Stress Induced Nuclear Granules form within the Nucleus in Response to Environmental Stress in *C. elegans*

By

Katherine Marie Sampuda

A Dissertation Submitted in Partial Fulfillment

of the Requirements for the Degree of

Doctor of Philosophy in Molecular Biosciences

Middle Tennessee State University

May 2017

Dissertation Committee:

Dr. Lynn Boyd, Chair

Dr. Matthew Elrod-Erickson

Dr. David Nelson

Dr. Jason Jessen

Dr. William Tansey

ACKNOWLEDGEMENTS

ABSTRACT

Protein misfolding caused by environmental stress can be damaging to a cell and it has been linked to many human diseases. Cells contend with misfolded proteins by employing an arsenal of protein quality control mechanisms (PQC). One PQC mechanism that aids in destroying misfolded and damaged proteins is the ubiquitin proteasome system (UPS). PQC mechanisms have been observed in the cytosol, endoplasmic reticulum, and mitochondria. However, little information is known about the PQC mechanisms in the nucleus. The nucleus has been suggested to be a site of protein degradation based on ubiquitin and proteasome localization in the nucleus under normal conditions. The research in this dissertation aims to understand how nuclear UPS is involved in environmental stress in *C. elegans.* Results from this study have shown that ubiquitin, proteasome, and TIA-1/TIAL RNA binding protein homolog (TIAR-2) localize into distinct structures termed stress induced nuclear granules (SINGs) in response to osmotic stress, oxidative stress, and starvation. SINGs were found to be enriched in K48 polyubiquitin chains and their formation was inhibited by proteasome inhibitors, which indicates SINGs being sites of protein degradation. Knockdown of ubiquitin conjugating enzymes *ubc-18*, *ubc-20,* and *ubc-22* decreased the appearance of SINGs during stress, which indicates they are part of the pathway leading to SING formation. Similar results were seen with knockdown of the ubiquitin ligase *chn-1* and nuclear import factors *ima-1, ran-1,* and *smo-1.* The formation of SINGs can be inhibited by a brief exposure to heat shock, which was found to be HSF-1 dependent. This finding suggests that increased chaperone expression is able to prevent SINGs. In addition, this experiment indicates that

the accumulation of misfolded proteins is required to induce SING formation. Embryos containing SINGs are unable to complete cell division suggesting that SINGs interfere with cell cycle progression. These results suggest a model in which the UPS is triggered in response to misfolded proteins in the nucleus.

TABLE OF CONTENTS

LIST OF TABLES

LIST OF FIGURES

LIST OF ABBREVIATIONS

26S   19S Regulatory Partical + 20S Catalytic Core Particle

C. elegans   Caenorhabditis

C-terminal   carboxyl-terminus

GFP   green fluorescent protein

H2B   histone protein

H_2O_2 hydrogen peroxide

K48   lysine 48

K63   lysine 63

L4   larval stage 4

mCh   mCherry

MG132   proteasome inhibitor

NaCl   sodium chloride

NPPs   nuclear pore proteins

NSBs   nuclear stress bodies

nSGs   nuclear stress granules

PML   promyelocytic leukemia

PQC   protein quality control

Q82   polyglutamate

RPT-1   regulatory particle triphosphatase

SINGs   stress induced nuclear granules

Ub   ubiquitin

UbAA   ubiquitin dialanine

uba   ubiquitin- activating enzyme

ubc   ubiquitin- conjugating enzyme

UPS   ubiquitin proteasome system

CHAPTER ONE

INTRODUCTION

1.1 General Introduction

Approximately 15% of the United States population is affected by infertility or impaired fecundity (Agarwal et al., 2008). Infertility can be linked to genetic and environmental factors, such as oxidative stress and starvation. Therefore, understanding how environmental stress exposure affects the organism as a whole and at a cellular level is important for preventing or treating infertility. Environmental stress is known to induce protein misfolding. When a protein becomes unfolded or partially unfolded it becomes structurally unstable and can aggregate with other proteins and interfere with normal cellular functions (Shibata and Morimoto, 2014). Accumulation of unfolded or damaged proteins may occur if the generation of those proteins is increased or if the ubiquitin proteasome system (UPS) is impaired (Huang and Chen, 2009). The accumulation of damaged proteins is a hallmark for cellular damage (Manetto et al., 1988).

A constant buildup of misfolded proteins is detrimental to the cell; therefore, the cell has evolved various protein quality control (PQC) mechanisms to correct, eliminate, or sequester misfolded proteins. One pathway that aids in clearing these damaged proteins is the UPS. The UPS is a pathway in which the 76 amino acid (8.5 kDa) polypeptide ubiquitin undergoes a series of three steps to be transferred onto a substrate that needs to be removed. Once a substrate is tagged by a polyubiquitin chain, a holoenzyme called proteasome recognizes the tag and destroys the substrate (Frankland-Searby and Bhaumik, 2012). The UPS has been well studied in the cytosol and evidence suggests that the system

plays a role in the nucleus (Nielsen et al., 2014). The background information to support this will be introduced by reviewing current knowledge of the UPS and compartment-specific mechanisms of PQC. Lastly, project objectives and summary will discussed.

1.2 Ubiquitin Proteasome System

1.2.1 Ubiquitin

Ubiquitin is a 76 amino acid polypeptide protein that is best known for its ability to target proteins for degradation by the 26S proteasome. It is also known to play key roles in DNA repair, endosomal sorting, signal translocation, protein-protein interactions, and autophagy (Wilkinson, 2005). This protein is highly conserved amongst eukaryotes. For instance, ubiquitin in *Caenorhabditis elegans* differs by one amino acid in *Homo sapiens* and three amino acids in *Saccharomyces cerevisiae.* Ubiquitin is characterized by having a β-grasp fold, seven lysine residues, and a diglycine at the C-terminal end of its sequence that is used when adding ubiquitin to proteins to evoke a specific event (Kraulis, 1991). In order for ubiquitin to be added to a protein three distinct enzymatic activities are needed called activation, conjugation, and ligation (Figure 1.1). This process is known as ubiquitination.
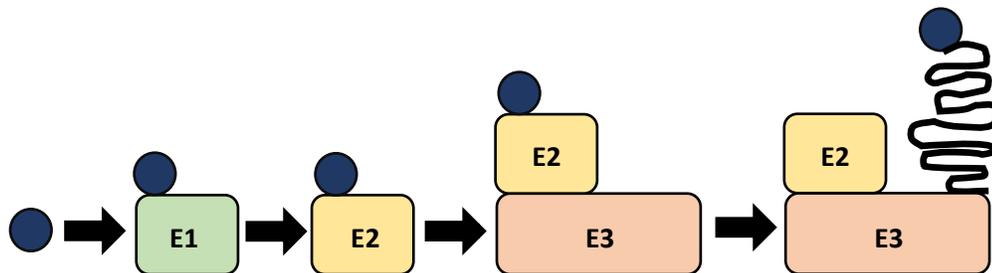
Figure 1.1: The Ubiquitin Pathway

Ubiquitin undergoes a series of three steps to be transferred onto a substrate that needs to be removed or relocated. First, ubiquitin must be bound to both ATP and to the ubiquitin activating enzyme **(E1)**. The next step involves transfer of ubiquitin to the ubiquitin conjugating enzyme **(E2)**. Generally, the E2 will from a complex with the ubiquitin ligase **(E3)** that recruits the substrate. Ubiquitin is then transferred over from the E2 to the substrate. This process can be repeated several times in order to form a polyubiquitin chain.

1.2.2 Ubiquitination

Ubiquitination is initiated by the binding of ATP to the ubiquitin activating enzyme (E1) that hydrolyzes ATP. E1 then adenylates the glycine of the C-terminal residue of ubiquitin and forms a thioester bond. The ubiquitin conjugating enzyme (E2) catalyzes the transfer of ubiquitin from the E1 to itself by transthiolation. The last step of ubiquitination

is mediated by the ubiquitin ligating enzyme (E3) that facilitates the transfer of ubiquitin from the E2 enzyme to the substrate (Figure 1.1). This reaction results in an isopeptide bond between the C-terminal glycine (Glycine 76) of ubiquitin and the epsilon amino group of the lysine on the target substrate (Ciechanover et al., 1982; Hershko et al., 1983).

1.2.3 Ubiquitinating Enzymes

1.2.3.1 Ubiquitin Activating Enzymes (E1)

E1s are ~100 kDa proteins that contain a Gly-X-Gly-X-X-Gly nucleotide-binding sequence that allows it to catalyze ubiquitin activation (McGrath et al., 1991). The function of E1 is to activate the C-terminus of ubiquitin by two reactions. The first reaction induces formation of an ubiquitin-adenylate intermediate. The next step involves a reaction between the intermediate formed and the cysteine residue from the E1 that results in an E1-ubiquitin thiol ester (Lake et al., 2001). In comparison to the other ubiquitin enzymes, there are fewer E1 enzymes. *H. sapiens* are known to have seven genes that encode E1s (UBA1-7), whereas, *D. melanogaster* and *C. elegans* has been reported to only have one E1 encoding gene (*Uba1* and *uba-1*) (Kulkarni and Smith, 2008; Pelzer et al., 2007; Watts et al., 2003) (Figure 1.1).

1.2.3.2 Ubiquitin Conjugating Enzymes (E2)

The second step of ubiquitination facilitates the transfer of ubiquitin from the E1 to the E2. The most prominent feature of E2s is the UBC domain. This region contains a centrally located cysteine residue that is essential in forming the thiolester bond between ubiquitin and E2 that aids in transferring ubiquitin from the E1 cysteine to the E2 cysteine (Bang et al., 2009). Another feature of this enzyme is the N-terminal motif that is rich in

basic residues. This motif is thought to function in E1 binding. In general, E2s are classified into four distinct classes (Class I-IV). Class I E2s contain a ~ 150 aa UBC domain, Class II E2s house the UBC domain with COOH extensions, Class III E2s contain the UBC domain and NH2 extensions, and Class IV E2s have the UBC domain and both types of extensions (Lake et al., 2001). E2s are more abundant than E1s with 37 E2 enzymes in *H. sapiens* and 24 in *C. elegans* (Stewart et al., 2016). Once ubiquitin is conjugated to the E2, it is transferred to the substrate by an E3 interaction that is dependent on the specific E3 utilized.

1.2.3.3 Ubiquitin Ligating Enzymes (E3)

Of the three steps of ubiquitination, E3s provide the highest level of substrate specificity provided by the specific type and multitude of E3 enzymes. In *H. sapiens*, there are greater than one thousand E3 enzymes that have been identified. They are classified into five families that include Homologuous to the E6-AP Carboxyl Terminus (HECT), RING-finger (Really Interesting New Gene), RING-in-Between-RING (RBR), U-box, and PHD-finger (Plant homeodomain). Each family of E3s participate in the transfer of ubiquitin to the substrate but vary in the mechanism of how they are transferred.

Some E3s can transfer ubiquitin directly to the substrate. For example, the HECT E3 family contain two connected lobes (C-and N-terminal lobes) that function to bring the E2 and the E3 in close proximity in order to transfer E2 bound ubiquitin over to the E3 and then to the specific substrate (Kumar et al., 1997) (Figure 1.2A).

Other E3s facilitate the transfer of ubiquitin from the E2 to the substrate by bringing the two closer. This type of activity is seen with the RING-finger family E3s. These

enzymes contain a zinc coordinating domain that houses a series of cysteine and histidine residues. This domain has been identified in the transfer of E2-dependent ubiquitination (Lorick et al., 1999). These E3 enzymes function as a scaffold to decrease the distance between the E2 and the substrate (Figure 1.2B). Once the enzyme brings these two closer, ubiquitin is directly transferred from the E2 to the substrate.

RBR E3s structural arrangement is composed of RING1-in-between-RING2 domains and share similarities with RING/HECT E3s. Examples of RBRs include Parkin and Human Homolog of Drosophila Ariadne-1 (HHARI). In the case of RBR E3s, the RING1 domain is responsible for recruiting and binding the E2-Ub complex. Ubiquitin from the E2 is then transferred to the RING2 on the E3 ligase (Streich and Lima, 2014). Once on the RING2, ubiquitin is transferred over from the E3 to the substrate (Bielskienė et al., 2015). The process of adding ubiquitin is different for each substrate, and this specificity is provided by the E3s. The enzymatic reaction of transferring ubiquitin to a substrate can be performed once or multiple times to produce a chain of ubiquitin molecules on the substrate.
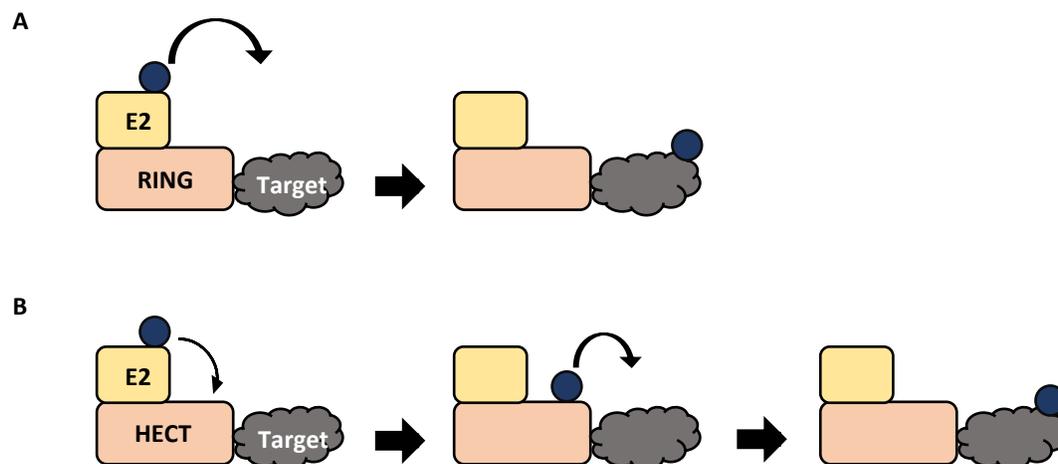
Figure 1.2: Activity of RING and HECT E3s

(A) RING finger domains function as a scaffold to enable the transfer of ubiquitin over to a substrate. **(B)** HECT domain E3s form a catalytic intermediate with ubiquitin to aid in the transfer of ubiquitin to the substrate.

1.2.4 Modes of Ubiquitination

There are three forms of ubiquitination: monoubiquitnation, multiubiquitination, and polyubiqitination. Monoubiquitination is the addition of a single ubiquitin molecule to a substrate (Figure 1.3A). This is often seen during endocytosis, membrane trafficking, and viral budding (Miranda and Sorkin, 2007). Multiubiquitination is the addition of a

single ubiquitin molecule to more than one lysine. Polyubiquitination is where multiple ubiquitin molecules are attached to a substrate as a chain (Figure 1.3A).

Ubiquitin has seven lysine (K) residues and an N-terminal methionine (M) that can be used for adding multiple ubiquitin molecules to a substrate. Depending on the identity of the seven lysine residues or methionine that is used will determine the type of polyubiquitin chain that is formed. The seven lysine residues are: lysine 6 (K6), lysine 11 (K11), lysine 27 (K27), lysine 29 (K29), lysine 33 (K33), lysine 48 (K48), and lysine 63 (K63). In addition to the lysine residues, the N-terminal methionine (M1) of ubiquitin can also participate in polyubiquitination. Two well characterized polypeptide chains are K48 and K63, where K48 chains typically lead to proteasomal degradation and K63 chains mediates endocytosis, Nuclear factor-kappa B (NF-κB) function, trafficking of proteins to aggresomes amongst other functions (Figure 1.3B) (Eddins et al., 2006; Nathan et al., 2013; Rodrigo-Brenni et al., 2010). Other atypical chains that are associated with proteasomal degradation include K6, K11, K27, and K29 (Ikeda and Dikic, 2008). Targeting a protein with a small post-translational modifier to invoke a particular response has been well-characterized with ubiquitin, but there are other proteins that act in a similar way. These proteins are called ubiquitin-like proteins (UBLs).
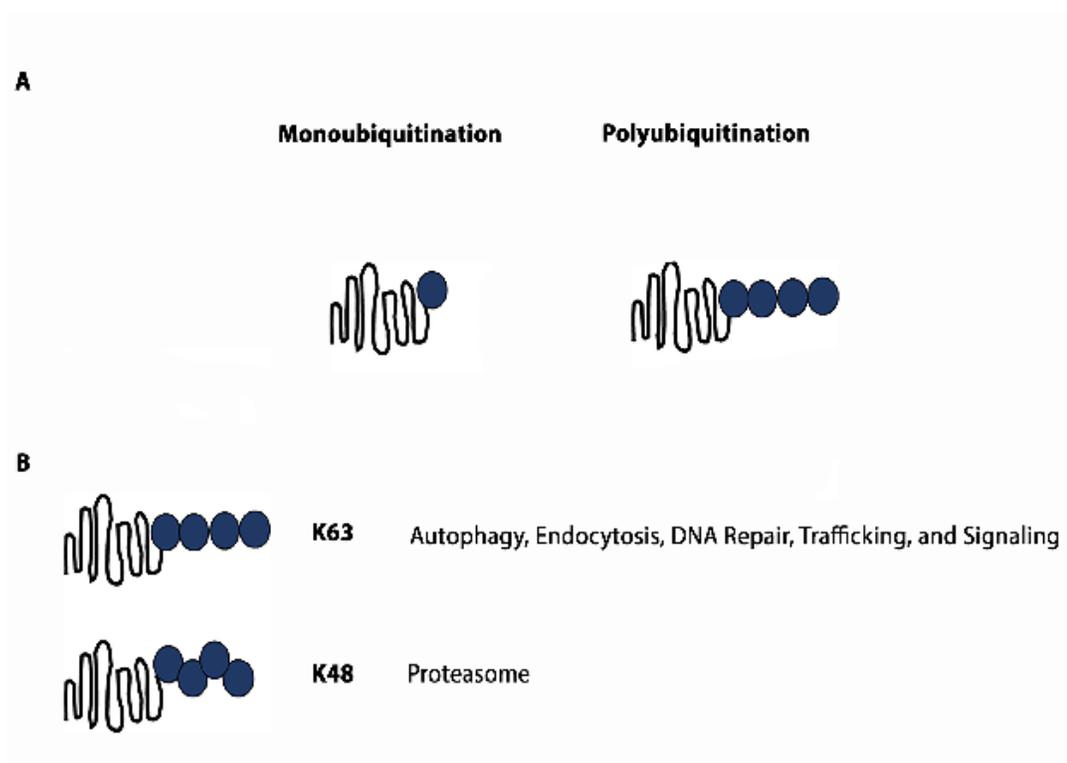
Figure 1.3: Ubiquitination

(A) This diagram represents two out of the three types of ubiquitination. Monoubiquitination is the addition of a single ubiquitin molecule to a substrate. Polyubiquitination is the addition of multiple ubiquitin molecules in a chain like fashion. **(B)** Two well characterized polyubiquitin chain types are K48 and K63 chains. K63 chains are known to be involvemed in autophagy. K48 chains are known to signal the proteasome for degradation.

1.2.5 Ubiquitin-like Proteins (UBLs)

UBL proteins contain a β-grasp fold and is structurally similar to ubiquitin. These proteins function by modifying a substrate through a series of three enzymatic steps that are closely related to the mechanism of ubiquitination (Herrmann et al., 2007). UBLs include SUMO (small ubiquitin-like modifier), NEDD8, ATG8, ATG12, UBL5, ISG15, and URM1. These proteins to play key roles in various cellular processes.

SUMO has been reported to be involved in nuclear transport, apoptosis, transcription, response to stress, and even required for cell cycle progression (Hong et al., 2001; Schimmel et al., 2014). Numerous nuclear proteins involved in signaling pathways such as cytokines, transcription, and DNA repair are known targets of this posttranslational modification. This modifier also regulates nuclear import. Evidence for this is based on the observation that RanGAP, a small GTPase that is involved in nuclear import, has been shown to interact more with a nuclear pore component (RanBP2) when it is sumoylated. Additionally, SUMO modification of proteins can lead to nuclear import. One example is seen where NF-κB essential modifier (NEMO), an IκB kinase regulator, is localized to the nucleus after being sumoylated (Huang et al., 2003). SUMO has also been linked to the localization of Promyelocytic Leukemia (PML) protein, a tumor suppressor protein, and other SUMO-modified proteins to PML nuclear bodies (Zhong et al., 2000). This UBL protein also plays an indirect role in protein degradation by recruiting special E3 ligases that ubiquitinate the polysumoylated protein to target it for degradation by the 26S proteasome (Hagen et al., 2010).

1.2.6 26S Proteasome

Once a substrate is tagged by a polyubiquitin chain of four or more ubiquitin proteins, the proteasome recognizes the ubiquitin tag and degrades the substrate (Frankland-Searby and Bhaumik, 2012). Proteasome subunits and their structure are well conserved amongst eukaryotes. The 26S proteasome is holoenzyme made up of one or two 19S regulatory caps and a 20S catalytic core (Figure 1.4A). The 19S cap consists of 19 proteins that are arranged as a base that binds to the 20S proteasome, and a lid that is comprised of 9 non-ATPase subunits. The function of the lid is to remove the ubiquitin molecules from substrates. This process of removing and recycling ubiquitin is performed by the Rpn11, a lid subunit (Tanaka, 2009). Once the polyubiquitin chain is cleaved, other deubiquitinating enzymes (DUBs) that are associated with the base further cleave this chain into monomeric ubiquitin molecules (Tanaka, 2009). The function of the 19S cap is to allow substrates to enter the 20S core to be degraded. The process of opening the lid is ATP-dependent.

Standard or constitutive proteasomes have a 20S catalytic core that contains four ring structures, which include two α-rings and two β-rings that are both compromised of 7 subunits. Each β-ring has three distinct proteolytic activities. The chymotrypsin-like activity (β5) cleaves peptide bonds that follow hydrophobic residues. The trypsin-like activity (β2) cleaves bonds after basic residues, and caspase-like or petidylglutamyl-peptide hydrolyzing activity (β1) cleaves after acidic residues (Figure 1.4B) (Dick et al., 1997). These three proteolytic activities enables this holoenzyme to degrade a wide range of substrates in an ATP-dependent manner. These substrates are degraded into 7 - 8 amino

acid polypeptides (Figure 1.4C). These polypeptides are further broken down by other enzymes and used in protein synthesis. There is diversity in the type of proteasomes. For instance, in vertebrates, there are more than 7 subunits (β1i, β2i, β5i) that are similar to other β subunits in the 20S. These β subunits are induced by microbial infections and interferon gamma (IFN-γ). These proteasomes that expresses these different subunits are referred to as immunoproteasomes. These proteasomes aid in regulating proinflammatory cytokine products, activate NF-κB pathway, and oxidative stress response (Tanaka, 2009).

The 26S proteasome normally appears in its assembled state. However, there are instances where the 26S proteasome dissociates into separate 19S cap and 20S core. For instance, oxidative stress has been shown to increase the disassembly of the 26S proteasome into independent 19S and 20S components (Wang et al., 2010). 26S disassembly is also observed in cases of low cellular NADH/NAD$^+$ and in cases of ATP deficiency when combined with mitochondrial impairment (Huang et al., 2013; Tsvetkov et al., 2014). The 26S proteasome can be found evenly distributed throughout the cytosol and nucleus in mammals and *S. cerevisiae*. The UPS is active in degrading misfolded proteins in the cytosol from different cell compartments.
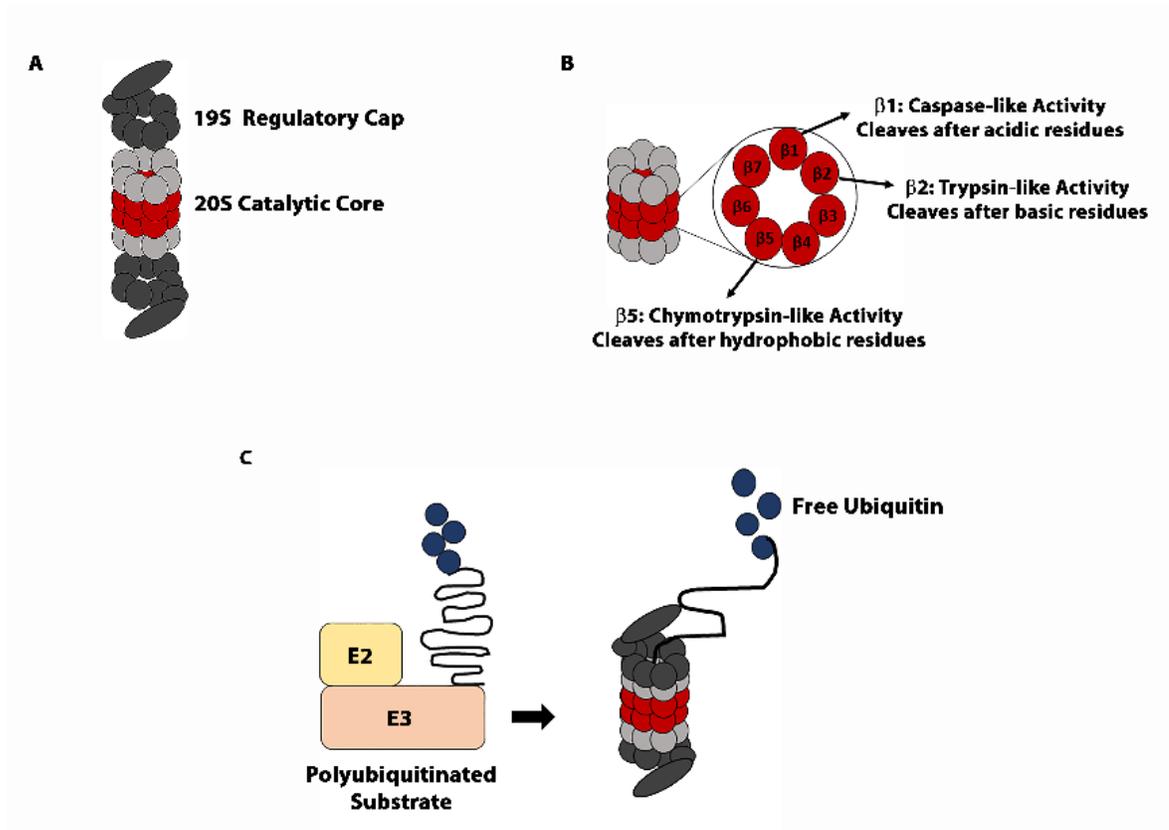
Figure 1.4: Ubiquitin Proteasome Pathway

(A) The 26S proteasome consists of both a 19S regulatory cap and a 20S catalytic core.

(B) The core contains three subunits (β1, β2, and β5) that are responsible for the proteolytic

activity required to cleave a substrate. **(C)** After a substrate has been polyubiquitinated, the

26S proteasome deubiqutinates ubiquitin molecules, unfolds, and degrades the substrate.

1.3 Compartment-Specific Mechanisms of Protein Quality Control

1.3.1 Areas of Protein Quality Control

Well-characterized areas of PQC in the cell include the cytosol, endoplasmic reticulum (ER), and mitochondria. Recently, studies have suggested that the nucleus is also a site of PQC. These areas of PQC have unique pathways for degrading or processing misfolded proteins. The cytosol, ER, and the mitochondria utilize both chaperone proteins and the UPS to process misfolded proteins (Amm et al., 2014). Chaperones function to recognize exposed hydrophobic patches on proteins and work to refold them back to their native state. If the protein is unable to fold that is targeted by the UPS for degradation (Bukau et al., 2006). Some misfolded proteins can be targeted by the chaperone itself for degradation. Those proteins are first identified by the chaperone, Hsp70 or Hsp90. If the chaperones are unable to fold the protein, CHIP (C-terminus of HSP70 Interacting Protein), a co-chaperone and an E3 ligase ubiquitinates Hsp90 and Hsp70 clients for proteasomal degradation. This co-chaperone is mainly concentrated in the cytoplasm and some in the nucleus under normal conditions, but is known to localize to the nucleus during different physiological states like heat shock (Gill, 2004a). CHIP is known to form different polyubiquitin chain types (K6, K11, K48, and K63) (Ikeda and Dikic, 2008). Chaperones and the UPS components are also detected in the nuclei of cells suggesting that similar PQC mechanisms are employed in this region of the cell (Shibata and Morimoto, 2014).

1.3.2 Nuclear Protein Quality Control

Recent studies have placed the UPS in the nucleus, which alludes to the concept of nuclear PQC (Mikecz, 2006; Nielsen et al., 2014). Supporting evidence includes nuclear

localization of the UPS and other PQC components, the characterization of nuclear proteolytic pathways in *S. cerevisiae,* and the localization of proteasome to known nuclear bodies.

1.3.3 Nuclear Localization of the UPS and Other Protein Quality Control Components

In both *S. cerevisiae* and mammalian cells, ubiquitin and 26S proteasome localize to the nucleus under normal conditions suggesting that the UPS functions in the nucleus (Mikecz, 2006). Studies in *S. cerevisiae* have characterized a nuclear proteolytic pathway. Experiments show that misfolded nuclear proteins are subjected to polyubiquitination by E3 ligases (San1, Slx-5-Slx8, and Doa10). San1 has also been reported to ubiquitinate misfolded cytoplasmic proteins that have been targeted to the nucleus for degradation (Heck et al., 2010). Currently, this pathway appears to unique to *S. cerevisiae*.

Chaperones (Hsp70, Hsp90, sHSPs) are imported into the nucleus under various conditions including acute exposure to stressors, such as heat shock. Certain chaperones are also found to be imported into the nucleus during G1 cell cycle phase (Shibata and Morimoto, 2014). However, the role that these chaperones play in the nucleus is not well understood. SUMO and CHIP can also become enriched in the nuclear compartment and are suggested to play a role in nuclear PQC. Studies in *S. cerevisiae* showed that CHIP plays a nuclear role by targeting signaling and misfolded proteins in nucleus for degradation (Nielsen et al., 2014). Experiments using heat shock and proteasome inhibitor treatment on *S. cerevisiae* showed high molecular weight SUMO conjugates that

accumulated in the nucleus (Tatham et al., 2011). This suggests that SUMO has a role in PQC.

1.3.4 Localization of Proteasome to Known Nuclear Bodies

The nuclei of various cultured cells and model organisms are known to develop distinct subnuclear structures under different stress conditions, changes in cell signaling, and altered metabolic state (Mähl et al., 1989; Sarge et al., 1993). These structures are often spherical and are most commonly referred to as nuclear bodies (NBs). NBs that form in response to stress include the following: heat-shock bodies (elevated heat), PML bodies (oxidative stress), paraspeckles, clastomes (osmotic stress), insulator bodies (osmotic stress), and nucleoplasmic speckles (Cotto et al., 1997; Everett, 2006; Lafarga et al., 2002; Schoborg et al., 2013).

Some of the aforementioned NBs contain components of the UPS (Table 1). These nuclear bodies include PML bodies, clastomes, and insulator bodies. Studies on PML bodies have shown that the proteasome and misfolded proteins are recruited to the PML body when cells are infected with a virus (Herpesviridae, Papillomaviridae, and Adenoviridae). This type of nuclear body is proposed to be a site of protein degradation (Antón et al., 1999; Dino Rockel and von Mikecz, 2002; Lallemand-Breitenbach and de Thé, 2010). Clastomes are also thought to be sites of proteolytic activity because they contain both ubiquitin and 26S proteasome complexes and were able to dissolve upon the addition of proteasome inhibitors (Lafarga et al., 2002). Insulator bodies were found to contain proteasome and are thought to act as a monitor of bound chromatin of insulator proteins (Schoborg et al., 2013). Numerous nuclear bodies have been recorded; however,

the function of these structures and how they relate to the cellular stress response remains ambiguous.

Table 1 List of Nuclear Body and Nuclear Granules

Name	Defining Components	UPS Components	BLAST Hits
Clastosome	19S, 20S Proteasome, c-fos, c-jun	Ubiquitin and 26S Proteasome	
Focal Clusters		Proteasome	
Insulator Bodies		Proteasome	
Nuclear Stress Granule	HSF1, HSF2, HAP	Ubiquitin	
Nuclear Speckles	Nsrp70	Proteasome	
PML Nuclear Bodies	PML Protein	Ubiquitin and 20S Proteasome	PML Not Found
Cajal Body	Coilin, SMN		Coilin Not Found
Histome locus body Nuclear Speckle	NPAT, FLASH, SRSF2, SRSF1, Malat1		NPAT Not Found
Paraspeckle Compartment	PSP1, p54nrb, Neat1		
Polycomb Body	Bmi1, Pc2		Polycomb Ground Proteins Not Found

1.4 Project Objectives and Summary

The aim of this study is to understand how nuclear UPS is involved in the response to cellular stress in the reproductive tissue. We chose *C. elegans* as our model organism because it has short life cycle (3 days), lifespan of 2-3 weeks, produces a large numbers of offspring, and both ubiquitin and the proteasome share homology with *H. sapiens*. Our data show that ubiquitin and 26S proteasome relocalize in response to salt stress, osmotic stress, oxidative stress, and starvation, forming 1-5 µm spheres that we term Stress Induced Nuclear Granules (SINGs) in both gonadal and embryonic nuclei. We found SINGs to be enriched in K48 polyubiquitin chains and their formation was inhibited by proteasome inhibitors. Based on our data, we believe that SINGs are sites of protein degradation that form during periods of cellular stress. Stressed embryos containing SINGs failed to complete cell division suggesting that SINGs play a role in interfering with the cell cycle. However, it is still unclear whether SING formation influences cell health or is an indirect result of cellular stress.

CHAPTER TWO

MATERIALS AND METHODS

Methods performed as described in Sampuda, K. M. et al 2017.

2.1 *C. elegans* **Strains and Maintenance**

C. elegans strains were cultured on nematode growth medium (NGM) with a bacterial lawn of *E. coli* strain OP50 and incubated at 20 °C, 25 °C, or 16 °C. Wild type and *ubc-18* mutants were grown at 20 °C and transgenic worms were incubated at 25 °C. The temperature sensitive *uba-1* mutant strain, RV110 was grown at 16 °C and shifted to 25 °C for 18 hours in order to reduce E1 activity before stress was administered. Strains used in this study are listed in Table 1.

Table 2 List of *C. elegans* Strains in this Study

Strain Name	Allele(s)	Source
AZ244	*ruIs57*[*pie-1*::GFP::tubulin + *unc-119*(+)]	CGC
BC10060	*sEx884* [rCes*C12C8.1*::GFP + pCeh361]	CGC
ERT261	jyEx128[vha-6p::GFP::ubiquitin cb-unc-119(+)];ttTi5605 II; unc-119 (ed9)	Emily Troemel
EU40	*skn-1*(*zu129*) IV/nT1 [*unc-?*(*n754*) *let-?*] (IV; V).	CGC
FGP8	*ruIs32* [*pie-1p*::GFP::H2B + *unc-119*(+)] III; *fgpIs20* [(pAA64) *pie-1p*::mCherry::*smo-1*(GG) + *unc-119*(+)]	CGC
JH1327	*axEx73* [*pie-1*p::*pie-1*::GFP + *rol-6(su1006)* + N2 genomic DNA]	CGC
JH2099	*axIs1486* [pCG51; LAP::*Y46G5A.13*(*tia-1.2*) + *unc-119*(+)]	Jennifer Schisa
JH2184	*axls1595*[*pie-1p*::GFP::*npp*-9(orf)::*npp-9* 3'UTR + *unc-119*(+)]	CGC
JH2338	*axls1489* [pCG61; *Ppie-1*::LAP::*pab-1*::*pie-1* 3' UTR + *unc-119*(ed3)] III	Jennifer Schisa
JH2458	*axIs1735*[*pie-1p*::LAP tag::*npp-10* (full length) + *unc-119* (+)]	CGC
JH2842	*ltIs37* [(pAA64) pie-1p::mCherry::*his-58* + *unc-119*(+)] IV; *axIs1522* [pie-1p::GFP::*pgl-1*::*pgl-1* 3'UTR + *unc-119*(+)]	CGC
JH2686	*axIs1844*[GFP:: *npp-7* + *unc-119*(+)]	CGC
LN129	*Ppie-1*::GFP::Ub + unc-119 (rcIs31): unc-119I(ed3)	Lynn Boyd
LN130	*Ppie-1*::GFP::Ub + *unc-119 (rcIs31); Ppie-1*::mCherry::*his-58 (itIs37)*	Lynn Boyd
LN154	*Ppie-1*::GFP::Ub + *unc-119 (rcIs31); rcSi1 [*Pmex-5::*rpt-1*::mCherry + *unc-119]II; unc-119 (ed3)*	Lynn Boyd
LN162	*avIs116 Ppie-1*::GFP::UbAA + *unc-119(+); Ppie-1*::mCherry::*his-58 (itIs37)*	Lynn Boyd
LW1089	*jjls1089*[*npp-1*::GFP + *unc-119*(+)]	CGC
N2 (Bristol)	Wild Type	CGC
OG497	*drSi13[hsf-1p::hsf-1*::GFP::*unc-54*' 3'UTR + *Cbr-unc-119*(+)] II	CGC
RV110	*uba-1(it129) IV*	Harold Smith
WY34	*ubc-18(ku354) III*	CGC
XA3546	*qaIs3546*[*unc-119*(+) + *pie-1*::GFP::*npp-8*]; *unc-119*(ed3)	CGC

2.2 Gene Knockdown by RNAi

RNAi was a technique used to knockdown the expression of genes by feeding worms bacteria that express dsRNA targeting each gene. RNAi clones for the UBC genes were obtained from the Ahringer library or the Vidal ORF library. The *ubc-18* RNAi is an ORF clone from the Ahringer library. Controls for the RNAi experiments used the L4440 plasmid (vector) without any gene insert in the HT115 bacterial strain. RNAi clones were streaked from glycerol stocks onto tryptic soy agar media with ampicillin (100 µg/mL) and tetracycline (10 µg/mL). Bacteria was grown overnight (~16 hours) in tryptic soy broth with ampicillin and tetracycline. NGM plates containing ampicillin and 0.2% lactose were seeded with overnight bacterial cultures. L4s were transferred to above plates and grown for 22 hours under ideal conditions for each respective strain.

2.3 Stress Treatment and Analyses

C. elegans were grown on OP50 containing NGM at their respective temperatures until they reached 1 day adults. Worms from this population were then moved to control and stressed conditions. Conditions involving liquid (control, salt stress, and oxidative stress) were performed by soaking day 1 adults in a watch glass containing 1 mL of solution at room temperature. Control (unstressed) individuals were soaked in M9 buffer (3 g KH_2PO_4, 6 g Na_2HPO_4, 5 g NaCl, 1 mL 1 M $MgSO_4$, H_2O to 1L) for 60 minutes. Salt stress was conducted by soaking worms in a 500 mM NaCl solution for 60 minutes. The worm strain JH2099 (GFP:: TIAR-2) was salt stressed for 120 minutes. The ERT261 (GFP::Ub) intestinal strain was salt stressed in 1 M NaCl for 60 minutes prior to imaging

by confocal microscopy. Oxidative stress was induced by soaking worms in a 10 mM H_2O_2 solution for 60 minutes. For starvation, synchronized L4 worms were moved to NGM plates without OP50 bacteria or peptone for a period of 48 hours prior to being examined.

2.4 Treatment with Proteasome Inhibitors

Proteasome inhibitor solutions were prepared the same day as the experiment by adding proteasome inhibitor stock solution to either M9 buffer or 500 mM NaCl. Proteasome inhibitors and concentrations tested include 20 µM MG132, 10 µM Lactacystin, and 20 µM Bortezomib. *In vivo* proteasome inhibitor experiments were performed by soaking day 1 adult worms in 20 µM MG132 for 60 minutes at room temperature. Worms were then transferred over to a solution containing both MG132 and 500 mM NaCl. Control worms were soaked in a 500 mM NaCl solution with no proteasome inhibitor for 60 minutes prior to imaging.

2.5 Heat Shock and Recovery

2.5.1 Prior Heat Shock Exposure

Day 1 adult worms grown at 25 °C were shifted to 34 °C for 60 minutes prior to 500 mM NaCl exposure. Worms were then moved to a 3% agar pad and then imaged by confocal microscopy. Control individuals stayed at the initial growing temperature (25 °C) before being exposed to salt stress.

2.5.2 Heat Shock

To induce heat shock, day 1 adults grown on an NGM plate with an OP50 bacterial lawn at 25 °C were shifted to 37 °C for 60 minutes prior to imaging. Control (25 °C) and stressed groups (37 °C) were transferred to a 3% agar pad, mounted on slides and examined with a laser scanning confocal microscope.

2.5.3 Recovery Post Stress

After exposure to stress, worms were placed on a new NGM plate set at 25 °C. Worms were imaged at 0, 2, and 24 hours post-stress for the presence of SINGs in oocytes. Three experiments were performed to give a total number of 45 worms that were imaged for SING recovery.

2.6 Embryonic Lethality and Cell Division Analysis

Embryos were extracted from day 1 adult worms by cutting under a dissecting microscope with a needle. Embryos were soaked in either M9 buffer (control) or 500 mM NaCl for 60 minutes. After which, embryos were then pipetted onto unseeded NGM plates and scored for hatching at 48 hours. Wild type and *ubc-18* (RNAi) embryos were extracted as described above and subjected to either M9 buffer, salt stress, or oxidative stress for 60 minutes. Embryos were then transferred to unseeded NGM plates and scored for hatching at 48 hours. Cell division analysis was conducted by taking time-lapse image series of

both control (M9 buffer) and salt stressed embryos expressing GFP::ub and mCh::H2B. Time-lapse movies are described in section 2.8.2.

2.7 Immunohistochemistry

2.7.1 Antibodies

Primary antibodies used were rabbit polyclonal anti-19S proteasome (sc-98797, Santa Cruz), mouse monoclonal anti-20S proteasome (MCP20, Enzo Lifesciences), mouse monoclonal anti-ubiquitin (P4D1, Santa Cruz), rabbit polyclonal anti-K48 ubiquitin (Apu2, Millipore), and rabbit anti-K63 ubiquitin (Apu3, Millipore). Secondary antibodies used were goat anti-mouse FITC (Abcam) and goat anti-rabbit TRITC (Jackson ImmunoResearch Laboratories).

2.7.2 Immunofluorescent Staining of *C. elegans*

Day 1 adult worms were placed in Egg Buffer and cut open on poly-L-lysine-coated slides to release the gonadal arms and embryos. Slides were placed in liquid nitrogen and fixed with 100% methanol at -20 °C for 20 minutes, followed by washing three times with PBS/ 0.1% Tween-20 for 5 minutes each. Slides were then blocked for 60 minutes with 30% normal goat serum in PBS/T at 23 °C, and incubated overnight with primary antibody (1:200) at 4 °C. Slides were washed with PBS/T, and incubated with secondary antibody (1:200) at 23 °C for 1.5 hours. All primary and secondary antibodies were made in

blocking buffer. Vectashield plus DAPI (Vector Labs, Burlingame, CA) was used for mounting each sample prior to confocal microcopy.

2.7.3 Detection of DNA and RNA in *C. elegans*

The cell-permeable SYTO14 green fluorescent nucleic acid stain (Life Technologies) was used to stain total RNA in oocytes. Fresh SYTO14 solution was used for each experiment. SYTO14 solution was made either in M9 buffer (unstressed) or 500 mM NaCl (stressed). Worms were dissected in 5 µm SYTO14 solution and incubated at room temperature for 15 minutes. Treated worms were then imaged by confocal microscopy. DAPI (NucBlue Fixed Cell ReadyProbes, Life Technologies) was used in the SYTO14 experiment to visualize DNA. One drop of DAPI (1 mg/ mL) was added directly to the top of the slide and incubated for 15 minutes prior to visualization.

2.8 Confocal Laser Scanning Microscopy

2.8.1 Fluorescence Microscopy of Live and Fixed Samples

All individual and time-lapse fluorescent images were acquired using the timelapse function on the ZEISS AxioObserver with a LSM 700 confocal module and a 63x/1.4 Plan-Apochromat oil DIC M27 objective. The microscope was operated using the Zen Black 2009 software. In live imaging and antibody staining experiments, the 408 nm laser was used to image DAPI, the 488 nm laser was used to excite SYTO14, GFP, and FITC fluorescence. The 555 nm laser was used to excite both mCherry and TRITC fluorescence. Image settings on the microscope were kept constant for each set

of experiments. The 488 and 555 laser were both set at 5% power, 800 gain, and a pixel dwell of 0.05 ms. The 408 laser was set at 5% power, 800 gain, and a pixel dwell of 0.05 ms. Dimensions of images acquired were 512 x 512 pixels at a depth of 12 bits. Images were analyzed with the ZEN 2009 software. Images in this dissertation are displayed in a linear fashion.

2.8.2 Time-lapse Imaging

A time-lapse series (30 frames with 1 minute intervals) of the worm strain LN154 (GFP::Ub and RPT-1:: mCh) was used to investigate the timing of colocalization events. All time-lapse experiments were imaged on the confocal at room temperature. A time-lapse series (30 frames with 0.5 minute intervals) of LN130 worms (GFP::Ub and mCh::H2B) was used for cell division experiments.

2.8.3 FRAP Analysis

Photobleaching experiments were performed using a Zeiss LSM700 laser scanning confocal microscope. Two pre-bleach images were acquired prior to photobleach in order to record the initial fluoresce. Bleaching was done via 40 passes across a user-defined region of interest using a 488 nm laser set at 100% laser power. Fluorescence was bleached to $\leq 20\%$ of initial intensity. Images were acquired every 1 second with the 488 nm laser set to 5% power. The background was subtracted from each data point and normalized to

unbleached areas using the equation: $[(ROI_b - ROI_{bg})/(ROI_{nb} - ROI_{bg})]/[(pbROI_b - pbROI_{bg})/(pbROI_{nb} - pbROI_{bg})]$.

2.9 SDS-PAGE

2.9.1 Imaging of Fluorescent Proteins Separated by SDS-PAGE

2x Laemmli loading buffer was added to each sample prior to running SDS PAGE. 1 x Loading buffer contained 1M Tris-HCl pH 6.8, 10% SDS, glycerol, β-mercaptoethanol, and 1% bromophenol blue in dH_20. Protein samples with Laemmli loading buffer were loaded into a 10% polyacrylamide gel. ColorPlus prestained protein marker (New England BioLabs Inc.), broad range (7-175 kDa) was used a protein ladder to compare size of resolved protein bands. 70 V were used to run the protein through the stacking gel in 1x running buffer, after which, the voltage was increased to 130 V for the remainder of the process. A 1:10 dilution of running buffer was made from a 10x stock containing 15.135 g Tris base, 72 g Glycine, 50 mL 10% SDS, and brought up to 500 mL dH_2O.

2.9.2 Silver Stain of SDS-PAGE Gel

The silver stain was conducted by initially washing the SDS-PAGE gel 2x in ultrapure water for 5 minutes. The gel was then placed in a fixative solution that contained 30% ETOH and 10% acetic acidic 2x for 15 minutes. The gel was washed 2x in 10% ETOH 2x for 5 minutes, followed by washing 2x in ultrapure water for 5 minutes. The gel was then incubated in a sensitizer working solution for 60 seconds and then washed 2x in ultrapure water for 60 seconds. After washing, the gel was incubated in Pierce silver stain

(Thermo Scientific) working solution for 30 minutes, then washed 2x in ultrapure water for 20 seconds. The developer solution was added and rocked until band appeared. After the desired band intensity was reached, the developer solution was removed and a stop solution of 5% acetic acid was added for 10 minutes and then removed. This step was repeated a total of two times. The gel was then imaged on a ChemiDoc Imager.

2.9.3 Detection of Fluorescent Proteins by Typhoon Imaging

To image GFP fluorescence in the SDS-PAGE gel, protein samples were resuspended in 2x loading buffer and incubated at 37 °C for 30 minutes prior to loading protein sample in the gel. After SDS-PAGE was completed, the gel was washed 1x in running buffer and then imaged using a Typhoon Trio + Variable Mode Imager (GE Healthcare Life Sciences), which is a fluorescent/phosphorescent image scanner. SDS gels were scanned on normal sensitivity at 580 BP 30/ Green 532 to visualize protein ladder (PMT 600) and 670 BP 30/ Green 532 (PMT 600) to view GFP.

2.10 Mass Spectrometry

2.10.1 Protein Preparation for Mass Spectrometry

Day 1 adult worms were isolated from large NGM plates by either washing off with M9 buffer (Unstressed) or 500 mM NaCl (stressed) and centrifuged at 6,500 rpm for 1 minute at room temperature. Stressed worms were rocked for 60 minutes in salt solution

prior to centrifugation. Unstressed worms were rocked for 60 minutes in M9 buffer. 0.5 mL worm pellets were used to create worm lysates.

Worm lysates were made by resuspending sample pellets in 0.75 mL of urea lysis buffer with protease inhibitors and 100 μL of 0.5 mm zirconium oxide beads followed by bead-beating for 6 minutes on 12 speed. Bead-beating was used as a mechanical method to break open the worms. After bead-beating, the lysate was incubated on ice for 30 minutes with repeated pipetting (10 passes) every 10 minutes. The lysate was spun at 20,000 x g for 10 minutes at 4 °C. The supernatant was then transferred to clean Eppendorf tube. A Pierce BCA protein assay kit was used to quantify the concentration of protein in each tube. A protein concentration of 11.527 mg for unstressed and 6.781 mg for stressed samples were then placed on dry ice and mailed to Cell Signaling Technology for mass spectrometry analysis (see section 2.11 for further details).

2.10.2 Analysis of Mass Spectrometry Data

Unstressed (M9 buffer) and stressed (500 mM NaCl) whole worm lysates were sent to Cell Signaling Technology for mass spectrometry analysis. Following tandem affinity purification and trypsin digestion, worm lysates were enriched for diGly-containing peptides using PTMScan Ubiquitin Branch Motif Immumoaffinity Bead (K-ε-GG) (ubiquitin remnant K-GG motif antibody #3925). Samples were then run in duplicate through LC-MS/MS. SEQUEST and the Core platform from Harvard University was used to evaluate MS/MS spectra. Peptide searches were performed against the current version of the NCBI *C. elegans* database with mass accuracy of +/-50 ppm (precursor ions) and

0.02 Da (product ions). Those results were then additionally filtered with a mass accuracy of +/-5 ppm (precursor ions) and detection of di-Gly motif. A 5% default false positive rate was used in filtering through the results. The list of proteins that were received by Cell Signaling Technology was thresholded based on the following parameters: a fold change of ≥ 2.5, max intensity $\geq 15,000,000$ AU, and a max % CV $\leq 20\%$. This list can be viewed in Table 3.

2.11 Statistical Analysis

Sample sizes and number of experiments performed are noted in each figure legend. In general, a total of 1020 oocytes were observed over three biological repeats unless otherwise noted in the figure legend. The type of statistical test that was performed for each experiment is indicated in each figure legend. Two sample z-tests were performed using VasarStats on the 20S and TIAR-2 antibody stains as well as on live images that include RNAi and stress experiments. The Fisher's exact test was performed on data that was $n < 5$. All error bars presented in this dissertation represent a 95% confidence interval and were derived using the modified Wald method on GraphPad. A log-rank test was used to determine significant differences in survivorship curves in the lifespan experiment. Data was considered to be statistically significant if $p < 0.05$.

CHAPTER THREE

STRESS INDUCES THE FORMATION OF NOVEL STRESS

INDUCED NUCLEAR GRANULES

3.1 Introduction

Environmental stress, such as salt stress and oxidative stress is known to induce protein damage that in turn affects PQC mechanisms such as the UPS and chaperones. Oxidative and hypertonic stress have been shown to increase ubiquitin conjugates indicating that stress is either inducing more ubiquitin conjugates or that the proteasome is disturbed (Burkewitz et al., 2012; Jahngen-Hodge et al., 1997). Certain stresses like heat shock enhance chaperone expression in order to cope with the increased number of damaged proteins (Morimoto, 1998). The heat shock response (HSR) is orchestrated by heat shock factor 1 (HSF1), a transcription factor. In unstressed states, HSF1 is repressed by heat shock protein 70 (HSP70) and heat shock protein 90 (HSP90). When proteotoxic stress such as heat shock occurs, HSF1 is released from HSP70 and HSP90. HSF1 then accumulates in the nucleus where it is responsible for stimulating the transcription of heat shock proteins (Morimoto, 1998). In addition to this response, HSF1 is also known to localize to nSGs and transcribe noncoding RNAs (Morton and Lamitina, 2013).

In addition to exogenous environmental stress, endogenous stresses associated with aging are another factor that influences PQC mechanisms. Aging is associated with the decline in proteostasis function and protein turnover. This may be due to a combination of

reduced in proteasome function and protein aggregation (Ferrington et al., 2005; Grune et al., 2004; Vernace et al., 2007). Contributing factors to proteasomal decline include decreased expression of proteasome subunits, disassembly of the 26S proteasome, and aggregation of the proteasomes themselves (Ferrington et al., 2005; Grune et al., 2004; Vernace et al., 2007). An example of altered proteasome state can be seen in flies where increased age is correlated with decreased ATP levels and 20S proteasome activity (Vernace et al., 2007) In addition to the UPS, chaperone expression is also known to decrease with age (David et al., 2010; Ben-Zvi et al., 2009). In older *C. elegans,* chaperone expression (*hsp-70* and *hsp-16.2*) in day 4 adults was significantly decreased in comparison to day 1 adults suggesting that proteostasis not only changes during age but it changes early in adulthood (Ben-Zvi et al., 2009). Currently, it is poorly understood how gonadal cells deal with stress. Insight into this will provide knowledge on how to treat infertility that results from exposure to environmental stress. We aim to understand how the nuclear UPS is affected by stress in the reproductive tissue of *C. elegans.*

3.2 Results

3.2.1 Ubiquitin Concentrates into Distinct Spheres within the Nuclei of Reproductive Tissue and Embryos

In this study, we are using *C. elegans* as a model to study cellular stress in the germline. *C. elegans* are primarily hermaphroditic and their reproductive germline contains two gonadal arms that consist of developing oocytes, sperm, and a uterus (Figure 3.1A). We aim to understand how stress affects the UPS by observing the subcellular localization

of ubiquitin in unstressed and stressed oocytes and embryos (Figure 3.1B). To visualize ubiquitin in the germline, we used an existing worm strain that expresses GFP::Ub (Ubiquitin) and mCh::H2B (Histone) (Hajjar et al., 2014).   Day 1 adult worms that were soaked in M9 buffer (86 mM NaCl) showed a diffuse pattern of ubiquitin within the cytoplasm and the nucleus of oocytes and embryos (Figure 3.1C and 3.1D). Interestingly, ubiquitin appeared to be more concentrated in the nucleus than in the cytoplasm of oocytes and embryos. After 60 minutes of soaking worms in a higher salt concentration (500 mM NaCl), ubiquitin relocalized into distinct spheres within the nucleus of oocytes and embryos (Figure 3.1C and 3.1D). In either of the two conditions, ubiquitin did not show any overlap with the histones.

To determine what concentration of salt induces the appearance of nuclear spheres, we soaked the worms in a range of salt concentrations. We found that as salt concentration increased so did the appearance of SINGs. A concentration of 500 mM NaCl was chosen because spheres were induced after 30 minutes of exposure and did not appear to cause lethality to adult worms (Figure 3.1E and 3.1F). The appearance of nuclear spheres during salt stress led us to ask whether osmotic stress also induced this phenomenon. Our results show that under unstressed conditions (M9 buffer) nuclear spheres are not present; however, they were induced in both 500 mM NaCl and 652 mM sucrose conditions (Figure 3.1G).

Since transgenic worms do not address the endogenous population of protein, an antibody stain of ubiquitin (P4D1) was performed on unstressed and stressed wild type day

1 adult worms. Results from this experiment showed that only salt stressed worms formed nuclear spheres containing endogenous ubiquitin (Figure 3.1H). This result suggests that the fluorescent reporter is a reliable reporter of the location of endogenous ubiquitin and that under stress conditions ubiquitin relocalizes into distinct spheres.   We will related to these nuclear spheres as "stress induced nuclear granules" (SINGs) for the remainder of this dissertation.

A Distal Gonad

Pachytene Arrested

Distal Tip

Embryos Sperm Oocytes

Proximal Gonad

B

M9 Buffer (Control) 500 mM NaCl

C

M9 Buffer 500 mM NaCl

GFP::Ub
mCh::H2B

10 μm

D

M9 Buffer 500 mM NaCl

GFP::Ub
mCh::H2B

10 μm

E

F

G

H

M9 Buffer 500 mM NaCl

Ubiquitin

10 μm
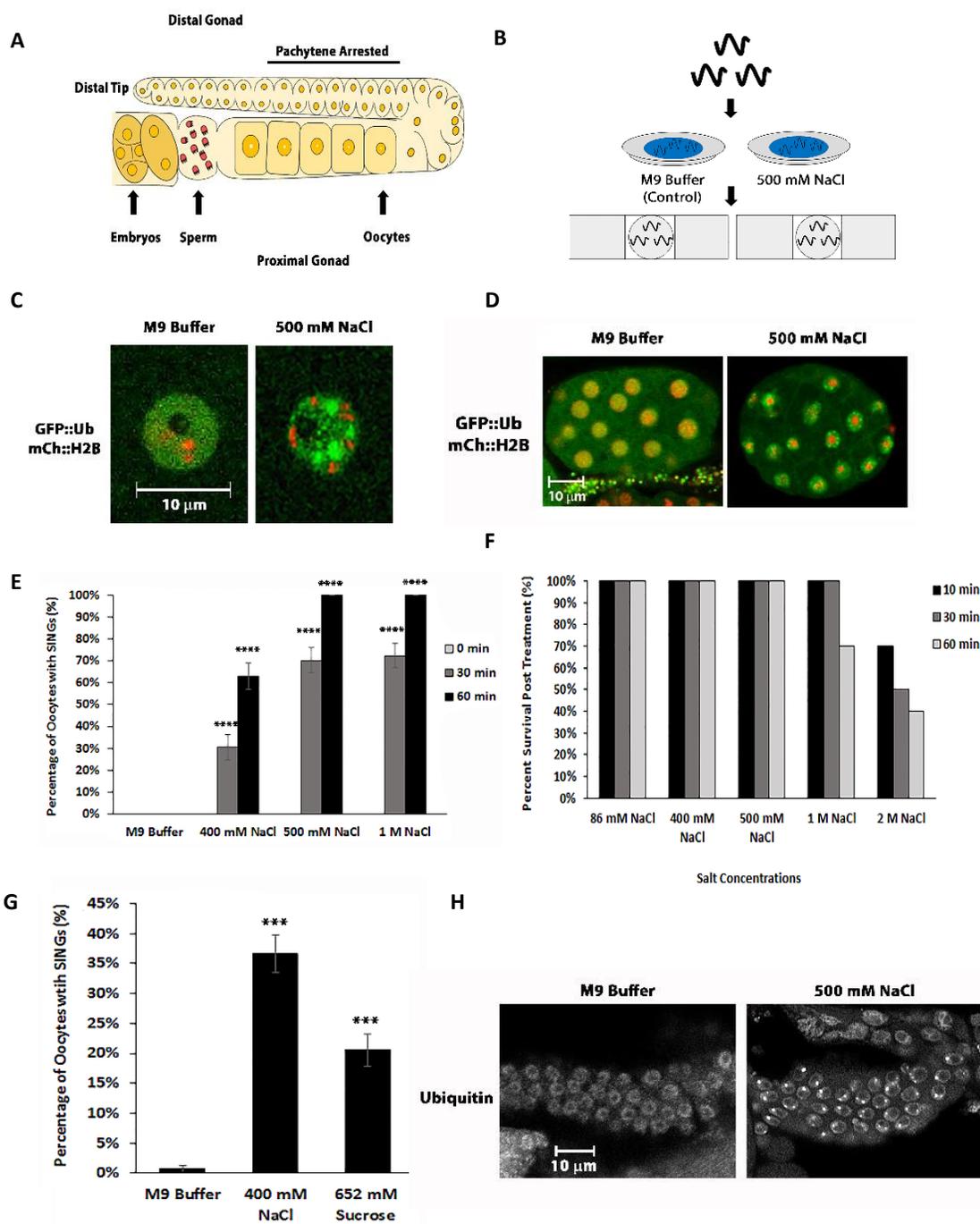
Figure 3.1: Salt Stress Induces Redistribution of Ubiquitin into Nuclear Stress Bodies

(**A**) Reproductive tissue of *C. elegans*. The *C. elegans* gonad is a U-shaped organ with mitotically dividing cells at the distal tip. The distal region of the gonad is syncytial and oocytes become increasingly cellularized and larger as they progress through the proximal region towards the spermatheca. (**B**) A schematic diagram of the application of stress to *C. elegans*. Salt stress was administered by placing young adult worms in a watch glass containing M9 buffer (unstressed condition) or in 500 mM NaCl (stressed condition) for 60 minutes. After which, worms were removed and placed on a slide to image. (**C**) Live imaging of GFP::Ub (green) and histones (mCh::H2B) in oocytes. During unstressed (M9 buffer) conditions ubiquitin was present in both the nucleus and the cytoplasm, but appeared to be more concentrated in the nucleus. In stressed (500 mM NaCl) conditions ubiquitin concentrated into stress bodies in the nucleus. A single oocyte is shown in each row. SINGs were found in salt stress (119/342 oocytes), but were absent in unstressed conditions (0/342 oocytes). A total of 342 oocytes were collected from 2 independent experiments ($n = 20$). (**D**) Live imaging of GFP::Ub (green) and histones (mCh::H2B) in embryos. SING formation was also noted to occur in stressed embryos. (**E**) The percentage of oocytes forming SINGs at varied concentrations of salt and time points. (**F**) The percent survival post treatment of unstressed and stressed conditions. Decreased survival was observed in worms soaked in 1M and 2M NaCl. (**G**) Osmotic stress induces SING formation. Graph representing the percentage of oocytes that formed SINGs when exposed to M9 buffer, 400 mM NaCl, and 652 mM sucrose. (**H**) Antibody staining of ubiquitin in the distal gonad. Gonads of unstressed and stressed adult *C. elegans* were dissected out

and stained with an ubiquitin antibody (green). Ubiquitin was found to be diffuse within the nucleus in unstressed populations (0/500 oocytes), but relocalized into SINGs in stressed populations (292/500 oocytes). A total of 500 oocytes were collected from 3 independent experiments. Statistical significance was calculated by a two-tailed z test: ***, $p < 0.001$. Scale bar indicates 10 µm.

3.2.2 SINGs are Enriched in K48 Polyubiquitin Chains

To determine if the ubiquitin present in SINGs is conjugated onto a substrate, we stressed a transgenic strain that harbors GFP::UbAA. This strain expresses ubiquitin with a dialanine in place of the diglycine at the C-terminus, preventing it from being covalently conjugated to substrates. After 60 minutes of soaking in either condition, GFP::UbAA remained diffuse, which suggests that SINGs contain conjugated ubiquitin (Figure 3.2A and 3.2B). To investigate whether a specific polyubiquitin chain is formed in SINGs during stress, immunofluorescent staining two well characterized polyubiquitin chains, K48 and K63, was performed on unstressed and stressed wild type worms. Immunofluorescent staining showed that only K48 polyubiquitin chains were present at nuclear spheres post-stress in oocytes and embryos (Figure 3.2C and Figure 3.2D). Since, K48 polyubiquitin chains are recognized by the proteasome, we decided to investigate proteasome involvement in SINGs.

A

Ub + H2B   UbAA + H2B

M9 Buffer

10μm

500 mM NaCl

B

60%

50%   ****

40%

30%

20%

10%

0%

Percentage of Oocytes with SINGs (%)

Ub   UbAA   Ub   UbAA
M9 Buffer M9 Buffer NaCl   NaCl

C

K63   K48

M9 Buffer

10 μm

500 mM NaCl

D

K48   Ubiquitin   Merged

M9 Buffer

10 μm

500 mM NaCl
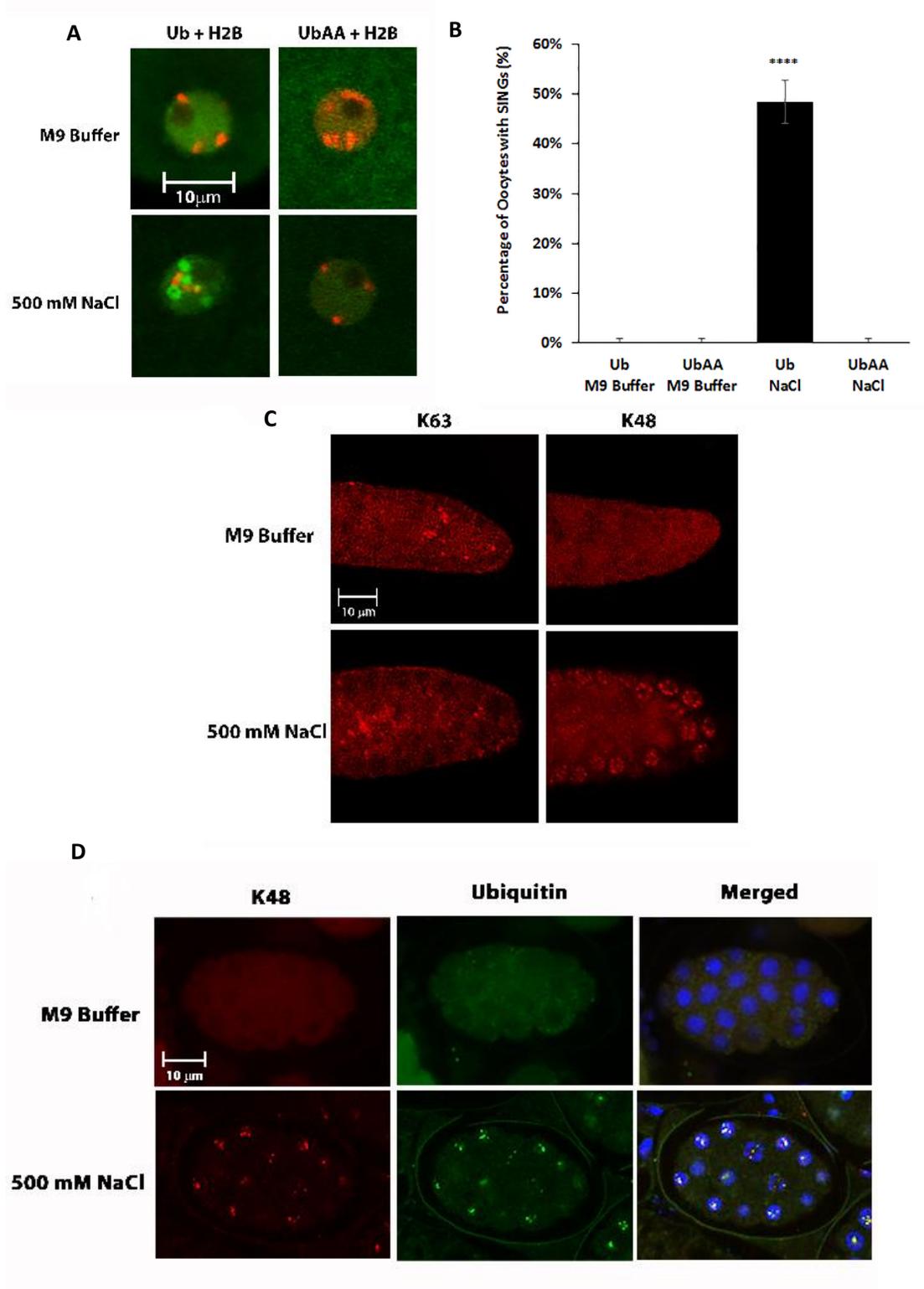
Figure 3.2: SINGs Contain Conjugated Ubiquitin and are Enriched in K48 Polyubiquitin Chains

(A) Unconjugated ubiquitin does not localize to SINGs. A worm strain expressing GFP::Ub (green) and mCh::H2B (red) shows localization of GFP::Ub to SINGs after soaking in 500 mM NaCl for 60 minutes. Whereas, GFP::UbAA does not localize to SINGs. GFP::UbAA lacks a C-terminal diglycine that is required for ubiquitin conjugation. **(B)** The percentage of oocytes forming SINGs in control and salt stress treated worms as described in A. Ub control and UbAA control and salt stressed worms showed no signs of SING formation (0/510 oocytes), whereas, Ub salt stressed did exhibit SING formation after stress exposure (247/510 oocytes). A total of 510 oocytes were observed at each time point. Statistical significance was calculated by a Fisher's Exact test: ****, $p < 0.0001$. **(C)** K63 and K48 polyubiquitin antibody staining in the distal gonad. During exposure to 500 mM NaCl, K48 chains localized into SINGs (552/600 oocytes), whereas, K63 chains show no localization to SINGs in response to stress (0/600 oocytes). **(D)** Ubiquitin (green) and K48 (red) antibody staining in embryos. Ubiquitin and K48 polyubiquitin chains appeared diffuse in M9 soaked embryos, and formed SINGs rich in ubiquitin and K48 polyubiquitin chains during stress. Scale bar indicates 10 µm.

3.2.3 26S Proteasome Colocalizes with Ubiquitin in SINGs

To test for the presence of proteasomes within SINGs we performed both live imaging and antibody staining of 19S proteasome. Live worms expressing RPT-1::GFP (19S cap) and mCh::H2B were tested for SING formation. Unstressed worms exhibited a diffuse expression of 19S proteasome within the cytosol and nucleus. Similar to ubiquitin, 19S proteasome also appeared to be highly concentrated within the nucleus. Salt stressed worms were found to form proteasome spheres within the nucleus (Figure 3.3A). To determine if these 19S proteasome spheres colocalized with ubiquitin in SINGs, a double immunofluorescence procedure to detect ubiquitin and 19S proteasome (RPT-3 subunit) was carried out on wild type worms. Upon the exposure to salt stress, both ubiquitin and 19S proteasome relocalized into spheres with the 19S proteasome colocalizing with ubiquitin in SINGs (Figure 3.3B). Next, we wanted to investigate whether the entire 26S proteasome complex was present in SINGs by conducting antibody staining on the PAS-6 (alpha 1) subunit of the 20S proteasome in both unstressed and stressed populations. Under control conditions, the 20S proteasome remains diffuse in the cytoplasm and the nucleus and only during stressed conditions formed nuclear spheres (Figure 3.3C). The results from this experiment show that the 20S is also present in SINGs, in addition to the 19S proteasome and ubiquitin.

A

M9 Buffer   500 mM NaCl

GFP::RPT-1
mCh::H2B

10 μm

B

19S Proteasome   Ubiquitin   Merged

M9 Buffer

10 μm

500 mM NaCl

C

20S   Ubiquitin   Merged

M9 Buffer

10 μm

500 mM NaCl
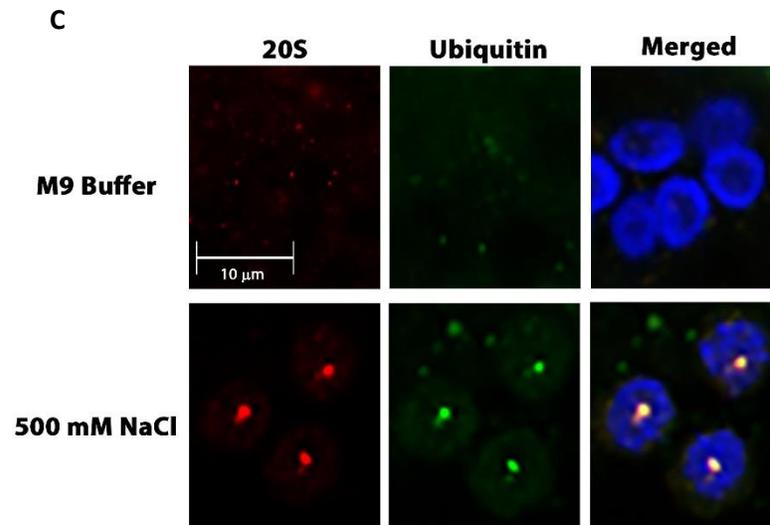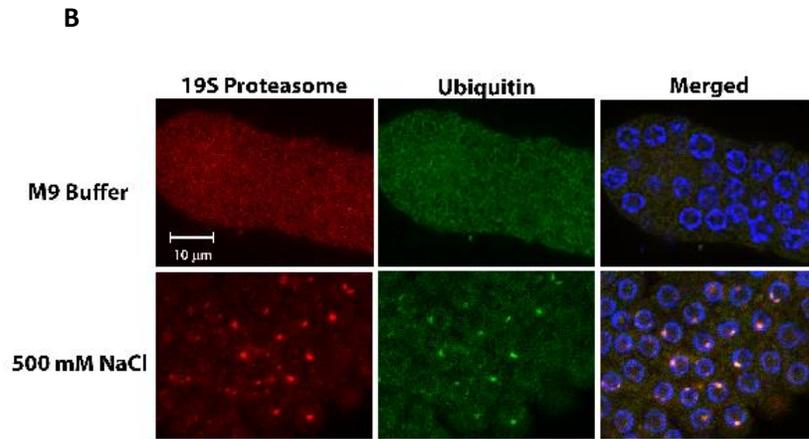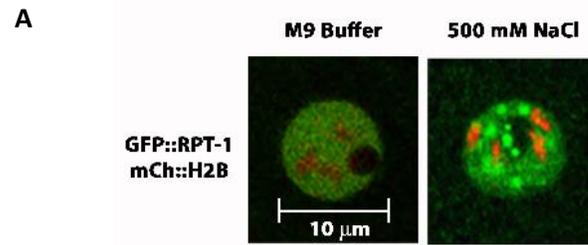
Figure 3.3: Stress Induces the Recruitment of the 26S Proteasome to SINGs

(A) Live imaging of RPT-1::GFP and mCh::H2B in proximal oocytes. In unstressed conditions (M9 buffer) proteasome remained diffuse in the cytosol and the nucleus (0/342 oocytes), but appeared more concentrated in the nucleus. Stressed conditions (500 mM NaCl) resulted in the rearrangement of proteasome into SINGs (117/342 oocytes). **(B)** Antibody staining of ubiquitin and 19S proteasome in the distal gonad. Gonads of unstressed and stressed young adult *C. elegans* were dissected out and stained with an ubiquitin antibody (green) and a 19S proteasome antibody (red). Both ubiquitin and proteasome where found to be diffuse within the nucleus in unstressed conditions (0/600 oocytes with SINGs), but relocalized into SINGs during salt stress (468/600 oocytes). **(C)** 20S proteasome subunit antibody staining. An antibody to the alpha 1 subunit of the 20S proteasome (green) was used to stain stressed (500 mM NaCl) and unstressed (M9) gonads. A region of the distal gonad is shown for each. In unstressed conditions, SINGs containing 20S proteasome do not form (10/200 oocytes). Under stressed conditions the 20S proteasome subunit colocalizes with K48 ubiquitin chains (red) in SINGs (153/200 oocytes). Statistical significance was calculated by a two-tailed z test: ***, $p < 0.0002$. Scale bar indicates 10 µm.

3.2.4 Ubiquitin Arrives to SINGs Before Proteasome

As ubiquitin is conjugated onto a substrate prior to its proteasomal degradation (Figure 1.4C), we evaluated the order by which ubiquitin and proteasome appears in SINGs. We conducted time-lapse studies of SING formation in stressed GFP::Ub and RPT-1::mCh worms. After data collection, individual frames were then assessed for the presence of either ubiquitin, proteasome, or both in SINGs. Results from the time-lapse images showed SINGs with either ubiquitin only or both ubiquitin and proteasome in SINGs, but not proteasomes at SINGs alone (Figure 3.4). This finding suggests that ubiquitin precedes proteasome in the formation of SINGs.
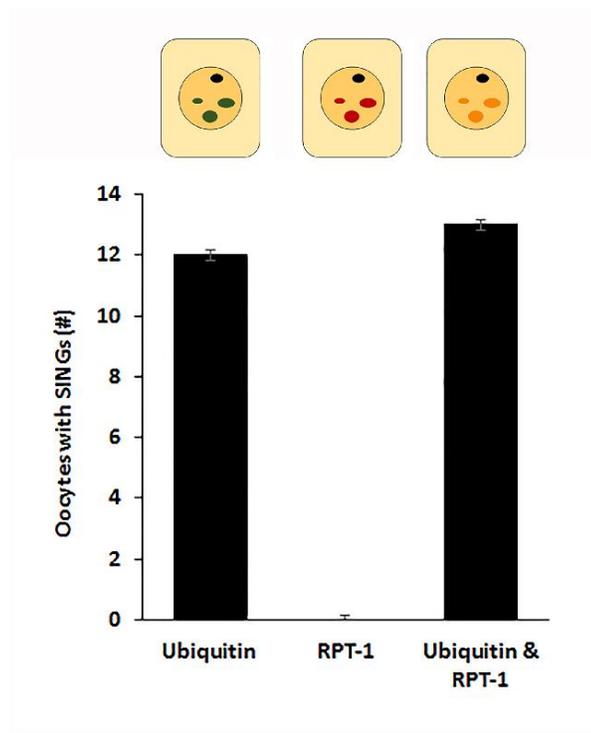
Figure 3.4: Ubiquitin Arrives to SINGs Prior to Proteasome

Time-lapse analysis of SINGs. Worms expressing GFP::Ub (green) and RPT-1::mCh (red) and soaked in 500 mM NaCl for 60 minutes were imaged for thirty minutes with an image taken every minute. When SINGs first appeared in the time-lapse series, they were assessed for the presence ubiquitin, RPT-1, or both ubiquitin and RPT-1. The numbers for each category are shown in the graph. RPT-1 alone was not observed at any of the initial SING sightings (0/25 SINGs). In comparison, SINGs with ubiquitin (12/25 SINGs) or both ubiquitin and RPT-1 (13/25 SINGs) were observed.

3.2.5 Ubiquitination is Required for SINGs to Form

Based on the presence of both ubiquitin and proteasome in SINGs, we wanted to determine whether ubiquitination was required to form SINGs. To answer this question, we performed three separate experiments. The first experiment was the knockdown of *uba-1* in GFP::Ub and RPT-1::mCh expressing worms. Stressed worms that were treated with control RNAi (vector only) expressed SINGs, whereas *uba-1* RNAi treated worms failed to form SINGs during stress (Figure 3.5A and 3.5B).

In addition to RNAi knockdown, we also used a temperature sensitive *uba-1 (it129)* worm strain. At lower temperatures (16 °C) no phenotype is present, but at higher temperatures an embryonic lethality phenotype appears. At higher temperatures ubiquitin is unable to conjugate onto a protein. To visualize SINGs in the temperature sensitive UBA-1 strain, we mated worms with RPT-1::mCh to the temperature sensitive E1 strain. At non-permissive temperatures (16 °C) SINGs were able to form during stress, but were not able to form under permissive temperatures (25 °C) (Figure 3.5C).

These results led us to investigate whether endogenous ubiquitin and proteasome formed SINGs in stressed temperature sensitive *uba-1* worms. Our data showed that only stressed wild type and control temperature sensitive (16 °C) worms expressed SINGs. However, temperature sensitive UBA-1 worms stressed at 25 °C did not show any appearance of SINGs (Figure 3.5D).

A

Vector   *uba-1* RNAi

500 mM NaCl

10μm

B

C

D

	19S Proteasome	Ubiquitin	Merged
Wild Type 500 mM NaCl			
uba-1 (it8ts) 16° C 500 mM NaCl			
uba-1 (it8ts) 25° C 500 mM NaCl			

10 μm
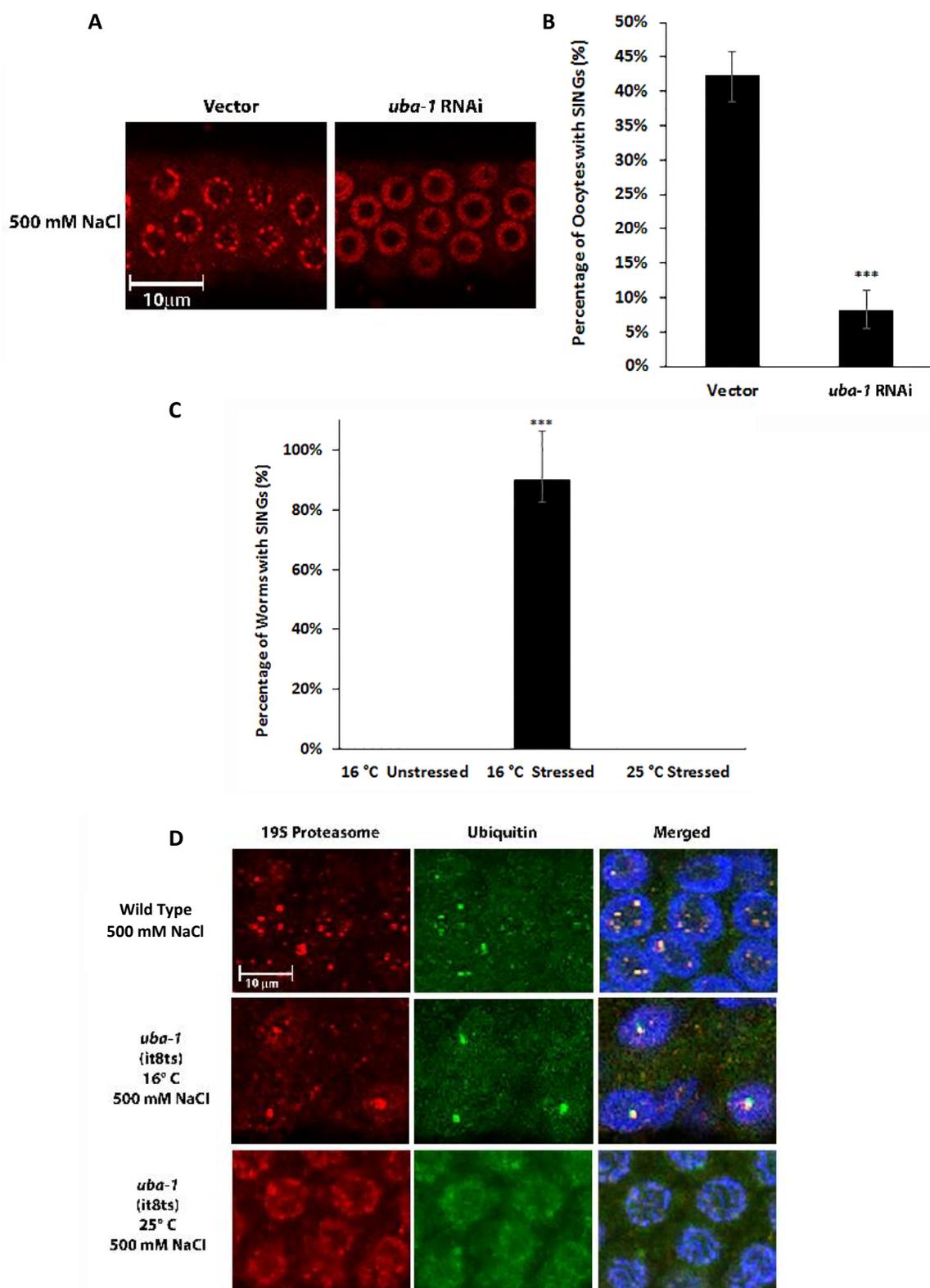
Figure 3.5: Ubiquitination is Required to Form SINGs

(**A**) Worms expressing RPT-1::mCh were subjected to *uba-1* RNAi for 24 hours prior to soaking in 500 mM NaCl for 60 minutes. The E1 enzyme, *uba-1*, is required for SING formation. (**B**) The percentage of oocytes forming SINGs after *uba*-1 RNAi treatment as described in A. Statistical significance was calculated by a two-tailed *z* test: ***, $p < 0.001$. (**C**) A temperature sensitive *uba-1* strain with an RPT::mCh tag was set at permissive and non-permissive temperatures prior to subjecting to salt stress. Unstressed worms at 16 °C and stressed worms at 25 °C showed not SING formation; whereas, the stressed 16 °C did exhibit SING formation. Statistical significance was calculated by fisher's exact test: ***, $p > 0.001$. (**D**) Antibody staining in *uba-1* mutants. Antibodies to ubiquitin and the 19S proteasome were used to stain wild type worms and a temperature sensitive mutant of *uba-1*. *uba-1* worms grown at 16 °C showed the presence of SINGs (551/600 oocytes) in response to salt stress (500 mM NaCl for 60 minutes). However, *uba-1* worms grown at 25 °C showed a reduction in SING formation (12/600 oocytes) when exposed to salt stress. Scale bar indicates 10 μm.

3.2.6 SING Formation is Dependent on Proteasome Activity

To determine whether proteasome activity is also required for the formation of SINGs by treating GFP::Ub and RPT-1::mCh transgenic worms with proteasome inhibitors (MG132, Bortezomib, and Lactacystin). Based on the result that ubiquitin arrives to SINGs prior to proteasome, we expected that inhibition of the proteasome would prevent proteasome localization to SINGs. However, our data show that in the presence of proteasome inhibitors neither ubiquitin-rich nor proteasome-rich SINGs formed during stress, whereas, osmotically stressed worms in the absence of proteasome inhibitors resulted in the appearance of SINGs (Figure 3.6A and 3.6B). This effect was unexpected, it is important to note that inhibition of the proteasome will reduce levels of free ubiquitin in the cell, which may partially explain this result.
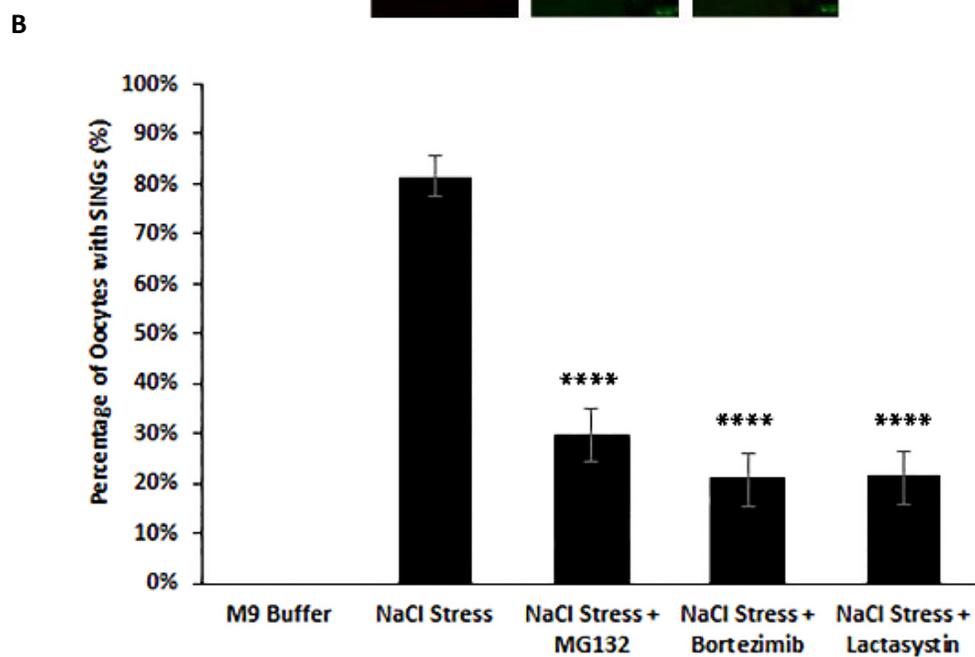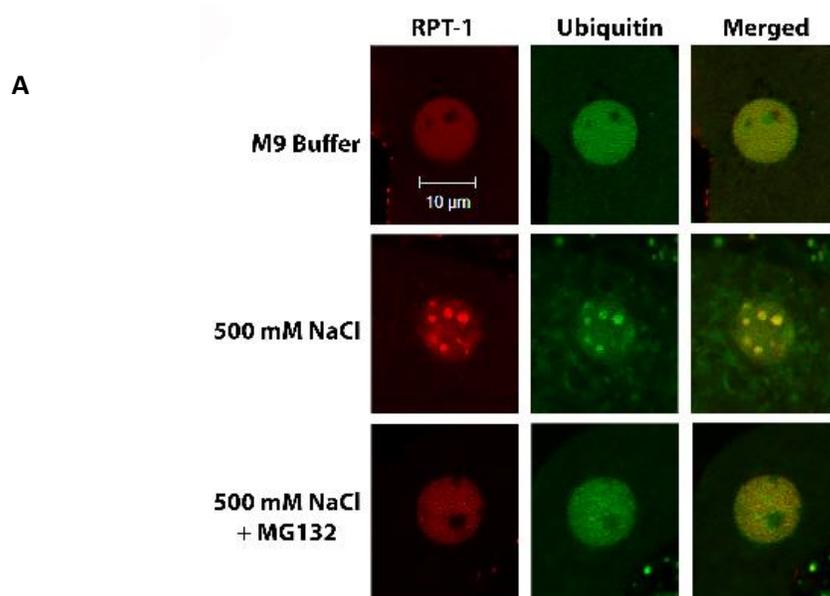
Figure 3.6: Proteasome Activity is Necessary for SING Formation

(A) Young adult *C. elegans* expressing GFP::Ub and RPT-1::mCh were either soaked in M9 buffer or 500 mM NaCl for 60 minutes. Worms soaked in M9 did not form SINGs. Under salt stress conditions, worms without the proteasome inhibitor MG132 formed SINGs, whereas, in the presence of MG132 SINGs did not form.   Scale bar indicates 10 μm.   **(B)** The percentage of oocytes forming SINGs after proteasome inhibitor treatment with MG132, Bortezomib, or Lactacystin. Statistical significance was calculated between salt stress and salt stress with proteasome inhibitor by a Fisher's Exact test: ****, $p <$ 0.0001.

3.2.7 Nuclear Import is Required to form SINGs

Section 1.3.4 mentioned that *S. cerevisiae* are known to degrade both nuclear and cytoplasmic proteins within the nucleus. Based on the studies done in *S. cerevisiae* and the observation that SINGs are strictly observed in the nucleus, we wanted to determine if cytoplasmic proteins contributed to the formation of SINGs during stress. To answer this question, the requirement for nuclear import in SING formation was tested by knocking down the three *C. elegans* importin genes (*ima-1, ima-2, and ima-3*) responsible for nuclear import (Figure 3.7A). Importin (IMA-1) is a protein that binds to the cargo protein located in the cytosol. Once bound, this complex can interact with the nuclear pore to pass through to the nucleus. After entry into the nucleus, Ran-GTP (RAN-1) induces IMA-1 to undergo a conformational change, which causes IMA-1 to dissociate from the cargo protein. The IMA-1 and RAN-1 complex then exits the nucleus back into the cytosol where they unbind. (Figure 3.7A) RNAi of *ima-1* showed a reduced number of nuclei with SINGs following stress treatment (Figure 3.7B and 3.7C). Ubiquitin levels in SINGs was more affected by *ima-1* RNAi knock down than proteasome.

Studies conducted in *S. cerevisiae* have shown that proteasome import is mediated by Arc3, an Arp2/3 homologue (Cabrera *et al.,* 2010). To test if this component is involved in the trafficking of proteasomes to SINGs, RNAi of *arx-5*, a homologue of Arp2/3, was performed on L4 larvae that expressed both GFP::Ub and RPT-1::mCh. Day 1 adult worms were then subjected to unstressed and stressed conditions. Results from this study show that *arx-5* RNAi reduced the levels of proteasome at SINGs (Figure 3.7B and 3.7C). In

addition to *arx-5*, we tested two other nuclear import components (Ran and SUMO) for their involvement in ubiquitin and proteasome localization to SINGs. Our results show that both *ran-1* (Ran) and *smo-1* (SUMO) RNAi reduced the number of nuclei with ubiquitin- and proteasome-rich SINGs (Figure 3.7B-3.7E).

A

B

| Vector | *ima-1* RNAi | *ran-1* RNAi | *arx-5* RNAi |

GFP:: Ub
500 mM NaCl

10 µm

C

D

| Vector | *smo-1* RNAi |

GFP:: Ub
500 mM NaCl

10 µm

E
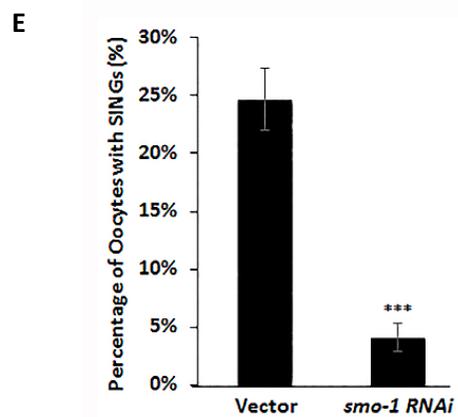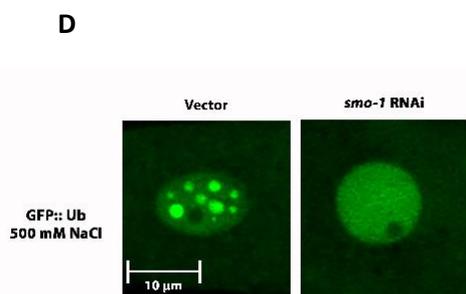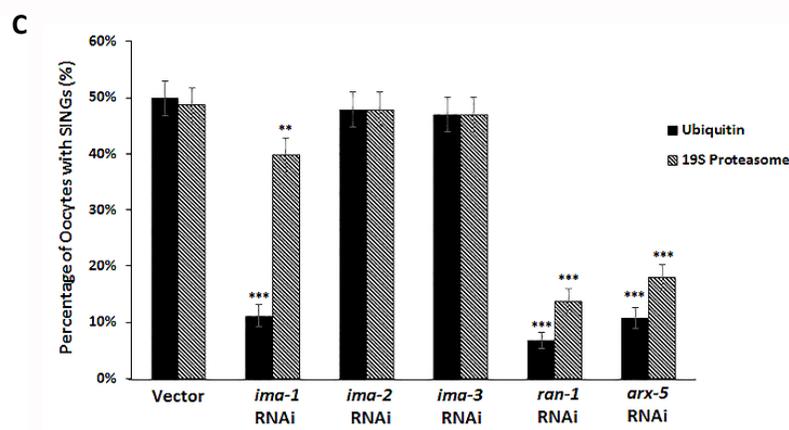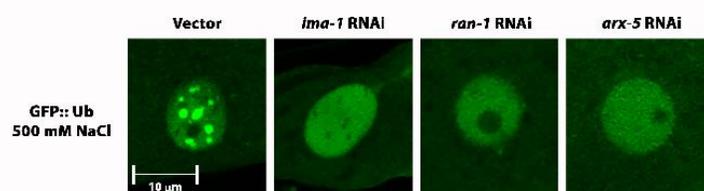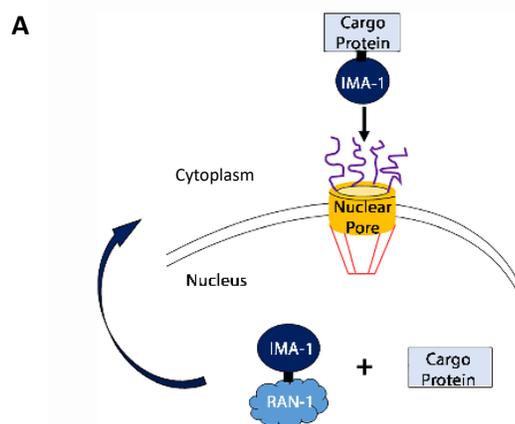
Figure 3.7: SINGs Formation Requires Nuclear Import

(A) Diagram of nuclear import. **(B)** RNAi of *ima-1, ran-1,* and *arx-5* reduces SING formation. Worms expressing GFP::Ub in the germline were soaked in 500 mM NaCl for 60 minutes. Proximal oocytes are shown. Control worms treated with vector RNAi formed SINGs normally. **(C)** The percentage of oocytes forming SINGs after treatment as described in B. Oocytes were scored for both GFP::Ub and RPT-1::mCh at SINGs.. **(D)** RNAi of *smo-1* reduces SING formation. RNAi of *smo-1* reduces SING formation in a worm strain expressing GFP::Ub in the germline. Proximal oocytes are shown. Scale bar indicates 10 µm. **(E)** The percentage of oocytes forming SINGs after treatment as described in D. Statistical significance was calculated by a two-tailed *z* test for C and E: **, $p < 0.01$; ***, $p < 0.001$.

3.2.8 *ubc-18, ubc-20/ubc-22,* and *chn-1* are Involved in SING Formation

We wanted characterized other features of the enzymatic pathway leading to the appearance of SINGs. As mentioned in Section 3.2.4, the E1 enzyme UBA-1 is required for SING formation. To determine which E2 enzyme was involved, an RNAi screen of the 24 E2 enzymes in *C. elegans* was performed by an undergraduate student (Mason Riley). GFP::Ub and mCh::H2B tagged worms were fed RNAi of vector or *uba-1* for 48 hours prior to salt stress. It was observed that a reduction in the number of nuclei with SINGs in

ubc-18 RNAi treated worms. This finding led us to hypothesize if *ubc-18* was also required in order for endogenous ubiquitin and proteasomes to be incorporated into/localize to SINGs during stress. Antibody staining for ubiquitin and proteasome (19S cap) was performed on wild type and *ubc-18* mutant worms. *ubc-18* mutant worms soaked in M9 buffer did not exhibited any SING formation (Figure 3.8A). However, stressed *ubc-18* mutant worms showed a significant decrease in the number of nuclei with SINGs when compared to the wild type stressed worms (Figure 3.8A). In addition to this result, we found two other E2 enzymes (*ubc-20* and *ubc-*22) that could potentially play a role in the formation of SINGs. We chose to test these two enzymes based off of the same E2 screen in which *ubc-18* was identified. In that screen, *ubc-20* and *ubc-22* only reduced the number of nuclei with SINGs by 30% and 29% (Mason Riley, personal communication). This partial reduction led us to investigate whether a knockdown of these two enzymes in combination would have an even greater influence on SING formation. We conducted a combination RNAi of both *ubc-20* and *ubc-22* in GFP::Ub and RPT-1::mCh transgenic worms and found that this significantly reduced the number of nuclei with SINGs compared to the stressed vector control (Figure 3.8B and 3.8C). However, the reduction that was seen in this combination was not as dramatic as the *ubc-18* result. *ubc-18* and *ari-1* are known to monoubiquitinate substrates (Rachel Klevit, personal communication). It is possible that *ubc-18* and *ubc-20/ubc-22* are working together to ubiquitinate substrates.

A unique feature of *ubc-18* that separates it from other E2s is its lack of reactivity to lysine, which makes the enzyme unable to function with many RING E3s. Further studies with *UBE2L3/ubc-18* has shown that this enzyme specificity interacts with HECT

and RBR E3 families (Wenzel et al., 2011). However, no reduction in SINGs were seen when the 16 HECT and 9 RBR E3s were individually knocked down. We did see a reduction in SING formation in a separate E3 screen when *chn-1* was knockdown with RNAi (Figure 3.8D and 3.8E). These experiments demonstrated that UBC-18, UBC-20/-22, and CHN-1 are involved in the formation of SINGs.

A

| 19S Proteasome | Ubiquitin | Merged |

Wild Type
500 mM NaCl

10 µm

ubc-18
(ku354)
M9 Buffer

ubc-18
(ku354)
500 mM NaCl

B

Vector | *ubc-20 & ubc-22* RNAi

500 mM NaCl
RPT-1:: mCh

10 µm

C

Percentage of Oocytes with SINGs (%)

***

Vector | *ubc-20 & ubc-22 RNAi*

D

Vector | *chn-1* RNAi

500 mM NaCl
RPT-1:: mCh

10 µm

E

Percentage of Oocytes with SINGs (%)

***

Vector | *chn-1* RNAi
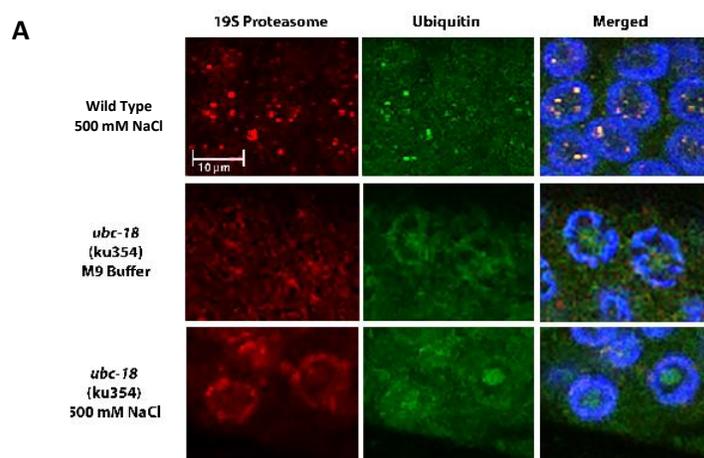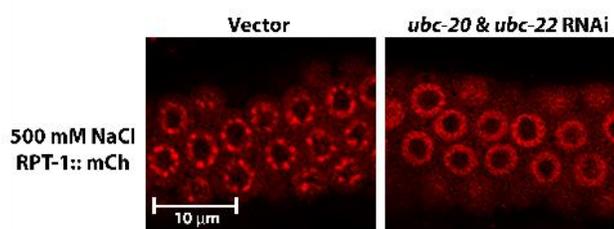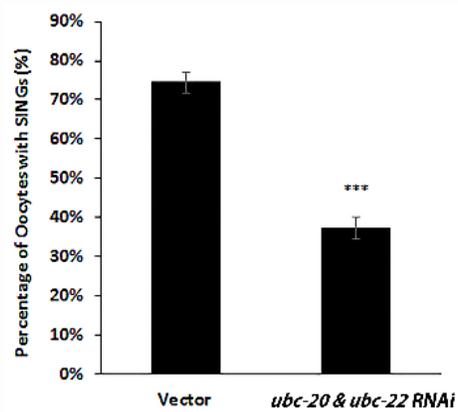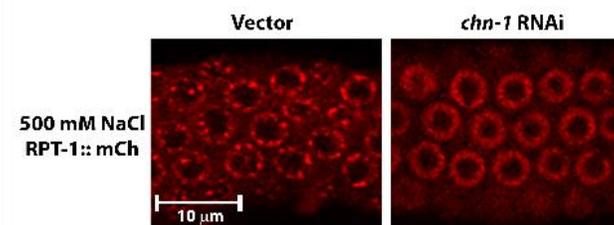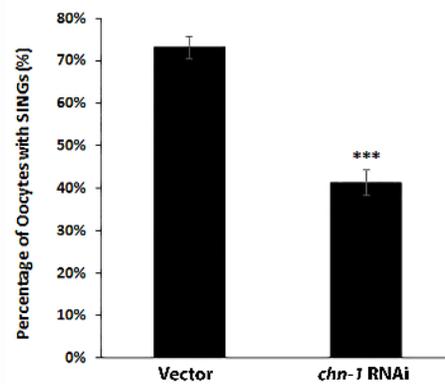
Figure 3.8: Ubiquitin Pathway Components Participating in SING Formation

(A) SINGs in *ubc-18* mutants. Antibodies to ubiquitin and the 19S proteasome were used to stain wild type worms and *ubc-18* mutants. SINGs were not induced in *ubc-18* mutants during salt stress (0/600 oocytes). **(B)** Worms expressing RPT-1::mCh were subjected to either control RNAi (vector) or RNAi of the *ubc-20* plus *ubc-22* E2 enzymes. This combined RNAi reduced the appearance of SINGs. **(C)** Quantification of the percentage of oocytes forming SINGs after treatment as described in B. **(D)** Worms expressing RPT-1::mCh were subjected to either control RNAi (vector) or RNAi of the *chn-1* E3 enzyme. Knockdown of *chn-1* reduced the appearance of SINGs. Scale bar indicates 10 μm. **(E)** Quantification of the percentage of oocytes forming SINGs after control RNAi and *chn*-1 RNAi treatment as described in D. Statistical significance was calculated by a two tailed *z* test: ***, $p < 0.001$. Scale bar indicates 10 μm.

3.2.9 Other Stressors Induce SINGs

To determine if SING formation can be induced by stressors other than high salt, day 1 adult worms expressing GFP::Ub and mCh::H2B were exposed to either 10 mM H_2O_2 for 60 minutes to induce oxidative stress or grown on media without peptone (bacteria food source) or bacteria (worm food source) to induce starvation conditions. In both conditions SINGs were induced in worms treated with control RNAi, and absent in *ubc-18* RNAi treated worms (Figure 3.9A and 3.9B). Our findings show that both oxidative stress and starvation are two other instances when SINGs are present. These findings provide evidence that SINGs may be involved in a general response to stressors that increase misfolded proteins or impair PQC.

Heat shock is another stress associated with misfolded proteins and is known to cause nuclear body formation. However, when worms expressing GFP::Ub and RPT-1::mCh or HSF-1::GFP (used as a control) were incubated at 37 °C for 1 hour to induce heat shock only the HSF-1::GFP worms formed HSF-1 nuclear stress granules (Figure 3.9C and 3.9D). These stress granules have been reported to form during heat shock and were selected to use as a positive control in this experiment (Morton and Lamitina, 2013). Although HSF-1 was not found to localize to SINGs, *hsf-1* was found to have a functional effect as described in the next section.

A

| | Vector | *ubc-18* RNAi |

10 mM H₂O₂
GFP::Ub
mCh::H2B

48 hr
Starvation
GFP::Ub
mCh::H2B

B

C

HSF-1:: GFP

D
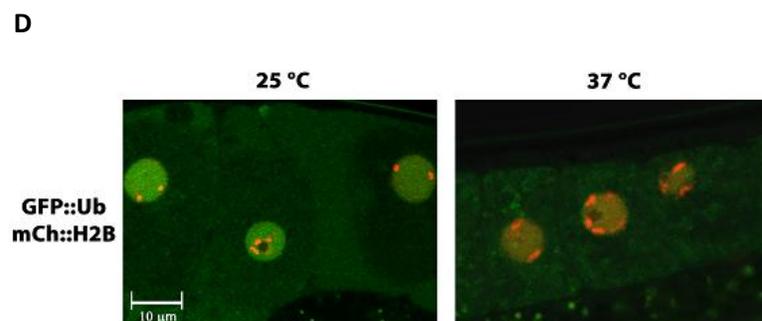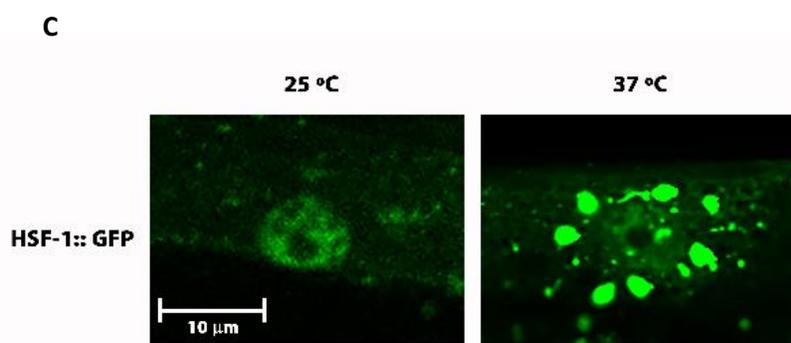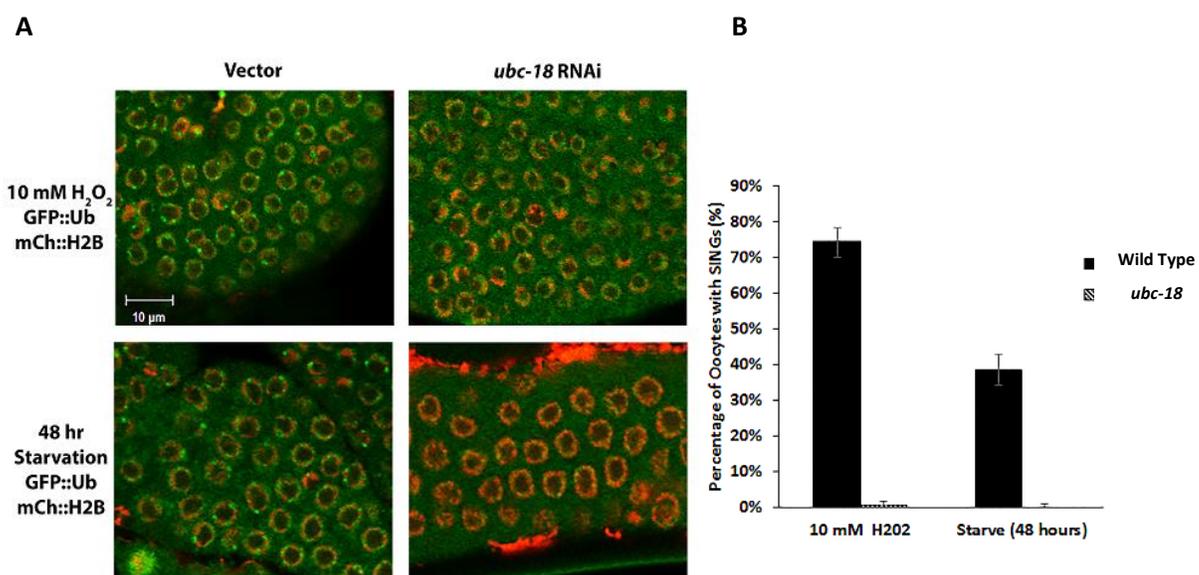
GFP::Ub
mCh::H2B

Figure 3.9: Oxidative Stress and Starvation Induce SING Formation

(A) Oxidative stress and starvation in gonads. Worms expressing GFP::Ub and mCh::H2B were grown on bacteria with control or *ubc-18* RNAi and subjected to 10 mM H_2O_2 for 30 minutes or starvation for 48 hours. Oxidative stress (145/250 oocytes) and starvation (164/250 oocytes) induced SING formation in vector treated worms. Distal gonads are shown. SINGs did not form in *ubc-18* worms soaked in H_2O_2 (0/250 oocytes) or starved (0/250 oocytes). **(B)** The percentage of oocytes forming SINGs in stressed vector and *ubc-18* treated worms salt stress treated worms as described in A. **(C)** Heat shock control forms HSF-1 nuclear granules after heat shock. HSF-1::GFP worms set at 37 °C showed nuclear granule formation following heat shock; whereas, worms set at 25 °C did not form granules. **(D)** Heat shock does not induce SINGs. Worms expressing GFP::Ub and mCh::H2B were subjected to heat shock by placing them at 37 °C for one hour. In control worms incubated at 25 °C for one hour, 0/600 oocytes showed SINGs. In the heat shock group, 0/600 oocytes showed SINGs. A total of 600 oocytes were collected from 2 independent experiments. Scale bar indicates 10 μm.

3.2.10 Heat Shock Reduces SINGs in an HSF-1 Dependent Manner

To determine if SING formation is a response to misfolded proteins, we tested whether increased chaperone expression induced by short heat pluses would influence SING formation. Prior to this experiment an GFP:: HSF-1 worm strain was used as a control to test for the increase expression of chaperones following heat shock. After 60 minutes of heat shock at 34 °C, GFP:: HSF-1 increased expression (Figure 3.10A). Based on these results, RPT-1::mCh expressing worms that were either treated with vector or were depleted of HSF-1 RNAi. These worms were maintained at either 25 °C or 34 °C for 60 minutes, followed by exposure to salt stress for 60 minutes. Worms that were depleted of HSF-1 RNAi expressed SINGs during stress, whereas, worms that were maintained at 34 °C and treated with empty vector prevented SING formation in the presence of stress (Figure 3.10B and 3.10C).

A HSP-70:: GFP 25º C 34º C

B Vector 500 mM NaCl 25° C 34° C 10 μm *hsf-1* RNAi 500 mM NaCl

C Percentage of Oocytes with SINGs (%) 70% 60% 50% 40% 30% 20% 10% 0% Vector *hsf-1* RNAi ■ 25° C ▨ 34° C *** **
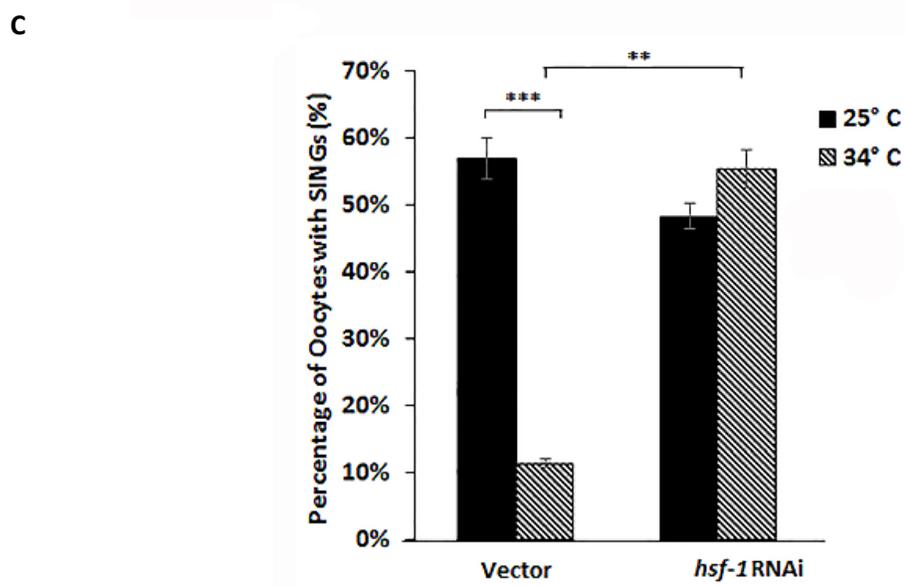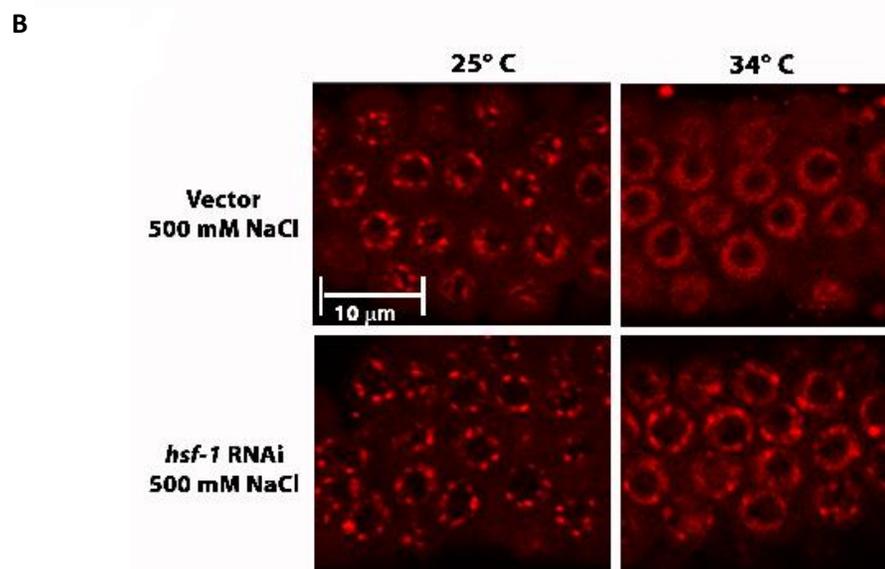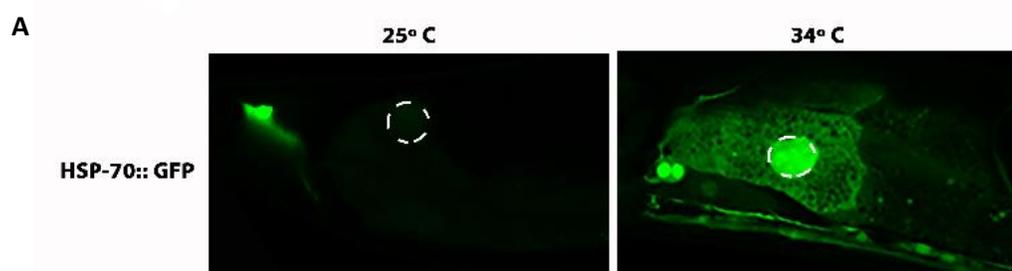
Figure 3.10: SING Formation Correlates with Reduced Protein Quality Control

(A) Live imaging of HSP-70::GFP in the intestine. GFP::HSP-70 expressing worms were exposed to heat shock at 34 °C for 60 minutes prior to imaging. Both control (25 °C) and heat shock worms (34 °C) showed HSP-70::GFP fluorescence in the cytoplasm and the nuclei. Heat shock treated worms exhibited a brighter fluoresce than control worms. The nucleus is outlined with an eclipse in worms for visualization. **(B)** Worms expressing RPT-1::mCh were incubated for 60 minutes at either 25 °C or 34 °C prior to soaking in 500 mM NaCl for 60 minutes. The brief heat shock reduced the occurrence of SINGs (x. When *hsf-1* was knocked down via RNAi, SING formation was normal even after heat shock. Scale bar indicates 10 μm. **(C)** The percentage of oocytes forming SINGs as described in B. Statistically relevant differences ***, $p < 0.0002$, and **, $p < 0.01$, two-tailed z test.

3.2.11 Older Reproductive *C. elegans* Form SINGs Earlier

PQC mechanisms are known to change with increased age (Section 3.1). Therefore, we investigated whether SING formation was influenced by age. Since adult hermaphrodites are only reproductively active for three days, we compared the timing of SING formation in day 1 adults to day 4 adults that expressed GFP::Ub and RPT-1::mCh. After salt stress treatment, the kinetics of SING formation of quicker in older adults. In day 4 adults, 21% of oocytes formed SINGs as early as 5 minutes post stress. At 30 minutes, when SINGs normally appear, only 16% of the oocytes formed SINGs. This experiment demonstrates that SING formation occurred at earlier time-points in older reproductively active worms than in young adults (Figure 3.11). These results suggest that SINGs are involved in PQC.
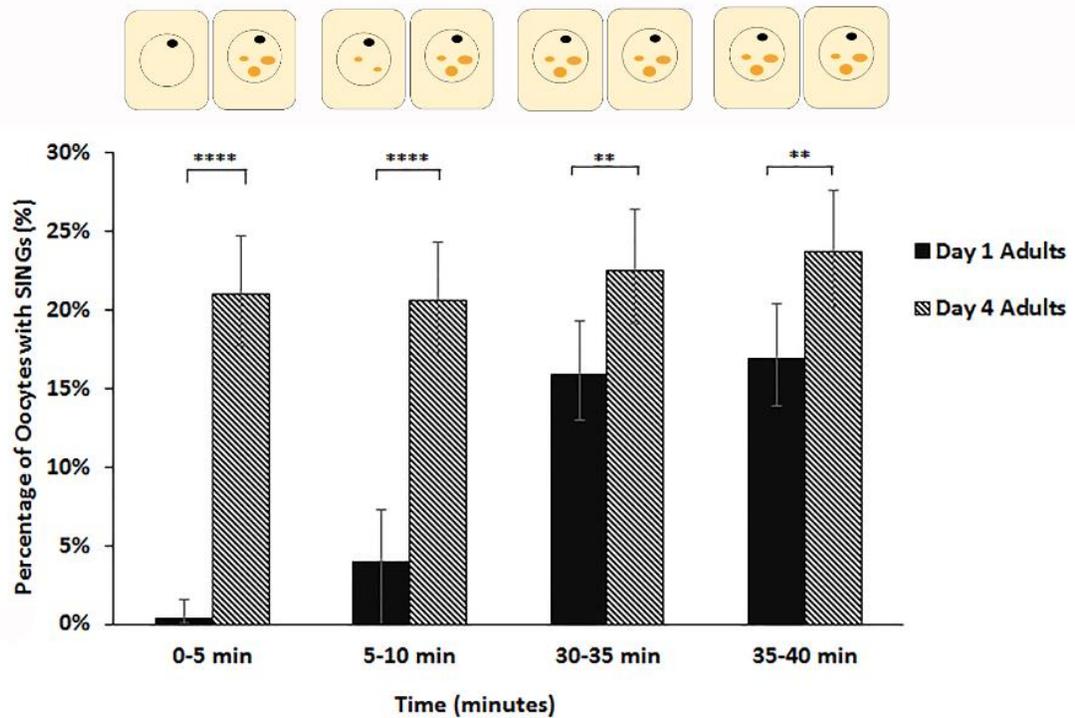
Figure 3.11: SING Formation is Rapidly Induced in Older Adults

Percentage of oocytes forming SINGs in day 1 and day 4 adults after exposure to 500 mM NaCl for the times indicated. Statistical significance was calculated by a Fisher's Exact test: **, $p < 0.01$ and ****, $p < 0.0001$.

3.3 Discussion

In this study, we addressed how stress affected nuclear UPS in *C. elegans.* Our results demonstrate a novel pathway in which environmental stress induces the redistribution of ubiquitin and 26S proteasome to distinct structures we call Stress Induced Nuclear Granules or SINGs. Since SINGs are characteristically present in *C. elegans* exposed to a range of stresses, including osmotic stress, oxidative stress, and starvation. We aimed to identify the molecular mechanisms responsible for forming these structures.

The GFP::UbAA experiment that indicated that ubiquitin conjugation was required for SING localization and the K48 antibody stain result showed that SINGs contain ubiquitin that is conjugated onto a substrate via K48 ubiquitin linkages. Based on the requirement for *uba-1,* GFP::UbAA, and the K48 antibody experiment, we conclude that SINGs are enriched in polyubiquitinated proteins and that they require ubiquitination to recruit ubiquitin and proteasome to SINGs. In addition to ubiquitination, proteasome activity is also required for both ubiquitin-rich and proteasome-rich SINGs to form. This finding was not expected because arrival of ubiquitin at SINGs was found to precede proteasome. Furthermore, ubiquitin-rich structures have been shown to form in other circumstances when UPS function is compromised, so the requirement for proteasome activity for SING formation was counter intuitive. The results from the proteasome inhibitor experiments are consistent with two possible mechanisms. The first scenario is that a proteolytic event proceeds the formation of SINGs, and the second scenario may be

that proteasome inhibition causes the reduction of the pool of free ubiquitin in the cell that would have been utilized in SING formation.

Our study also showed that nuclear import via *ima-1, ran-1,* and *smo-1* are necessary for SING formation. The observation that ubiquitin appears to be more affected by *ima-1* RNAi suggests a model in which ubiquitin is being shuttled into the nucleus. The result that *smo-1* RNAi affected SING formation was not surprising because SUMO is known to be involved in nuclear import of proteins (Gill, 2004b). These experiments indicate that nuclear import is required in the development of SINGs. However, it is unclear as to what is being imported into the nucleus that induces SING formation. It may be that either ubiquitinated substrates, proteasomes themselves, or an additional factor is being transported into the nucleus under stressed conditions to initiate the formation of SINGs.

The finding that increased chaperone expression prevents SING formation and that SINGs form more rapidly in older adults suggests that SINGs may be involved in a nuclear PQC pathway. These results are consistent with studies performed in *C. elegans* were PQC components such as chaperones were shown to decline with age (Ben-Zvi et al., 2009). We found that this PQC pathway requires the ubiquitin pathway components *uba-1, ubc-18, ubc-20/-22, chn-1* to form SINGs during stress.

C. elegans ubc-18 is similar to the *H. sapiens UBE2L3* gene. This gene is known for its role in cell cycle progression/regulation, ubiquitination of p105 (NFκB1, a p50 precursor), DNA repair, and mitophagy (Geisler et al., 2014; Han et al., 2014; Wenzel et

al., 2011). As mentioned previously, this enzyme is known to specifically interact with HECT and RBR E3 ligases (Wenzel et al., 2011). In our study, no one E3 was found to be required in SING formation, which suggesting that multiple E3s participate in SING formation. *ubc-20* and *ubc-22* are both similar to the *H. sapiens* gene *UBE2K*. This enzyme is capable to forming K48 linked chains and is known for its ability to target huntingtin protein for degradation (Haldeman et al., 1997). The finding that *ubc-18, ubc-20,* and *ubc-22* are required in SING formation during stress suggests that these enzymes are targeting proteins for proteasomal degradation.

In conclusion, our results suggest a model where environmental stress induces protein misfolding that promotes the ubiquitination of those proteins and localizes them to SINGs. Based on our findings, we propose that either protein degradation or protein sequestration occurs at SINGs. The identification and characterization of a PQC mechanism in the nucleus aid increases our general knowledge regarding the nuclear PQC in *C. elegans.* Future studies to determine the identity of these misfolded proteins that localize to SINGs and this will help to determine the function of these structures.

CHAPTER FOUR

DETERMINE THE IDENTITY OF THE PROTEIN

CONSTITUENTS OF SINGS

4.1 Introduction

Exposure to environmental stress can induce the appearance of distinct nuclear subdomains that include nuclear stress granules (nSGs) and nuclear stress bodies (NSBs). nSGs are induced by heat and have been found to contain ubiquitin, chaperones (HSF1 and HSF2), and pre-mRNA processing factors. They are considered to be discrete nuclear subdomains because they do not colocalize with other subnuclear bodies such as PML bodies. The function of nSGs are currently unknown; however, studies have suggested three possible functions (1) sites of storage or recycling of transcription factors, (2) areas formed to protect the genome from stress, and (3) sites of active transcription (Jolly et al., 1999, 2004; Rizzi et al., 2004). Similarly, NSBs are also known to react to stress by forming discrete structures within the nucleus. Numerous NSBs have been described and are defined by their key components, yet only a small subset are known to contain UPS machinery (Table 1). Currently, the function of NSBs is poorly understood; however, numerous functions have been proposed, which include acting as a general response to stress by sequestering factors that regulate gene expression, and playing a protective role to the cell by sequestering RNA or proteins during harmful conditions. The appearance of SINGs during stress has led us to investigate the protein constituents of SINGs in order

to determine which proteins are being targeted to these structures during stress and if SINGs are similar to other known nuclear bodies. Understanding what proteins localize to SINGs will aid in addressing their function(s) in the cell.

4.2 Results

4.2.1 Mass Spectrometry Data

In order to identify possible SING targets, protein lysates from unstressed and stressed worm lysates were sent to Cell Signaling Technology for mass spectrometry analysis. This company was chosen based on their ability to specifically immunoprecipitate peptides containing a di-Gly branch post tryptic digest, marking these out as sites of ubiquitination. We initially immunoprecipitated germline GFP::Ub in both unstressed and stressed conditions prior to sending the samples to Cell Signaling Technology. For unstressed conditions, worms were soaked in M9 buffer for 60 minutes prior to being spun down in a 1.5 mL Eppendorf tube. In stressed conditions, worms were soaked in 500 mM NaCl for 60 minutes prior to centrifugation. To confirm that we immunoprecipitated GFP-tagged ubiquitinated proteins from our samples and only heated the samples to 37 °C for 30 minutes prior to running an SDS-PAGE to prevent denaturation of GFP fluorophore. This temperature allowed for the GFP fluorophore to stay intact in the gel thus allowing the visualization of GFP using a typhoon scanner. In addition to imaging GFP fluorescence, we performed a silver stain on the gel to total proteins in each lane. Results from this showed that we were able to successfully immunoprecipitate GFP-tagged ubiquitinated proteins. This technique allowed for the GFP::Ub conjugates to be

pulled out of the all labeled tissues (reproductive tissue and embryos), but did not allow for the isolation of SINGs themselves. The mass spectrometry analysis yielded only 13 proteins total in both samples, with actin being the most abundant protein being detected in the stressed sample.

Since we did not have the ability to isolate SINGs themselves along with the observation that SINGs appear in four of the main tissues of the worm, we decided to send whole worm lysates for mass spectrometry analysis. Lysates were produced from salt stressed and control worms as described above and sent to Cell Signaling Technology. Prior to MS-MS analysis, Cell Signaling Technology subjected protein lysates to a di-Gly capture, which immopreciptated ubiquitin conjugates from all tissues (Figure 4.1A). To determine which proteins from the mass spectrometry results are targeted to SINGs, we filtered the list based on high abundance in order to increase the likelihood of finding SING targets. To prioritize hits from the mass spectrometry results, we filtered the protein list by the fold change, max intensity, and max coefficient of variation (% CV). Proteins were initially sorted by a fold change including only those proteins that were $\geq$ 2.5 fold in the stressed vs control sample. A high fold change indicates peptides were found to be more abundant in stressed conditions (high salt) than in control (M9 buffer). Next, the list was filtered by a max intensity of $\geq$ 15,000,000 AU. A high max intensity indicates the abundance of that peptide in the sample. Finally, the proteins were filtered by a low max % CV $\leq$ 20%, which is a measure of variation between the two mass spectrometry runs. The list of filtered proteins are represented in Table 3.

Since PAB-1(Poly (A)-binding protein) was our top hit from Table 3, we decided to look for the presence of PAB-1 in SINGs. This protein recognizes and binds to the 3'polyadenylated region of mRNA. Once bound to mRNA, this protein functions to stimulate translation of mRNA, poly (A) synthesis, and stabilizes the 3' polyadenylated region. PAB-1 is a cytosolic protein and is essential in the development of the postembryonic germline at all stages (Ko et al., 2013). PAB-1 is known to localize to RNP foci in oocytes during osmotic stress, heat shock, and anoxia (Jud et al., 2008). To test whether PAB-1 was present in SINGs, we performed live imaging on unstressed and stressed worms that express GFP::PAB-1 in the germline. PAB-1 appeared to be diffuse within the cytosol in both unstressed and stressed conditions (Figure 4.1B). Small foci located by the nuclear envelope were observed in both conditions, which is consistent with those from Jud et al (2008). No nuclear PAB-1 foci were found to form during either condition, indicating that PAB-1 does not localize to SINGs (Figure 4.1B).
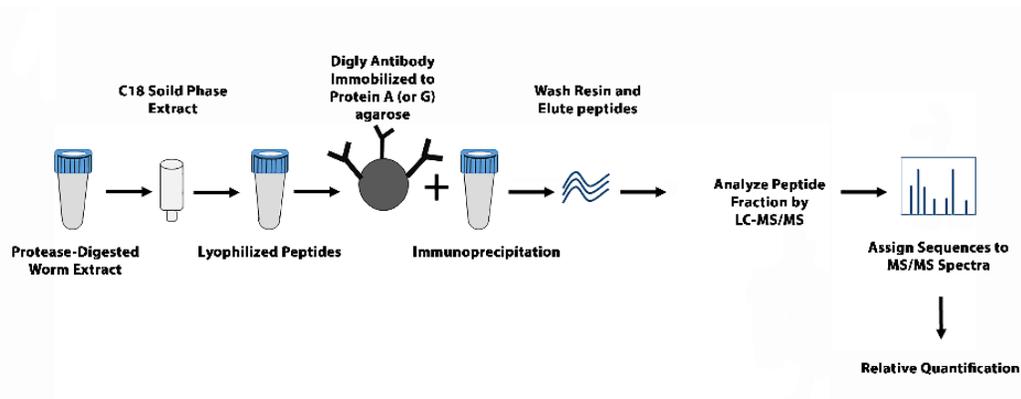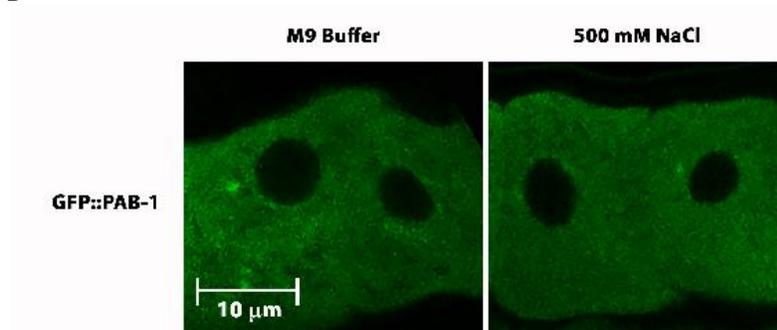
Figure 4.1: Mass Spectrometry Analysis on diGly Remnants

(A) Schematic diagram of how the mass spectrometry samples were processed at Cell Signaling Technology. Protease-digested worm extracts were concentrated and purified by C18 solid phase extraction and lyophilization. Samples were then exposed to an ubiquitin remnant K-GG motif antibody and immunoprecipitated. Resin and unbound protein were washed away. The samples were then analyzed by LC-MS/MS spectral analysis. **(B)** Live imaging of GFP::PAB-1 in the proximal gonad. Expression of GFP::PAB-1 appeared cytosolic in both unstressed (M9 buffer) and stressed (500 mM NaCl) worms (0/340 oocytes). Scale bar indicates 10 μm.

Table 3 List of Sorted Mass Spectrometry Results

Fold Change Condition B: A	Gene Name	Protein Name	Description
65.4	*pab-1*	**PolyA Binding protein family member**	Aid in Regulating mRNA and Translation
65.3	*syp-4*	**hypothetical protein H27M09.3**	Bridging paired meiotic chromosomes
37.6	*hcp-2*	**HoloCentric chromosome binding Protein family member**	Segregation of Meiotic Chromosome and Mitotic Sister Chromatids, Mitotic Spindle Organization, and Embryonic Development
32.4	*col-119*	**COLlagen family member**	Structural Unit of the Cuticle, Involved in Lipid Storage
23.6	*pod-2*	**Polarity and Osmotic sensitivity Defect family member**	in de novo Fatty Acid Biosynthesis, Embryonic Polarity, and Osmotic Protection of the Eggshell
20.3	*rpl-23*	**Ribosomal Protein, Large subunit family member**	Large Ribosomal Subunit
16.5	*R102.5*	**hypothetical protein R102.5**	Involved in Embryonic Development
11.6	*rpl-10*	**Ribosomal Protein, Large subunit family member (rpl-10)**	Large Ribosomal Subunit
11.4	*mlc-3*	**Myosin Light Chain family member (mlc-3)**	Normal Locomotion, Development before and after Fertilization
9.0	*cey-2*	**Y-box family member (cey-2)**	Bind DNA/RNA and Involved in Transcripition/Translation
8.7	*rps-14*	**Ribosomal Protein, Small subunit family member (rps-14)**	Component of the 40S Ribosome

		Table 3 (Cont.)	
5.9	*rpl-4*	**Ribosomal Protein, Large subunit family member (rpl-4)**	Large Ribosomal Subunit
5.6	*hpo-34*	**hypothetical protein F29G6.3**	Involved in Body Morphogenesis and Reproduction
5.3	*rpn-9*	**proteasome Regulatory Particle, Non-ATPase-like family member (rpn-9)**	19S Proteasome Subunit
5.2	*R07H5.8*	**hypothetical protein R07H5.8**	Involved in Endocytosis, Reproduction, Secretion, and Larval Development
5.1	*ngp-1*	**Nuclear/nucleolar GTP-binding Protein family member (ngp-1)**	Embryonic Development, Genitalia Development
5.1	*H43I07.3*	**hypothetical protein H43I07.3**	Glucosylation
5.0	*cdo-1*	**hypothetical protein F56F10.3**	Cysteine Catabolism
5.0	*Y48G8AL.13*	**hypothetical protein Y48G8AL.13**	Unknown Function
5.0	*Y48G8AL.13*	**hypothetical protein Y48G8AL.13**	Unknown Function
4.6	*col-133*	**COLlagen family member (col-133)**	Structural Unit of the Cuticle, Embryonic Development
4.5	*pas-2*	**Proteasome Alpha Subunit family member (pas-2)**	20S Proteasome Subunit
4.4	*rps-13*	**Ribosomal Protein, Small subunit family member (rps-13)**	Small Ribosomal Subunit
4.3	*F35G12.12*	**hypothetical protein F35G12.12**	Proteasomal Subunit

		Table 3 (Cont.)	
3.9	*rack-1*	**RACK1 (mammalian Receptor of Activated C Kinase) homolog family member (rack-1)**	Distal Tip Cell Migration, P Cell Nuclear Migration, and Normal Brood Sizes.
3.9	*rpn-3*	**proteasome Regulatory Particle, Non-ATPase-like family member (rpn-3)**	19S Proteasome Subunit
3.8	*rpa-0*	**Replication Protein A homolog family member (rpa-0)**	Acidic Ribosomal Subunit
3.6	*rpl-2*	**Ribosomal Protein, Large subunit family member (rpl-2)**	Large Ribosomal Subunit
3.3	*nlt-4*	**NOT-Like (yeast CCR4/NOT complex component) family member (ntl-4)**	Intracellular Lipid Transport
3.3	*eif-3.B*	**Eukaryotic Initiation Factor family member (eif-3.B)**	Involved in Apoptosis, Endocytosis, Reproduction, Lipid Storage, and Translation Initiation Activity
3.3	*unc-54*	**UNCoordinated family member (unc-54)**	Transcribes the Major Myosin Heavy Chain of Muscle in *C. elegans*
3.2	cth-2	**hypothetical protein ZK1127.10**	Unknown Function
3.2	rps-4	**Ribosomal Protein, Small subunit family member (rps-4)**	Small Ribosomal Subunit
3.2	C16A3.6	**hypothetical protein C16A3.6**	Involved in Embryonic Development, Genitalia Development, Larval Development, and Receptor-mediated Endocytosis
3.1	rpl-15	**Ribosomal Protein, Large subunit family member (rpl-15)**	Large Ribosomal Subunit
3.1	F45F2.10	**hypothetical protein F45F2.10**	Involved in reproduction and embryonic development

		Table 3 (Cont.)	
3.1	**ptr-23**	**PaTched Related family member (ptr-23)**	Aids in Transcribing Osmosensitive mRNAs during Osmotic Stress
3.1	**rpl-3**	**Ribosomal Protein, Large subunit family member (rpl-3)**	Large Ribosomal Subunit
2.8	**let-418**	**LEThal family member (let-418)**	Represses Germline-Specific Genes and Regulates Postembryonic Vulval Development
2.8	**pab-1**	**PolyA Binding protein family member (pab-1)**	Aid in Regulating mRNA and Translation
2.8	**C06A8.1**	**hypothetical protein C06A8.1**	Unknown Function
2.8	**yop-1**	**YOP (yeast membrane trafficking protein) homolog family member (yop-1)**	Involved in Trafficking of Membrane/Vesicles
2.7	**rps-1**	**Ribosomal Protein, Small subunit family member (rps-1)**	Small Ribosomal Subunit
2.7	**Y54E10BR.3**	**hypothetical protein Y54E10BR.3**	Predicted to E3 Ligase Activity (zinc ion binding activity)
2.6	**cdc-42**	**Cell Division Cycle related family member (cdc-42)**	Controls Polarity of Individual Cells and Embryogenesis by Regulating PAR Proteins
2.6	**F22F7.1**	**hypothetical protein F22F7.1**	Unknown Function
2.5	**fat-6**	**Fatty acid desaturase family member (fat-6)**	Involved in Fatty Acid Desaturation
2.5	**rpl-15**	**Ribosomal Protein, Large subunit family member (rpl-15)**	Large Ribosomal Subunit
2.5	**rpl-6**	**Ribosomal Protein, Large subunit family member (rpl-6)**	Large Ribosomal Subunit

4.2.2 TIAR-2 Localizes to SINGs during Stress

Next, we wanted to determine if SINGs were similar to other known nSGs. To answer this we looked for the localization of a stress granule component (TIAR-2) to SINGs during stress (Kedersha et al., 2005). TIAR-2 is known to form nuclear foci under osmotic stress (Jud et al., 2008). To address if TIAR-2 localizes to SINGs in the reproductive tissue, we used a GFP::TAIR-2 reporter worm strain. Unstressed worms displayed a diffuse GFP::TAIR-2 nuclear and cytoplasmic signal (Figure 4.2B). Upon the addition of salt stress, the GFP::TAIR-2 strain formed nuclear foci rich in TIAR-2 protein, which is constant with the literature (Figure 4.2B). TIAR-2 is the orthologue of the human TIA-1 and TIAL1 proteins, which have been implicated in reproduction and adult lifespan of *C. elegans*, hyperosmotic stress response, and heat shock response (Figure 4.2A) (Jud et al., 2008; Kedersha et al., 1999).

We next validated that TIAR-2 localizes to SINGs by conducting antibody stains of ubiquitin and 19S proteasome on GFP::TIAR-2 expressing worms. The reason why we chose to do antibody staining in transgenic worms was due to the fact that no commercially available antibody raised against TAIR-2 to detect the *C. elegans* orthologue of this protein. Results from the antibody stains show that GFP::TIAR-2 colocalizes with ubiquitin and 19S proteasome in SINGs (Figure 4.2C). Since SING formation requires ubiquitination and proteasome activity, we wanted to test whether if TIAR-2 localization required these activities. We performed *uba-1* RNAi and proteasome inhibitor experiments on GFP::TIAR-2 expressing worms. *uba-1* knockdown revealed that TIAR-2 does not form

nuclear spheres under salt stress conditions (Figure 4.2F). Proteasome inhibitor experiments were performed using 20 µM MG132 on GFP::TIAR-2 worms. These results demonstrated that the proteasome inhibitor treatment reduced the accumulation of TIAR-2 in the nucleus (Figure 4.2D and 4.2E). The ubiquitination and proteasome activity experiments, showed that TIAR-2 localizes to SINGs under salt stress.

TIAR-2

- Stablize RNA
- Regulating alternative and constitutive splicing events
- Regulate translation (Reduces ribosomal machinery during stress and cellular homeostasis)
- Apoptosis/Autophagy
- Embryonic Development
- Cell Poliferation
- Stress

GFP::TIAR-2

M9 Buffer   500 mM NaCl

10 μm

C

	19S Proteasome	GFP::TIAR-2	Merged
M9 Buffer			
500 mM NaCl			

10 μm

D

GFP:TIAR-2

500mM NaCl   500 mM NaCl + MG132

10 μm

E

F

Figure 4.2: SINGs Contain the TIAR-2 protein
(A) Diagram representing the different functions of TIAR-2. **(B)** Live imaging of GFP::TIAR-2 in oocytes. During unstressed conditions (M9 buffer) TIAR-2 was present in both the cytosol and the nucleus, but was more concentrated in the nucleus (1/340 oocytes). In stressed conditions (500 mM NaCl), TIAR-2 concentrated into distinct stress bodies (129/340 oocytes). **(C)** Antibody staining of 19S proteasome in GFP::TAIR-2 expressing worms. Worms expressing GFP::TIAR-2 were soaked in M9 or 500 mM NaCl for 60 minutes and then stained with an antibody to the 19S proteasome. In M9 treated worms, few oocytes showed nuclei with both TIAR-2 and proteasome colocalization (38/600 oocytes). Whereas, in salt stressed worms, the number of TIAR-2 and proteasome colocalization events increased (212/600 oocytes). **(D)** Day 4 adults were soaked in a watch glass containing for 500 mM NaCl with or without MG132 for 60 minutes. Worms that were not treated with MG132 showed TIAR-2 in SINGs, whereas MG132 treated worms showed fewer TIAR-2 containing SINGs. Scale bar indicates 10 µm. **(E)** Quantification of the percentage of TIAR-2 in SINGs as described in D. Statistical significance was calculated by a Fisher's Exact test: ****, $p < 0.0001$. **(F)** Graph representing the percentage of LAP::TIAR-2 in SINGs in vector and *uba-1* RNAi. Statistical significance was calculated by a two tailed *z* test: ***, $p < 0.001$.

4.2.3 NPPs, Tubulin, and PGL-1 are not Constituents of SINGs

In addition to PAB-1 and TIAR-2, we tested other proteins identified in the MS screen their aggregation or appearance in SINGs. Germline reporters of fluorescently labeled nuclear pore proteins (NPPs), tubulin, and P granule abnormality protein 1 (PGL-1) were subjected to salt stress. A total of four NPPs were tested for their aggregation in salt stress conditions. NPP-7, NPP-9, and NPP-10 were not found to react to salt stress. Whereas, NPP-1 reacted to stress by forming perinuclear foci that did not colocalize with SINGs (Figure 4.3A and 4.3B). GFP::tubulin in both unstressed and stressed conditions remained in the cytoplasm and under stress conditions expressed minor rearrangement (Figure 4.3D). In addition, PGL-1 protein was also not found to localize to SINGs under salt stress (Figure 4.3C). These experiments show that not all proteins are targeted to SINGs during stress.

A

NPP-1 NPP-7 NPP-9 NPP-10

M9 Buffer

10 µm

500 mM NaCl

B

M9 Buffer 500 mM NaCl

GFP::NPP-1
RPT-1::mCh

10 µm

C

M9 Buffer 500 mM NaCl

GFP::PGL-1

10 µm

GFP::Tubulin
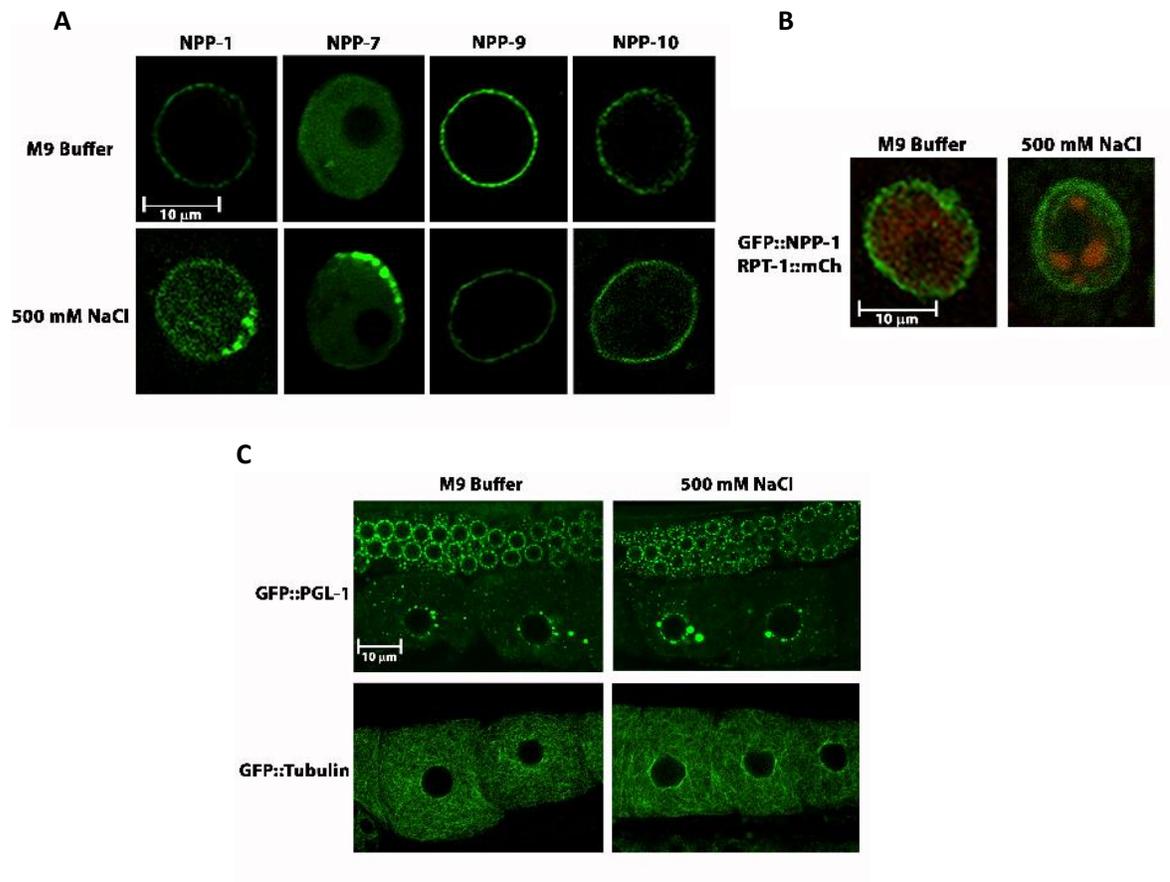
Figure 4.3: Nuclear Pore Proteins, Tubulin, PGL-1, and SMO-1 do not Localize to SINGs during Salt Stress

(A) Worm strains expressing GFP::NPP were exposed to both M9 buffer and 500 mM NaCl for 60 minutes. The NPPs responded to stress by occasionally forming concentrated areas of protein at the periphery of the nucleus: NPP-1 (19/250 oocytes) and NPP-7 (14/250 oocytes). A total of 250 oocytes were collected 10 worms. **(B)** NPP-1 was crossed into a RPT-1::mCh expressing worm and then subjected to unstressed and salt stressed conditions. SINGs were not found to colocalize with NPP-1 (48/50 oocytes). A total of 50 proximal oocytes were collected from 10 worms. **(C)**. Tubulin and PGL-1 do not localize to SINGs during salt stress. GFP::tubulin worms were soaked in M9 buffer or 500 mM NaCl for 60 minutes and then observed under confocal microcopy. Both unstressed and stressed GFP::tubulin did not localize to SINGs (50/50 oocytes). A total of 50 oocytes were collected from 10 worms. Minor rearrangement of cytoplasmic tubulin was seen in stressed GFP::tubulin populations. GFP:: PGL-1 worms were soaked in M9 buffer or 500 mM NaCl for 60 minutes and then observed under confocal microcopy. Both unstressed and stressed GFP::PGL-1 did not localize to SINGs (240/240 oocytes). A total of 240 oocytes were collected from 6 worms. Scale bar indicates 10 µm.

4.2.4 SING Formation is Independent of SKN-1

SINGs are induced by oxidative stress, which leads us to consider that SINGs may be involved in the oxidative stress pathway. Nuclear factor (erythroid-derived2)-like 2 (Nrf2) is a transcription factor that is known to transcribe genes involved in superoxide metabolism during oxidative stress to protect the cell (Ma, 2013). The worm homolog of Nrf2 is SKN-1 (SKiNhead). To investigate whether SKN-1 is required to form SINGs under oxidative stress, antibody staining of ubiquitin and 19S proteasome was performed on stressed wild type and *skn-1 (zu129)* mutants. *skn-1* mutants and wild type worms formed SINGs in response to both osmotic and oxidative stress (Figure 4.4). This result indicates that the appearance of SINGs under both types of stress are operating under a separate stress pathway that is independent of *skn-1*.
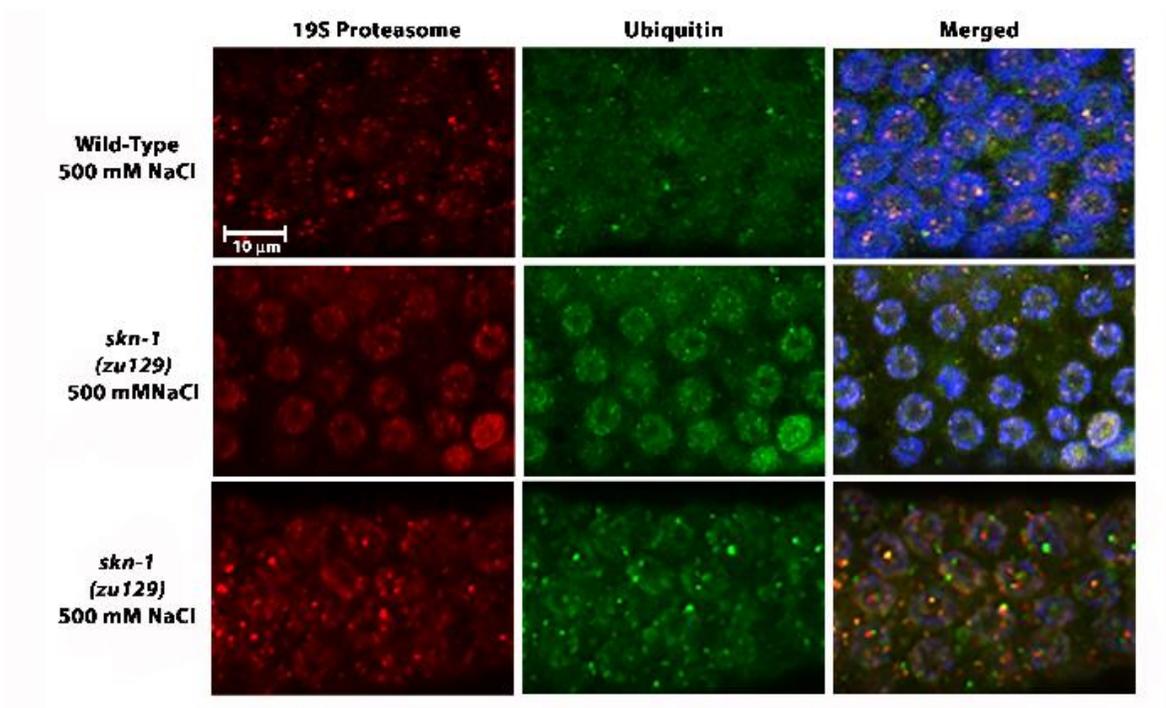
Figure 4.4: *skn-1* **is not Required for SING Formation**

Antibody staining was conducted on dissected gonads from *skn-1*(*zu129*) mutants or their heterozygous siblings. Worms were subjected to 500 mM NaCl for 60 minutes or 10 mM H_2O_2 for 30 minutes prior to dissection and staining. Gonads from heterozygous worms (7/100 oocytes) or *skn-1* mutants (7/100 oocytes) soaked in M9 were absent of SINGs. Heterozygous worms soaked in 500 mM NaCl (96/100 oocytes) or 10 mM H_2O_2 (83/100 oocytes) have SINGs as expected. *skn-1* (*zu129*) worms soaked in 500 mM NaCl (78/100 oocytes) or 10 mM H_2O_2 (74/100 oocytes) also have SINGs. A total of 600 oocytes were collected from 2 independent experiments. Scale bar indicates 10 µm.

4.2.5 SINGs are Distinct Nuclear Bodies

Numerous discrete structures are known to form in the nucleus under stress conditions and among them include protein aggregates and nuclear bodies. Protein aggregates are characterized as being poorly soluble, visible with microscopy, increase during stress, and are relatively immobile. Based on literature, one method to detect if SINGs are protein aggregates is to see if they are mobile by using a method known as FRAP (fluorescent recovery after photobleaching) (Brignull et al., 2006; Iliev et al., 2006). This technique allows a user to photobleach fluorophores within a select area of a cell and observe if any fluorescence comes back to the area as a consequence of the diffusion or trafficking of unbleached fluorescent proteins into the bleached area. In this way, FRAP enables the measurement of protein diffusion/mobility rates within live cells. In order to determine if SINGs were sites of protein aggregation that arise in response to stress, we conducted FRAP analysis on SINGs (GFP::Ub) and compared the behavior to a protein aggregate control (Q82::GFP) that is based on the Huntington protein. For the control strain, Q82::GFP is expressed in the muscle and encodes 82 glutamine residues attached to GFP that are known to form protein aggregates in the cytoplasm (Morley et al., 2002). Based on the results of the FRAP analysis, SINGs showed a higher mobility than the Q82::GFP cytoplasmic muscle aggregates, which showed minimal recovery post-bleach (Figure 4.5A).

Many nuclear bodies are known to appear during stress and even contain components of the UPS. One nuclear body known to form during stress and contain both ubiquitin and

proteasome is PML bodies. Two identifying components of PML bodies are SUMO and PML proteins. To investigate whether SINGs are similar to PML bodies, we performed live imaging on unstressed and stressed worms expressing GFP::*smo-1* (SUMO). After being osmotically stressed, GFP::*smo-1* remained diffuse and did not form any concentrated regions of observable SUMO (Figure 4.5B). In addition to live imaging, we performed a BLAST search and did not find a worm homologue of the PML protein.

There are other NSBs that have been shown to contain RNA. We wanted to investigate whether SINGs contained RNA by using a SYTO14 stain. This stain is used to detect the presence of both DNA and RNA when excited at a certain wavelength. In both unstressed and stressed worms the SYTO14 stain localized to the nucleoli and DNA, but was not found to be concentrated in other regions of the nucleus (Figure 4.5C).
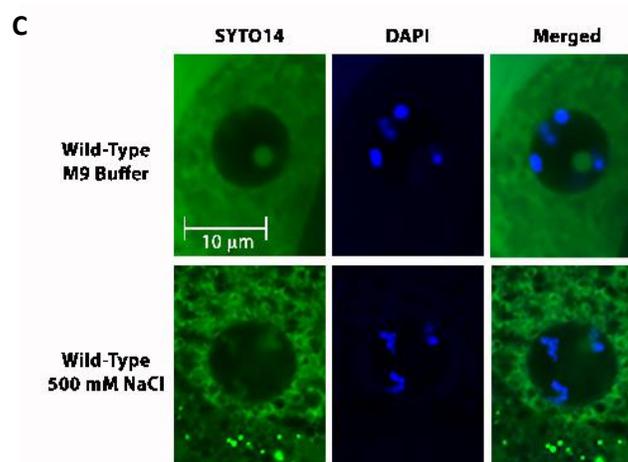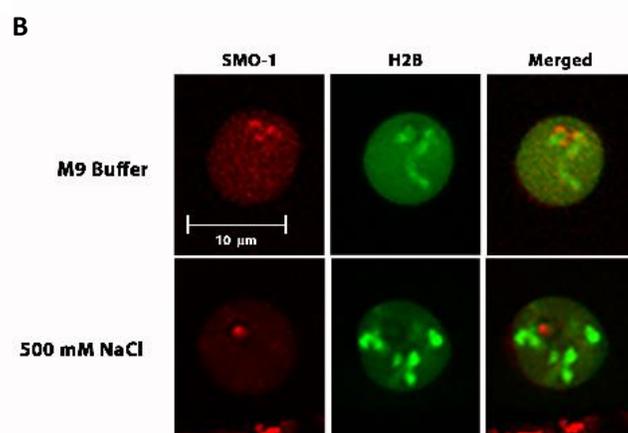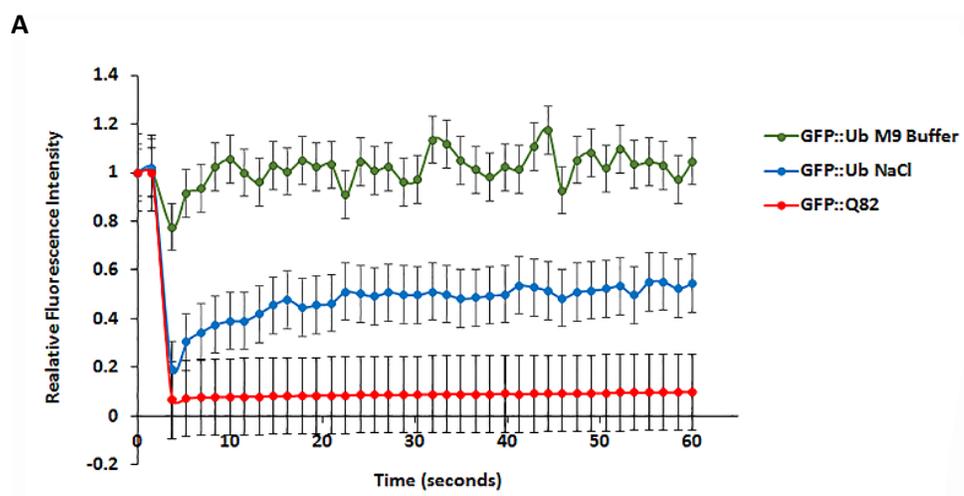
Figure 4.5: SINGs are Distinct Nuclear Bodies

(**A**) FRAP analysis of Q82::GFP in muscle cells compared to GFP::Ub in the nuclei of salt stressed oocytes. The Q82::GFP shows little recovery of fluorescence over a one minute period, whereas, GFP::Ub in SINGs recovers to approximately 50% of initial level after one minute. Graph shows the data from 10 individual FRAP experiments with standard errors indicated. A total of 10 SINGs were derived from proximal oocytes collected from 3 independent experiments. (**B**) Worms expressing GFP:: H2B and mCh:: *smo-1* were soaked in M9 and 500 mM NaCl for 60 minutes. Nucleolus showed SMO-1 localization in control and salt stress groups, but did not localize to SINGs (80/80 oocytes). A total of 80 proximal oocytes were collected from 2 independent experiments. (**C**) SYTO14 staining in wild type worms. In both unstressed and stressed worms, SYTO14 was found to colocalize with the histones and be concentrated within the nucleolus and the cytoplasm of the oocyte (80/80 oocytes). A total of 80 proximal oocytes were collected from 2 independent experiments. Scale bar indicates 10 µm.

4.3 Discussion

The goal of this study was to identify proteins that localize to SINGs and determine if SINGs are novel NSBs. To address these questions, we performed mass spectrometry analysis and tested worm strains with fluorescently labeled proteins. The findings from this study concluded that SINGs are novel NSBs that were found to contain TIAR-2 in the presence of stress.

Based on the PGL-1, tubulin, and NPP data, SING formation is not a general response for all proteins within the oocyte. In addition, FRAP analysis demonstrated that GFP::Ub recovered more readily than the protein aggregate control. This finding suggests that SINGs are dynamic and rapid protein exchange is occurring. Therefore, SINGs are not likely to be sites of protein aggregation or failed protein degradation as seen for some structures such as Lewy bodies. SINGs appear to be similar to PML bodies and clastomes due to the presence of ubiquitin and proteasome during stress. However, our data shows that SINGs contain no noticeable levels of RNA or SUMO. BLAST results also indicated that worms do not have a homologue of the PML protein. RNA, SUMO, and PML protein are all found to localize to PML bodies. As previously mentioned, SINGs do not form in response to heat shock, which also distinguishes SINGs from PML bodies and clastomes. Based on these findings, we believe that SINGs are not protein aggregates and that they are distinct from other known NSBs.

Results from the mass spectrometry data indicated that PAB-1 was ubiquitinated more during stress. However, we found that PAB-1 did not appear to localize to SINGs

under stress. This result may be due to the low presence of PAB-1 in SINGs or that it is being quickly degraded. Future studies will address whether PAB-1 is being quickly degraded by soaking GFP::PAB-1 worms in MG132 prior to stress exposure. Since, PAB-1, did not appear to localize to SINGs under stress, we decided to compile a list of possible proteins targets that either had a fluorescent label or a reliable antibody available. Currently, we have two possible proteins (SYP-4 and CDC-42) that either have an antibody or transgenic worm strain available. Future experiments will be geared towards discovering if these proteins localize to SINGs during stress.

PAB-1 and TIAR-2 are both stress granule markers and are known to localize to RNPs (Large ribonucleoprotein) during heat shock, anoxia, and arrested ovulation. However, under salt stress only TIAR-2 is known to form nuclear foci, which we have reproduced in the lab (Jud et al., 2008). The antibody staining and the proteasome inhibitor results provide evidence that TIAR-2 localizes to SINGs during stress. In conclusion, our findings suggests a novel pathway where misfolded proteins induced by stress undergo proteolysis at SINGs, providing evidence that SINGs are playing a role in the nuclear PQC.

CHAPTER FIVE

CHARACTERIZATION OF THE PROPERTIES OF SINGS IN DIFFERENT TISSUE TYPES

5.1 Introduction

According to the Centers for Disease Control and Prevention, 6.7 million women are affected by impaired fecundity in the United States (Winkelman et al., 2016). Impaired fecundity can be contributed to many factors, but an important one to consider is environmental stress. Common stressors that have been attributed to decreased fecundity include oxidative stress, osmotic stress, and starvation. One study showed that starving pregnant mice for 48 hours at various time points during their pregnancy resulted in miscarriages (Wood, 2003). Similar results were seen in *C. elegans*, where if food was withheld from the organism reproductive processes such as oogenesis, egg production, and egg laying were delayed (Seidel and Kimble, 2011). Oxidative stress is thought to be another causative agent of infertility and has been shown to affect fertility in both natural and assisted pregnancies (Agarwal et al., 2014; Ruder et al., 2009). The role of oxidative stress in infertility is not understood completely; however, there seems to be a correlation between increased reactive oxidation species (ROS) and infertility in both males and females (Agarwal et al., 2005). Another stress that is known to affect assisted pregnancies is salt stress. An example of this can be see with cryopreserved gametes, embryos, and sperm which often experience salt stress during thawing procedures (Hammadeh et al., 1999).

The studies that have been conducted with these stressors have been focused on aging, stress tolerance, and fecundity. Currently, it is known that stress can have a physiological response such as extended lifespan or reduced fecundity, but it is unclear as to what happens at a cellular level during stress. Understanding how the organism is affected as a whole and at a cellular level during environmental stress is important for preventing/treating infertility. The stressors discussed in this section are all associated with protein damage, which is thought to be a contributing factor of infertility. We aim to investigate the downstream consequences of SING formation by looking at adult lifespan, cell division, and embryo viability in *C. elegans.*

5.2 Results

5.2.1 SINGs Persist in Reproductive Tissue but not in Muscle or Intestine

Unpublished data from the Boyd lab showed that similar ubiquitin-rich nuclear bodies formed during stress in the muscle (Jacob Sanders) and intestine (Lynn Boyd), indicating that this event may not be constrained to the germline and may be a general response to cellular stress. We wanted to address whether SINGs persisted in each of these three tissues. Results from this experiment showed that the SINGs in the germline persisted for over 72 hours; whereas both muscle and intestine SINGs disappeared within 24 hours after initial SING formation (Figure 5.1A). Additional studies using the intestinal GFP::Ub expressing strain showed that *ubc-18* is required in the formation of ubiquitin-rich nuclear bodies during stress. This result indicates that the nuclear bodies seen in the intestine are similar to the SINGs that form in the reproductive tissue (Figure 5.1B and 5.1C).

A

B

| Vector M9 Buffer | Vector 1 M NaCl | *ubc-18* RNAi 1 M NaCl |

GFP::Ub

10 μm
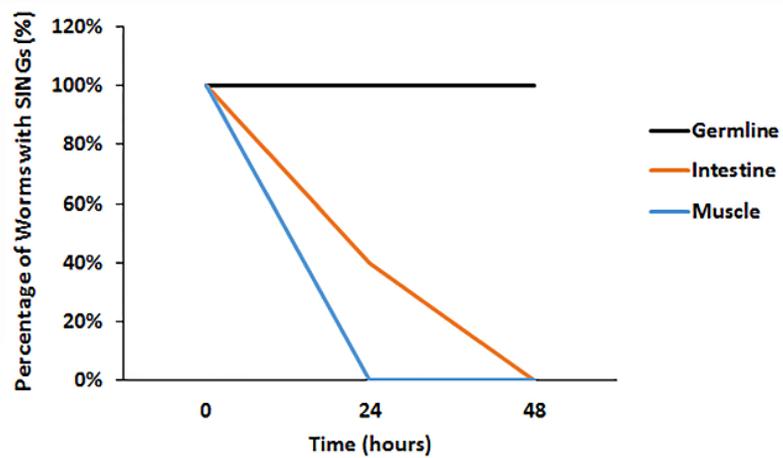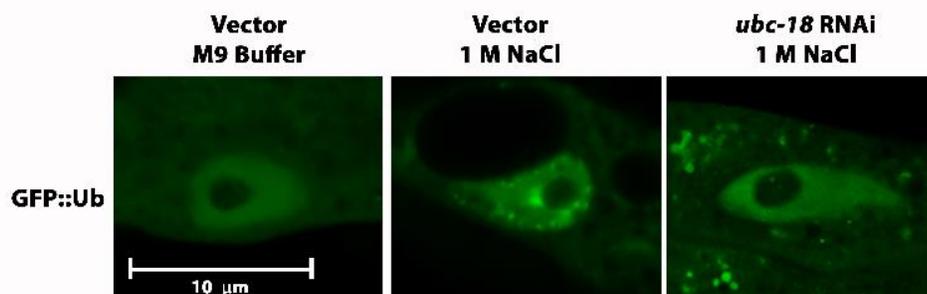
C
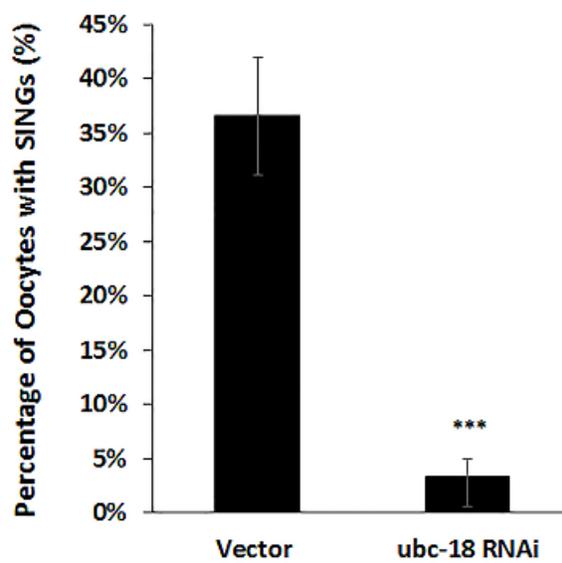
Figure 5.1: Other Tissues Form SINGs

(**A**) Graph represents the percentage of worms with SINGs at 0, 24, and 48 hour time points. $n = 10$ worms. SINGs were present in 10/10 worms for each tissue at time zero. At 24 and 48 hours, SINGs were still detected in the germline. The intestine had a reduced number of SINGs present at 24 hours (4/10 worms), and had no SINGs present at 48 hours. The muscle recovered within 24 hours after stress. (**B**) Live imaging of GFP::Ub in the intestine. In unstressed vector and *ubc-18* RNAi GFP::Ub appeared diffuse in the cytoplasm and the nucleus. Under salt stress, GFP::Ub concentrated into spheres within the nucleus. Scale bar indicates 10 µm. (**C**) Quantification of the percentage of GFP::Ub in spheres as described in B. Statistical significance was calculated by a Two tailed *z* test: ***, $p < 0.001$.

5.2.2 Embryos with SINGs Fail to Hatch

The appearance of SINGs in multiple tissues led us to investigate whole organism consequences of SING formation by observing changes in lifespan and reproductive success. Lifespan assays were performed by Mason Riley (Undergraduate) and showed that lifespan of stressed L4 larvae remained unchanged. This result suggests that exposure to salt stress prior to adulthood had no noticeable effect on adult lifespan.

Since SINGs appear in both osmotic and oxidative stressed embryos, we wanted to determine if the reproductive success of an organism was altered by the formation of SINGs. We performed embryonic lethality assays on unstressed (M9 buffer) and stressed (500 mM NaCl) embryos expressing GFP:Ub and mCh::H2B. Embryos were extracted from unstressed and stressed adult worms. Embryos were then checked for the presence of SINGs, and observed at 48 hours for hatching. Embryos that contained SINGs failed to hatch (0%), whereas, unstressed and stressed embryos that did not contain SINGs successfully hatched (100%) (Figure 5.2). Based on the presence of stressed embryos without SINGs, we performed a separate experiment on ten worms to determine what percentage of embryos formed SINGs. The small scale study revealed that 22/38 embryos (58%) of the stressed embryos formed SINGs. The aforementioned results suggest that salt stress does not perturb the lifespan of the organism but there is a correlation between the presence of SINGs and reduced reproductive success.

Based on the presence of SINGs in gonadal tissue, we wanted to know whether oocytes that had SINGs were able to be fertilized. Day 1 adults were exposed to M9 buffer

or 500 mM NaCl for 60 minutes and then moved to a fresh NGM plate to lay eggs at 0, 6, 12, and 16 hours. The numbers of eggs laid and hatched were recorded at 48 hours. M9 treated worms at each time-point had a higher number of eggs laid and hatched than the salt stressed group. In the salt stressed treated group, the number of eggs laid increased over time. This data suggests that some oocytes with SINGs are able to be fertilized (Figure 5.2). The aforementioned results suggest that salt stress does not perturb the lifespan of the organism but there is a correlation between the presence of SINGs and reduced reproductive success.

A
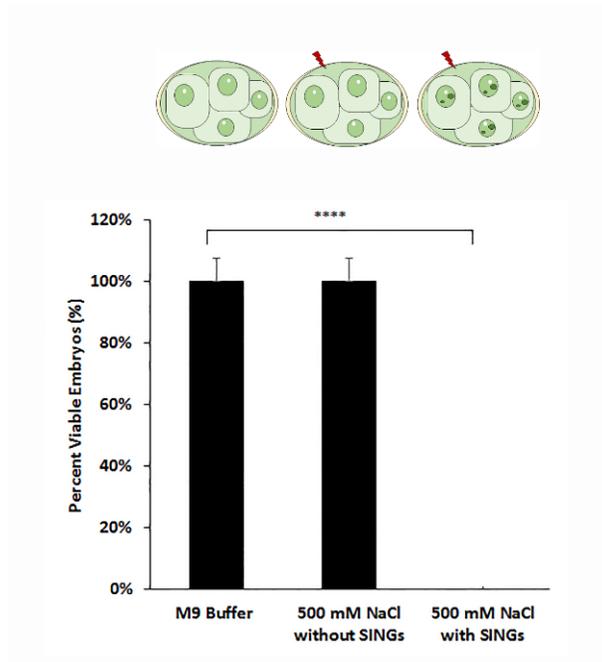
B
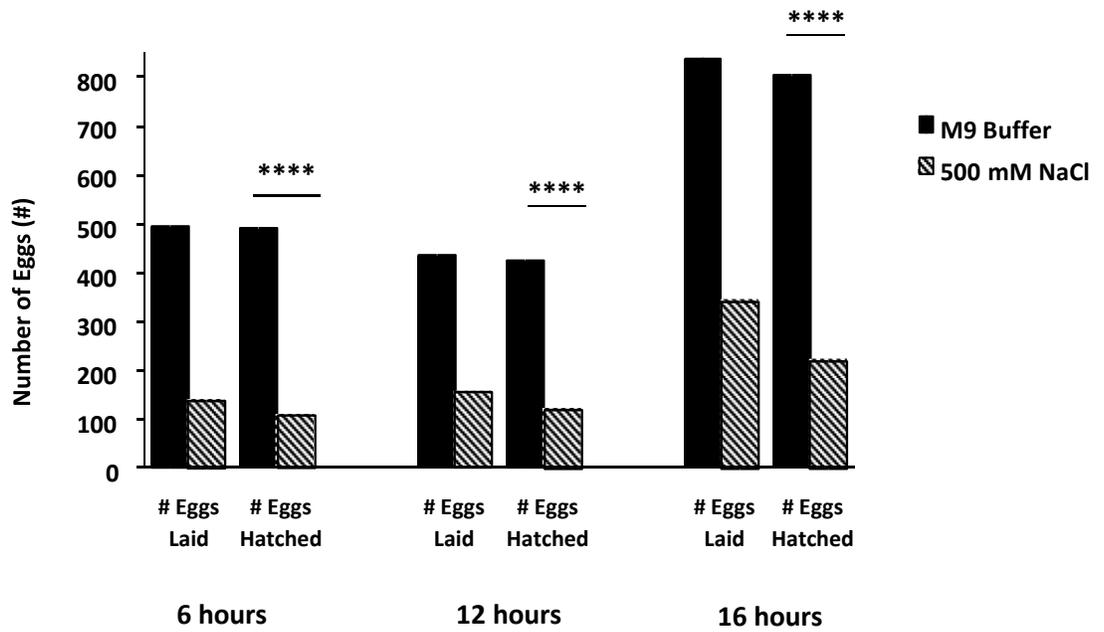
Figure 5.2: Embryos with SINGs are Unable to Hatch

Hatching rate of embryos that contain SINGs. Embryos were dissected from gravid adults and then soaked in M9 (unstressed) or 500 mM NaCl (stressed) for one hour. Stressed embryos were screened under the confocal microscope for the presence of SINGs. Embryos with SINGs (0/40 embryos) showed a 0% hatch rate versus a 100% hatch rate for unstressed embryos or stressed embryos without SINGs (40/40 embryos).

5.2.3 *ubc-18* Mutant Embryos Survive Cellular Stress

Next, we wanted to address whether embryos that were unable to form SINGs also experienced embryonic lethality. Wild type and *ubc-18* mutant embryos were placed in either unstressed, salt stress, or oxidative stress conditions and then scored for hatching. We found that 97% of the unstressed wild type embryos hatched and only 61% of salt stressed embryos hatched, which is consistent with our previous findings (Figure 5.3). In comparison to wild type, 86% of unstressed *ubc-18* mutant embryos hatched, whereas, 89% of salt stressed *ubc-18* mutant embryos hatched (Figure 5.3). This finding suggests that *ubc-18* embryos may have a lower hatching rate than the wild type unstressed but are more resistant to salt stress. Studies performed by the Fay lab have shown that *ubc-18* is associated with a reduced brood size but did not report the hatching rate (Fay et al., 2003). Prior to these results, *ubc-18* was not found to be associated with increased stress

resistance. Another interesting finding from this experiment was that *ubc-18* mutant embryos that underwent oxidative stress did not show increased survival as did the salt stressed embryos (Figure 5.3). This observation could be attributed to other detrimental effects that may be occurring during oxidative stress aside from SING formation.
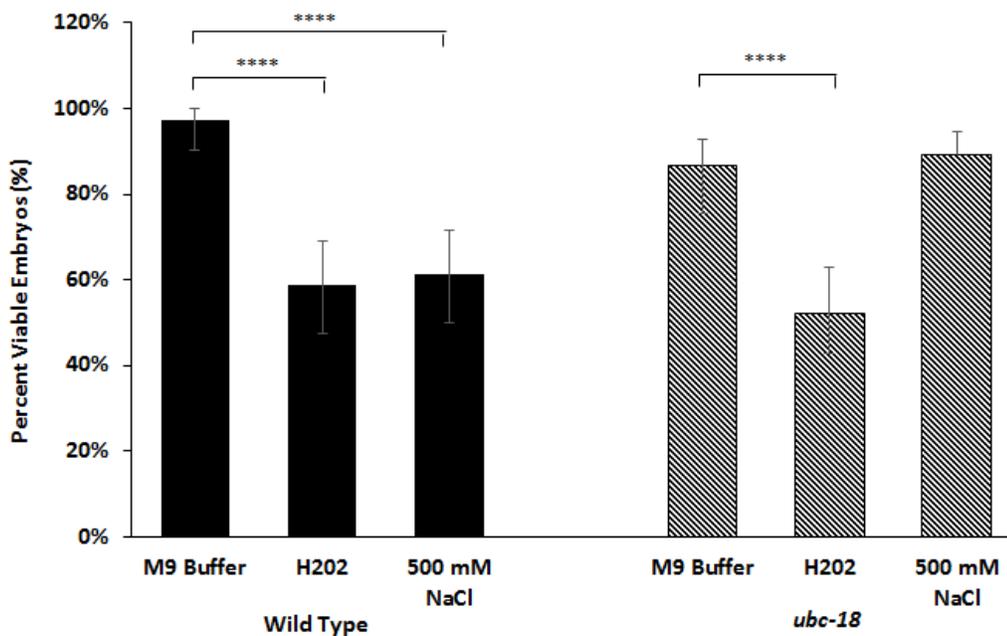
Figure 5.3: Stressed Embryos without SINGs Successfully Hatch

(**A**) Hatching rate of embryos that contain SINGs. Embryos were dissected from gravid adults and then soaked in M9 (unstressed) or 500 mM NaCl (stressed) for one hour. Stressed embryos were screened under the confocal microscope for the presence of SINGs. Embryos with SINGs (0/40 embryos) showed a 0% hatch rate versus a 100% hatch rate for unstressed embryos or stressed embryos without SINGs (40/40 embryos). (**B**) Quantification of eggs laid and hatched in stressed worms after 6, 12, and 16 hours.

5.2.4 Embryos with SINGS Fail to Hatch and Complete Cell Division

To understand why embryos were failing to hatch, we decided to test if SINGs affected cell division during embryogenesis by performing time-lapse microscopy experiments. We hypothesize that embryos with SINGs are not able to undergo successful early cell division. Results from this experiment showed that unstressed embryos successfully progress through prophase, metaphase, and anaphase within 15 minutes, which is indicated by the asterisk (Figure 5.4). However, stressed embryos with SINGs were not able to complete cell division within 15 minutes and appeared to halt during various stages in the cell cycle (Figure 5.4). Figure 5.4 shows stressed cells that are halted at prophase, indicated by an asterisk, and metaphase, indicated by the arrow.
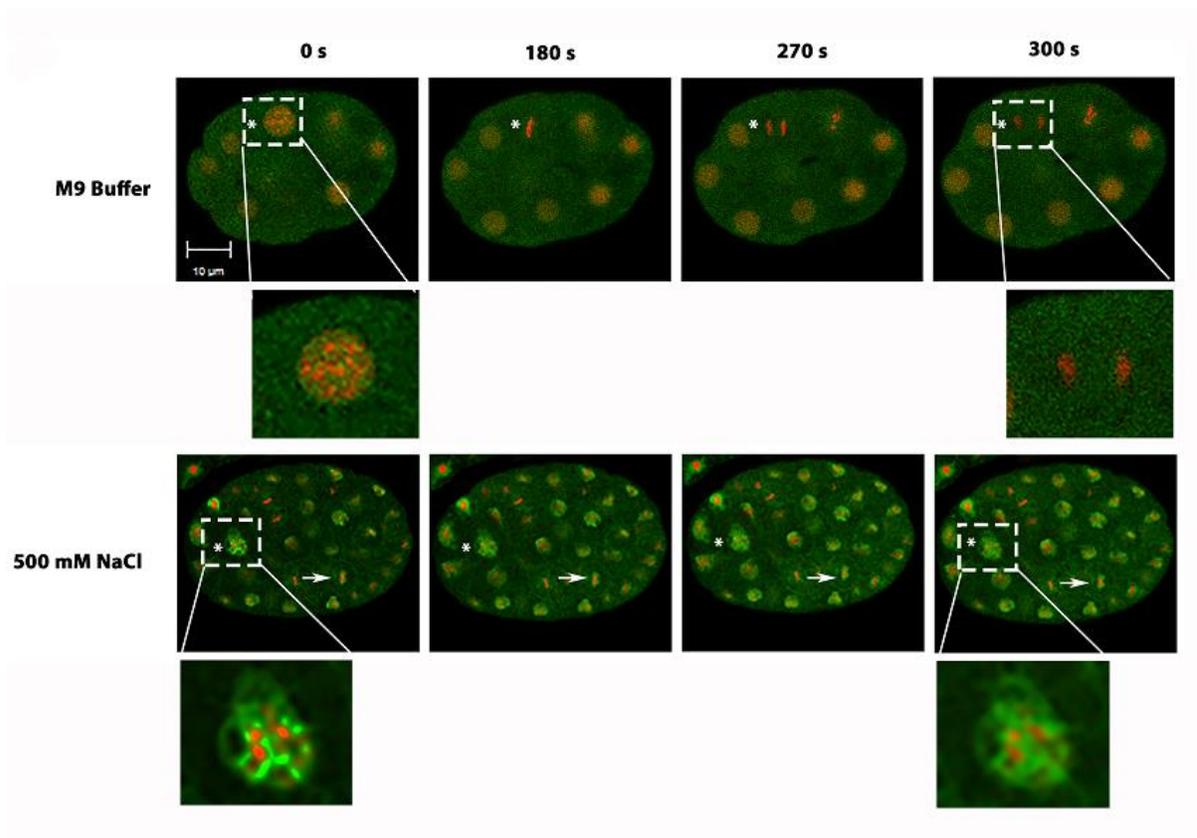
Figure 5.4: Embryos with SINGs Fail to Complete Cell Division

Time-lapse imaging on unstressed and stressed embryos expressing GFP::Ub and mCh::H2B. Ten embryos from the unstressed and ten embryos from the salt stressed groups were observed on the confocal microscope with time-lapse imaging for 15 minutes each. Many cells in each unstressed embryo were able to complete cell division within 5 minutes. Cells in salt stressed embryos showed no progression through the cell division cycle. The asterisk in the M9 embryo shows a cell that proceeds through prophase, metaphase, and anaphase of the cell cycle. The asterisk in the 500 mM NaCl embryo shows a nucleus that has SINGs and remains in prophase. The arrow shows a nucleus with SINGs that remains in metaphase throughout the 15 minute observation period. Outlined cells show an enlarge view of the nuclei with asterisks. Scale bar indicates 10 μm.

5.3 Discussion

In this study, we examined the downstream consequences of SING formation by looking at the persistence of SINGs in multiple tissues, cell division, and embryonic viability in *C. elegans.* A major finding from this study was that embryos with SINGs were unable to hatch and complete cell division. Additionally, *ubc-18* mutants that were unable to form SINGs were able to successfully hatch and proceed through cell division.

SINGs were found to form in multiple tissues including muscle, intestine, embryos, and reproductive tissue. Similar to the reproductive tissue, *ubc-18* was also found to be required to form intestinal SINGs. All three of these tissues formed SINGs at different times and salt concentrations, but only the muscle and intestine recovered from stress. SINGs that formed in the reproductive tissue were observed to persist over 24 hours. These findings suggests that SINGs are a general response to stress.

In *C.elegans*, exposure to hypertonicity induced protein damage which was found to initiate the accumulation of glycerol, an organic osmolyte (Huang and Stern, 2004). These molecules are thought to act as chemical chaperones that aid in refolding proteins back to their native conformation (Bolen and Baskakov, 2001). Osmolytes are also thought to aid in protein-protein and protein-DNA interactions (Kedersha et al., 2005). The hypodermis and the intestine of *C. elegans* have both been proposed to have a role in osmoregulation (Huang and Stern, 2004; Lamitina et al., 2006). The fact that SINGs took longer to form in the muscle and the intestine could be due to evaluated levels of glycerol in both of these tissues, which may be providing a protective mechanism during stress that

aids in reduction in SINGs after 24 hours. In addition, oocyte production is constantly occurring in *C. elegans*, so when SINGs form the tissue is dispensable compared to the muscle and intestine. This may be why SINGs persist in oocytes and embryos.

The observation that SINGs were seen to persist in embryos led to the discovery that stressed embryos with SINGs fail to hatch, and further studies showed that SINGs correlated with cell cycle arrest. Cell cycle arrest has also been documented to occur in muscle cells that are located by the kidneys in response to salt stress. This event is thought to provide a protective mechanism to cells because once they are removed from the stress cell division resumes (Kültz et al., 1998). Our findings demonstrate that both osmotic and oxidative stress halt cell division in embryos of *C. elegans*. This event is only seen in embryos with SINGs, suggesting that SINGs are directly interfering with cell division.

The finding that the inhibition of SING formation led to an increased hatching rate during stress may be explained by studies in *ubc-18* mutant worms. *ubc-18* mutants show increased longevity and survival under stress caused by dietary restrictions. This E2 enzyme is known to interact with a HECT E3 ligase WWP-1 to increase longevity by ubiquitinating substrates involved in regulating increased lifespan induced by dietary restriction (Carrano et al., 2009). Based on literature, it is possible that SING formation and the increased hatching rate may be independent activities of *ubc-18*. A deeper understanding of the role SINGs play during cell division is needed in order to understand why cell division is impaired.

Based on our mass spectrometry results from Table 3, embryonic lethality may be attributed to ubiquitination of developmental proteins that are necessary for embryogenesis. Three potentially ubiquitinated proteins from that list include SYP-4, CDC-42, and POD-2 which are all known to play a role in embryonic development. SYP-4 is one of four proteins that aid in constructing the synaptonemal complex. This complex is known for mediating chromosome repairing and synapsis. If one of these four proteins is missing, then crossover between chromosomes during prophase I will not take place (Brockway et al., 2014). Another developmental protein identified from our list is CDC-42, which is a Rho GTPase that has been identified in controlling cyclin-D1 levels that are used in progressing through the cell cycle (Melendez et al., 2011; Perona et al., 1997; Vanni et al., 2005). CDC-42 also plays a crucial role in determining cell polarity and PAR protein localization in one-cell embryos in *C. elegans* (Gotta et al., 2001). POD-2 (polarity and osmotic sensitivity defect) is an acetyl-CoA carboxylase which is involved in protecting the eggshell from salt stress and for proper embryonic polarity (Tagawa et al., 2001). Additional studies would need to be conducted to test whether these three proteins localize to SINGs under stressed conditions. If either of these three proteins are found to colocalize with SINGs, this may aid in explaining why stressed embryos are unable to complete embryogenesis.

In conclusion, our data shows that exposure to environmental stress induces SING formation in embryos and correlates with cell cycle arrest. Upon the inhibition of SING formation, stressed embryos are able to successfully progress through the cell cycle. These results suggests that SINGs are interfering in cell division by either altering gene

expression or proteolysis during this process. Future studies are required to determine how cell division is affected by the presence of SINGs. The finding that the cell cycle is impaired by stress may shed light onto why organisms exposed to environmental stress experience problems in reproductive capability.

CHAPTER SIX

SING A NEW SONG ABOUT NUCLEAR

PROTEIN QUALITY CONTROL

6.1 Outcomes and Conclusions

The buildup of misfolded proteins is one of the identifying characteristics of over 45 degenerative diseases in humans (Gallagher et al., 2014). Amongst those diseases, roughly 15 have shown protein accumulation in the nucleus (Gallagher et al., 2014). Nuclear quality control pathways for DNA and RNA are well understood. However, less is known about nuclear PQC mechanisms. The main function of PQC mechanisms is to maintain the integrity of the proteome by either refolding, degrading, or sequestering misfolded proteins. Exposure to environmental stress can cause a burden to the cell by increasing the number of misfolded proteins present. Environmental stress has also been linked to infertility; however, it is unclear as to how stress exposure leads to this outcome. Our study was aimed to understand the cellular mechanism of stress response. Specifically, we wanted to know how the UPS was involved in the stress response in gonadal cells. To answer this question, we identified key enzymes in SING formation, putative substrates of these enzymes which localize to SINGs, and determined the downstream effects of SING formation on reproductive function.

We discovered that environmental stress, such as osmotic and oxidative stress, induces the rearrangement of both ubiquitin and 26S proteasome into SINGs (Figure

6.1). These structures were found to be involved in PQC based on the *hsf-1* dependent heat shock result and the rapid appearance of SINGs in aged worms. Based on this, SINGs appear to occur in response to the accumulation of misfolded proteins. In an attempt to find SING targets, we found that TIAR-2 is localized to SINGs in stressed conditions (Figure 6.1). We found that embryonic lethality and cell cycle arrest were consequences of SING formation in stressed embryos. SINGs appear to play a detrimental role to the cell, based on the findings that prevention of SINGs resulted in normal cell division and successful hatching. SINGs appearance in other tissues suggest that the formation of SINGs is a general response to protein misfolding.

The findings from this study suggest a novel PQC pathway in the nucleus that responds to a collapse in proteostasis in the reproductive tissue of *C. elegans.* Based on our limitations, we were unable to determine if proteins in SINGs were actively being degraded. Our mass spectrometry data suggests that some developmental proteins are targets of SINGs, but further studies are needed to determine if this is true. Proteasome components were also found in the mass spectrometry data, which suggests that certain proteasome components are targeted during stress. This finding is consistent with what is seen the Goldberg study were oxidative stress induced the ubiquitination of certain proteasome subunits (Besche et al., 2014). These results suggest three possible roles that SINGs play in PQC during stress. SINGs could be sites of protein degradation, sequestered proteins, or sequestered proteasomes.

The finding that SINGs appear under different stressed conditions could be beneficial to pharmaceutical and biotechnology companies. SINGs could be used as a bioindicator to screen for pharmaceutical drugs or chemicals that cause germline stress like ROS production. Example of a chemicals and drugs to test for causing germline stress include common household products, personal products, cosmetics, NSAIDs (non-steroidal anti-inflammatory drugs), chemotherapy drugs, antipsychotics, estrogens/androgens, and others. Using SINGs as a bioindicator would be a fast and inexpensive method to screen through those drugs and products before going into animal testing, which is expensive and takes longer to screen through drugs. This method could also be employed to test for products to alleviate germline stress. For instance, chemotherapy drugs are known to cause germline stress, which could affect the reproductive capability of the person. These individuals could be given a drug to counteract germline stress, which SINGs could aid in screening through preliminary drugs.
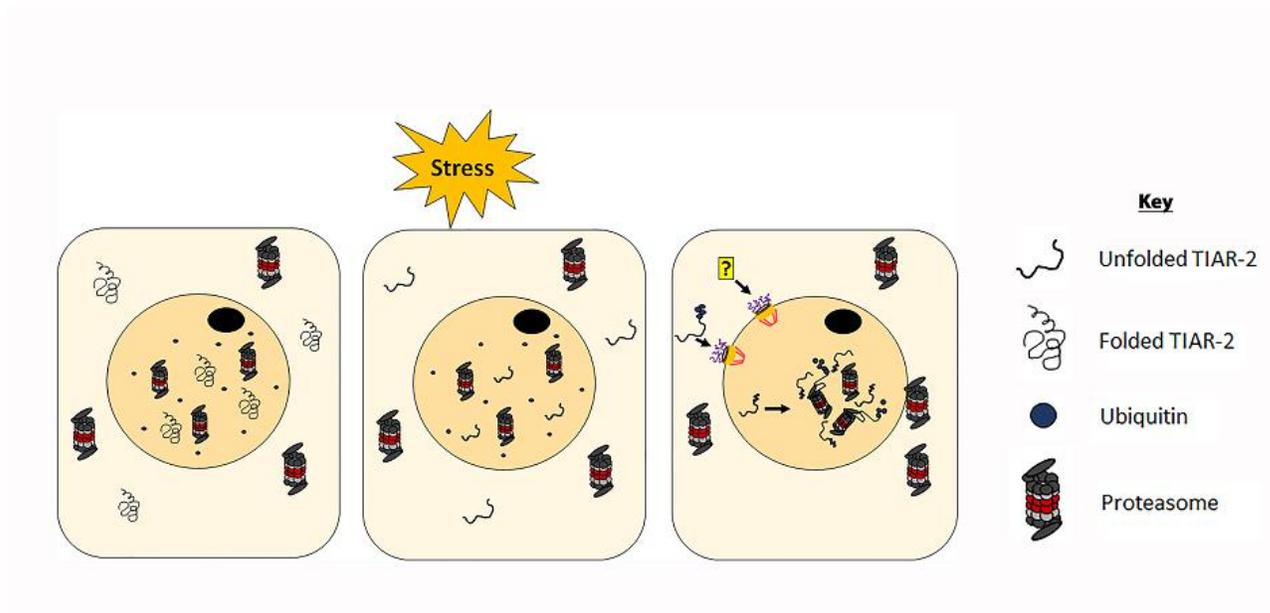
Figure 6.1: Model for SING Formation

Unstressed cells experience a healthy protein homeostasis. When cells are exposed to stressors that induce protein misfolding, the ubiquitin system adds K48-linked ubiquitin chains to the misfolded proteins. The ubiquitinated proteins and proteasomes localize to SINGs in the nucleus.

REFERENCES

Agarwal, A., Gupta, S., and Sharma, R. (2005). Oxidative stress and its implications in female infertility – a clinician's perspective. Reprod. Biomed. Online *11*, 641–650.

Agarwal, A., Makker, K., and Sharma, R. (2008). REVIEW ARTICLE: Clinical relevance of oxidative stress in male factor infertility: An update. Am. J. Reprod. Immunol. *59*, 2–11.

Agarwal, A., Virk, G., Ong, C., and du Plessis, S.S. (2014). Effect of oxidative stress on male reproduction. World J. Mens Health *32*, 1–17.

Amm, I., Sommer, T., and Wolf, D.H. (2014). Protein quality control and elimination of protein waste: The role of the ubiquitin–proteasome system. Biochim. Biophys. Acta BBA - Mol. Cell Res. *1843*, 182–196.

Antón, L.C., Schubert, U., Bacík, I., Princiotta, M.F., Wearsch, P.A., Gibbs, J., Day, P.M., Realini, C., Rechsteiner, M.C., Bennink, J.R., et al. (1999). Intracellular localization of proteasomal degradation of a viral antigen. J. Cell Biol. *146*, 113–124.

Bang, Y.-L., Nguyen, T.T.T., Trinh, T.T.B., Kim, Y.J., Song, J., and Song, Y.-H. (2009). Functional analysis of mutations in UDP-galactose-4-epimerase (GALE) associated with galactosemia in Korean patients using mammalian GALE-null cells. FEBS J. *276*, 1952–1961.

Besche, H.C., Sha, Z., Kukushkin, N.V., Peth, A., Hock, E.-M., Kim, W., Gygi, S., Gutierrez, J.A., Liao, H., Dick, L., et al. (2014). Autoubiquitination of the 26S proteasome on Rpn13 regulates breakdown of ubiquitin conjugates. EMBO J. *33*, 1159–1176.

Bielskienė, K., Bagdonienė, L., Mozūraitienė, J., Kazbarienė, B., and Janulionis, E. (2015). E3 ubiquitin ligases as drug targets and prognostic biomarkers in melanoma. Medicina (Mex.) *51*, 1–9.

Bolen, D.W., and Baskakov, I.V. (2001). The osmophobic effect: natural selection of a thermodynamic force in protein folding. J. Mol. Biol. *310*, 955–963.

Brignull, H.R., Morley, J.F., Garcia, S.M., and Morimoto, R.I. (2006). Modeling polyglutamine pathogenesis in *C. elegans*. Methods Enzymol. *412*, 256–282.

Brockway, H., Balukoff, N., Dean, M., Alleva, B., and Smolikove, S. (2014). The CSN/COP9 Signalosome Regulates Synaptonemal Complex assembly during meiotic prophase I of *Caenorhabditis elegans*. PLoS Genet. *10 (11): e1004757.*

Bukau, B., Weissman, J., and Horwich, A. (2006). Molecular chaperones and protein quality control. Cell *125*, 443–451.

Burkewitz, K., Choe, K.P., Lee, E.C.-H., Deonarine, A., and Strange, K. (2012). Characterization of the proteostasis roles of glycerol accumulation, protein degradation and protein synthesis during osmotic stress in *C. elegans*. PLOS ONE *7*, e34153.

Carrano, A.C., Liu, Z., Dillin, A., and Hunter, T. (2009). A conserved ubiquitination pathway determines longevity in response to diet restriction. Nature *460*, 396–399.

Ciechanover, A., Elias, S., Heller, H., and Hershko, A. (1982). "Covalent affinity" purification of ubiquitin-activating enzyme. J. Biol. Chem. *257*, 2537–2542.

Cotto, J., Fox, S., and Morimoto, R. (1997). HSF1 granules: a novel stress-induced nuclear compartment of human cells. J. Cell Sci. *110*, 2925–2934.

David, D.C., Ollikainen, N., Trinidad, J.C., Cary, M.P., Burlingame, A.L., and Kenyon, C. (2010). Widespread protein aggregation as an inherent part of aging in *C. elegans*. PLoS Biol. *8*, e1000450.

Dick, L.R., Cruikshank, A.A., Destree, A.T., Grenier, L., McCormack, T.A., Melandri, F.D., Nunes, S.L., Palombella, V.J., Parent, L.A., Plamondon, L., et al. (1997). Mechanistic studies on the inactivation of the proteasome by lactacystin in cultured cells. J. Biol. Chem. *272*, 182–188.

Dino Rockel, T., and von Mikecz, A. (2002). Proteasome-dependent processing of nuclear proteins is correlated with their subnuclear localization. J. Struct. Biol. *140*, 189–199.

Eddins, M.J., Carlile, C.M., Gomez, K.M., Pickart, C.M., and Wolberger, C. (2006). Mms2-Ubc13 covalently bound to ubiquitin reveals the structural basis of linkage-specific polyubiquitin chain formation. Nat. Struct. Mol. Biol. *13*, 915–920.

Everett, R.D. (2006). Interactions between DNA viruses, ND10 and the DNA damage response. Cell. Microbiol. *8*, 365–374.

Ferrington, D.A., Husom, A.D., and Thompson, L.V. (2005). Altered proteasome structure, function, and oxidation in aged muscle. FASEB J. *19* (*6*): 644-646.

Frankland-Searby, S., and Bhaumik, S.R. (2012). The 26S proteasome complex: an attractive target for cancer therapy. Biochim. Biophys. Acta *1825*, 64–76.

Gallagher, P.S., Oeser, M.L., Abraham, A., Kaganovich, D., and Gardner, R.G. (2014). Cellular maintenance of nuclear protein homeostasis. Cell. Mol. Life Sci. CMLS *71*, 1865–1879.

Geisler, S., Vollmer, S., Golombek, S., and Kahle, P.J. (2014). The ubiquitin-conjugating enzymes UBE2N, UBE2L3 and UBE2D2/3 are essential for Parkin-dependent mitophagy. J. Cell Sci. *127*, 3280–3293.

Gill, G. (2004a). SUMO and ubiquitin in the nucleus: different functions, similar mechanisms? Genes Dev. *18*, 2046–2059.

Gill, G. (2004b). SUMO and ubiquitin in the nucleus: different functions, similar mechanisms? Genes Dev. *18*, 2046–2059.

Gotta, M., Abraham, M.C., and Ahringer, J. (2001). CDC-42 controls early cell polarity and spindle orientation in *C. elegans*. Curr. Biol. CB *11*, 482–488.

Grune, T., Jung, T., Merker, K., and Davies, K.J.A. (2004). Decreased proteolysis caused by protein aggregates, inclusion bodies, plaques, lipofuscin, ceroid, and "aggresomes" during oxidative stress, aging, and disease. Int. J. Biochem. Cell Biol. *36*, 2519–2530.

Hagen, M. van, Overmeer, R.M., Abolvardi, S.S., and Vertegaal, A.C.O. (2010). RNF4 and VHL regulate the proteasomal degradation of SUMO-conjugated Hypoxia-Inducible Factor-2α. Nucleic Acids Res. *38*, 1922–1931.

Hajjar, C., Sampuda, K.M., and Boyd, L. (2014). Dual roles for ubiquitination in the processing of sperm organelles after fertilization. BMC Dev. Biol. *14*, 6.

Haldeman, M.T., Xia, G., Kasperek, E.M., and Pickart, C.M. (1997). Structure and function of ubiquitin conjugating enzyme E2-25K: the tail is a core-dependent activity element. Biochemistry (Mosc.) *36*, 10526–10537.

Hammadeh, Askari, Georg, Rosenbaum, and Schmidt (1999). Effect of freeze–thawing procedure on chromatin stability, morphological alteration and membrane integrity of human spermatozoa in fertile and subfertile men. Int. J. Androl. *22*, 155–162.

Han, X., Zhang, L., Chung, J., Pozo, F.M., Tran, A., Seachrist, D.D., Jacobberger, J.W., Keri, R.A., Gilmore, H., and Zhang, Y. (2014). UbcH7 regulates 53BP1 stability and DSB repair. Proc. Natl. Acad. Sci. *111*, 17456–17461.

Heck, J.W., Cheung, S.K., and Hampton, R.Y. (2010). Cytoplasmic protein quality control degradation mediated by parallel actions of the E3 ubiquitin ligases Ubr1 and San1. Proc. Natl. Acad. Sci. U. S. A. *107*, 1106–1111.

Herrmann, J., Lerman, L.O., and Lerman, A. (2007). Ubiquitin and ubiquitin-like proteins in protein regulation. Circ. Res. *100*, 1276–1291.

Hershko, A., Heller, H., Elias, S., and Ciechanover, A. (1983). Components of ubiquitin-protein ligase system. Resolution, affinity purification, and role in protein breakdown. J. Biol. Chem. *258*, 8206–8214.

Hong, Y., Rogers, R., Matunis, M.J., Mayhew, C.N., Goodson, M., Park-Sarge, O.-K., and Sarge, K.D. (2001). Regulation of heat shock transcription factor 1 by stress-induced SUMO-1 modification. J. Biol. Chem. *276*, 40263–40267.

Huang, L., and Chen, C.H. (2009). Proteasome regulators: activators and inhibitors. Curr. Med. Chem. *16*, 931–939.

Huang, P., and Stern, M.J. (2004). FGF signaling functions in the hypodermis to regulate fluid balance in *C. elegans*. Dev. Camb. Engl. *131*, 2595–2604.

Huang, Q., Wang, H., Perry, S.W., and Figueiredo-Pereira, M.E. (2013). Negative regulation of 26S proteasome stability via calpain-mediated cleavage of Rpn10 subunit upon mitochondrial dysfunction in neurons. J. Biol. Chem. *288*, 12161–12174.

Huang, T.T., Wuerzberger-Davis, S.M., Wu, Z.-H., and Miyamoto, S. (2003). Sequential modification of NEMO/IKKγ by SUMO-1 and ubiquitin mediates NF-κB activation by genotoxic stress. Cell *115*, 565–576.

Ikeda, F., and Dikic, I. (2008). Atypical ubiquitin chains: new molecular signals. "Protein modifications: beyond the usual suspects" Review Series. EMBO Rep. *9*, 536–542.

Iliev, A.I., Ganesan, S., Bunt, G., and Wouters, F.S. (2006). Removal of pattern-breaking sequences in microtubule binding repeats produces instantaneous tau aggregation and toxicity. J. Biol. Chem. *281*, 37195–37204.

Jahngen-Hodge, J., Obin, M.S., Gong, X., Shang, F., Nowell, T.R., Gong, J., Abasi, H., Blumberg, J., and Taylor, A. (1997). Regulation of ubiquitin-conjugating enzymes by glutathione following oxidative stress. J. Biol. Chem. *272*, 28218–28226.

Jolly, C., Usson, Y., and Morimoto, R.I. (1999). Rapid and reversible relocalization of heat shock factor 1 within seconds to nuclear stress granules. Proc. Natl. Acad. Sci. U. S. A. *96*, 6769–6774.

Jolly, C., Metz, A., Govin, J., Vigneron, M., Turner, B.M., Khochbin, S., and Vourc'h, C. (2004). Stress-induced transcription of satellite III repeats. J. Cell Biol. *164*, 25–33.

Jud, M.C., Czerwinski, M.J., Wood, M.P., Young, R.A., Gallo, C.M., Bickel, J.S., Petty, E.L., Mason, J.M., Little, B.A., Padilla, P.A., et al. (2008). Large P body-like RNPs form in C. elegans oocytes in response to arrested ovulation, heat shock, osmotic stress, and anoxia and are regulated by the major sperm protein pathway. Dev. Biol. *318*, 38–51.

Kedersha, N., Stoecklin, G., Ayodele, M., Yacono, P., Lykke-Andersen, J., Fritzler, M.J., Scheuner, D., Kaufman, R.J., Golan, D.E., and Anderson, P. (2005). Stress granules and processing bodies are dynamically linked sites of mRNP remodeling. J. Cell Biol. *169*, 871–884.

Kedersha, N.L., Gupta, M., Li, W., Miller, I., and Anderson, P. (1999). RNA-binding proteins TIA-1 and TIAR link the phosphorylation of eIF-2 alpha to the assembly of mammalian stress granules. J. Cell Biol. *147*, 1431–1442.

Ko, S., Kawasaki, I., and Shim, Y.-H. (2013). PAB-1, a *Caenorhabditis elegans* Poly(A)-Binding Protein, Regulates mRNA Metabolism in germline by Interacting with CGH-1 and CAR-1. PLOS ONE *8*, e84798.

Kraulis, P.J. (1991). Similarity of protein G and ubiquitin. Science *254*, 581–582.

Kulkarni, M., and Smith, H.E. (2008). E1 ubiquitin-activating enzyme UBA-1 plays multiple roles throughout *C. elegans* development. PLoS Genet. *4* (*7*): e1000131.

Kültz, D., Madhany, S., and Burg, M.B. (1998). Hyperosmolality causes growth arrest of murine kidney cells. Induction of GADD45 and GADD153 by osmosensing via stress-activated protein kinase 2. J. Biol. Chem. *273*, 13645–13651.

Kumar, S., Kao, W.H., and Howley, P.M. (1997). Physical Interaction between Specific E2 and Hect E3 Enzymes Determines Functional Cooperativity. J. Biol. Chem. *272*, 13548–13554.

Lafarga, M., Berciano, M.T., Pena, E., Mayo, I., Castaño, J.G., Bohmann, D., Rodrigues, J.P., Tavanez, J.P., and Carmo-Fonseca, M. (2002). Clastosome: a subtype of nuclear body enriched in 19S and 20S proteasomes, ubiquitin, and protein substrates of proteasome. Mol. Biol. Cell *13*, 2771–2782.

Lake, M.W., Wuebbens, M.M., Rajagopalan, K.V., and Schindelin, H. (2001). Mechanism of ubiquitin activation revealed by the structure of a bacterial MoeB–MoaD complex. Nature *414*, 325–329.

Lallemand-Breitenbach, V., and de Thé, H. (2010). PML nuclear bodies. Cold Spring Harb. Perspect. Biol. *2*, a000661.

Lamitina, T., Huang, C.G., and Strange, K. (2006). Genome-wide RNAi screening identifies protein damage as a regulator of osmoprotective gene expression. Proc. Natl. Acad. Sci. U. S. A. *103*, 12173–12178.

Lorick, K.L., Jensen, J.P., Fang, S., Ong, A.M., Hatakeyama, S., and Weissman, A.M. (1999). RING fingers mediate ubiquitin-conjugating enzyme (E2)-dependent ubiquitination. Proc. Natl. Acad. Sci. *96*, 11364–11369.

Ma, Q. (2013). Role of Nrf2 in oxidative stress and toxicity. Annu. Rev. Pharmacol. Toxicol. *53*, 401–426.

Manetto, V., Perry, G., Tabaton, M., Mulvihill, P., Fried, V.A., Smith, H.T., Gambetti, P., and Autilio-Gambetti, L. (1988). Ubiquitin is associated with abnormal cytoplasmic filaments characteristic of neurodegenerative diseases. Proc. Natl. Acad. Sci. U. S. A. *85*, 4501–4505.

McGrath, J.P., Jentsch, S., and Varshavsky, A. (1991). UBA 1: an essential yeast gene encoding ubiquitin-activating enzyme. EMBO J. *10*, 227–236.

Melendez, J., Grogg, M., and Zheng, Y. (2011). Signaling role of Cdc42 in regulating mammalian physiology. J. Biol. Chem. *286*, 2375–2381.

Mikecz, A. von (2006). The nuclear ubiquitin-proteasome system. J. Cell Sci. *119*, 1977–1984.

Morimoto, R.I. (1998). Regulation of the heat shock transcriptional response: cross talk between a family of heat shock factors, molecular chaperones, and negative regulators. Genes Dev. *12*, 3788–3796.

Morley, J.F., Brignull, H.R., Weyers, J.J., and Morimoto, R.I. (2002). The threshold for polyglutamine-expansion protein aggregation and cellular toxicity is dynamic and influenced by aging in Caenorhabditis elegans. Proc. Natl. Acad. Sci. U. S. A. *99*, 10417–10422.

Morton, E.A., and Lamitina, T. (2013). *Caenorhabditis elegans* HSF-1 is an essential nuclear protein that forms stress granule-like structures following heat shock. Aging Cell *12*, 112–120.

Nathan, J.A., Tae Kim, H., Ting, L., Gygi, S.P., and Goldberg, A.L. (2013). Why do cellular proteins linked to K63-polyubiquitin chains not associate with proteasomes? EMBO J. *32*, 552–565.

Nielsen, S.V., Poulsen, E.G., Rebula, C.A., and Hartmann-Petersen, R. (2014). Protein quality control in the nucleus. Biomolecules *4*, 646–661.

Pelzer, C., Kassner, I., Matentzoglu, K., Singh, R.K., Wollscheid, H.-P., Scheffner, M., Schmidtke, G., and Groettrup, M. (2007). UBE1L2, a Novel E1 Enzyme Specific for Ubiquitin. J. Biol. Chem. *282*, 23010–23014.

Perona, R., Montaner, S., Saniger, L., Sánchez-Pérez, I., Bravo, R., and Lacal, J.C. (1997). Activation of the nuclear factor-kappaB by Rho, CDC42, and Rac-1 proteins. Genes Dev. *11*, 463–475.

Rizzi, N., Denegri, M., Chiodi, I., Corioni, M., Valgardsdottir, R., Cobianchi, F., Riva, S., and Biamonti, G. (2004). Transcriptional activation of a constitutive heterochromatic domain of the human genome in response to heat shock. Mol. Biol. Cell *15*, 543–551.

Rodrigo-Brenni, M.C., Foster, S.A., and Morgan, D.O. (2010). Catalysis of lysine 48-specific ubiquitin chain assembly by residues in E2 and ubiquitin. Mol. Cell *39*, 548–559.

Ruder, E.H., Hartman, T.J., and Goldman, M.B. (2009). Impact of oxidative stress on female fertility. Curr. Opin. Obstet. Gynecol. *21*, 219–222.

Sampuda, K.M., Riley, M., Boyd, L. (2017). Stress induced nuclear granules form in response to accumulation of misfolded proteins in *Caenorhabditis elegans*. BMC Cell Biology. 18 (1), 1 - 18.

Schimmel, J., Eifler, K., Sigurðsson, J.O., Cuijpers, S.A.G., Hendriks, I.A., Verlaan-de Vries, M., Kelstrup, C.D., Francavilla, C., Medema, R.H., Olsen, J.V., et al. (2014). Uncovering SUMOylation dynamics during cell-cycle progression reveals FoxM1 as a key mitotic SUMO target protein. Mol. Cell *53*, 1053–1066.

Schoborg, T., Rickels, R., Barrios, J., and Labrador, M. (2013). Chromatin insulator bodies are nuclear structures that form in response to osmotic stress and cell death. J. Cell Biol. *202*, 261–276.

Seidel, H.S., and Kimble, J. (2011). The Oogenic germline starvation response in *C. elegans*. PLoS ONE *6*, e28074.

Shibata, Y., and Morimoto, R.I. (2014). How the nucleus copes with proteotoxic stress. Curr. Biol. CB *24*, R463–R474.

Stewart, M.D., Ritterhoff, T., Klevit, R.E., and Brzovic, P.S. (2016). E2 enzymes: more than just middle men. Cell Res. *26*, 423–440.

Streich, F.C., and Lima, C.D. (2014). Structural and functional insights to ubiquitin-like protein conjugation. Annu. Rev. Biophys. *43*, 357–379.

Tagawa, A., Rappleye, C.A., and Aroian, R.V. (2001). Pod-2, along with pod-1, defines a new class of genes required for polarity in the early *Caenorhabditis elegans* embryo. Dev. Biol. *233*, 412–424.

Tanaka, K. (2009). The proteasome: Overview of structure and functions. Proc. Jpn. Acad. Ser. B Phys. Biol. Sci. *85*, 12–36.

Tatham, M.H., Matic, I., Mann, M., and Hay, R.T. (2011). Comparative proteomic analysis identifies a role for SUMO in protein quality control. Sci. Signal. *4*, rs4.

Tsvetkov, P., Myers, N., Eliav, R., Adamovich, Y., Hagai, T., Adler, J., Navon, A., and Shaul, Y. (2014). NADH binds and stabilizes the 26S proteasomes independent of ATP. J. Biol. Chem. *289*, 11272–11281.

Vanni, C., Ottaviano, C., Guo, F., Puppo, M., Varesio, L., Zheng, Y., and Eva, A. (2005). Constitutively active Cdc42 mutant confers growth disadvantage in cell transformation. Cell Cycle Georget. Tex *4*, 1675–1682.

Vernace, V.A., Arnaud, L., Schmidt-Glenewinkel, T., and Figueiredo-Pereira, M.E. (2007). Aging perturbs 26S proteasome assembly in *Drosophila melanogaster*. FASEB J. Off. Publ. Fed. Am. Soc. Exp. Biol. *21*, 2672–2682.

Wang, X., Yen, J., Kaiser, P., and Huang, L. (2010). Regulation of the 26S proteasome complex during oxidative stress. Sci. Signal. *3*, ra88.

Watts, R.J., Hoopfer, E.D., and Luo, L. (2003). Axon pruning during *Drosophila metamorphosis*: evidence for local degeneration and requirement of the ubiquitin-proteasome system. Neuron *38*, 871–885.

Wenzel, D.M., Lissounov, A., Brzovic, P.S., and Klevit, R.E. (2011). UbcH7 reactivity profile reveals Parkin and HHARI to be RING/HECT hybrids. Nature *474*, 105–108.

Wilkinson, K.D. (2005). The discovery of ubiquitin-dependent proteolysis. Proc. Natl. Acad. Sci. *102*, 15280–15282.

Winkelman, W.D., Katz, P.P., Smith, J.F., Rowen, T.S., and Infertility Outcomes Program Project Group (2016). The Sexual impact of infertility among women seeking fertility care. Sex. Med. *4*, e190–e197.

Wood, H. (2003). Food and fertility. Nat. Rev. Neurosci. *4*, 858–859.

Zhong, S., Salomoni, P., and Pandolfi, P.P. (2000). The transcriptional role of PML and the nuclear body. Nat. Cell Biol. *2*, E85–E90.

Ben-Zvi, A., Miller, E.A., and Morimoto, R.I. (2009). Collapse of proteostasis represents an early molecular event in *Caenorhabditis elegans* aging. Proc. Natl. Acad. Sci. U. S. A. *106*, 14914–14919.